FACULTY OF
PHARMACEUTICAL SCIENCES

APPLICATION OF A MU-OPIOID BIO-ASSAY FOR TOXICOLOGICAL SCREENING AND FOR EVALUATION OF BIASED SIGNALING OF DESIGNER OPIOIDS

Marie Deventer

A Master dissertation for the study program Master in Pharmaceutical Care

Academic year: 2018 – 2019

GHENT
UNIVERSITY

FACULTY OF
PHARMACEUTICAL SCIENCES

APPLICATION OF A MU-OPIOID BIO-ASSAY FOR TOXICOLOGICAL SCREENING AND FOR EVALUATION OF BIASED SIGNALING OF DESIGNER OPIOIDS

Marie Deventer

A Master dissertation for the study program Master in Pharmaceutical Care

Academic year: 2018 – 2019

GHENT
UNIVERSITY

SUMMARY

New psychoactive substances or NPS, notorious for encompassing an exceptionally wide variety of structure analogues of known, banned drugs, are a growing problem. Apart from the fact that new substances enter the drug market at a staggering rate, their structural diversity allows them to circumvent the currently used (targeted) detection techniques such as immunoassays and liquid chromatography coupled to mass spectrometry, which all require pre-existing knowledge about the identity of the substance. In clinical and forensic settings, this means that presence of these drugs in biological matrices is not detected, which sparked the design of a new detection approach which is activity-based screening, firstly developed for screening of cannabinoids. With opioids being one of the fastest growing groups of NPS and being responsible for a large number of (sometimes fatal) intoxications, a similar assay for the detection of these substances was concocted. In short, it is based on the fact that activation of the μ opioid receptor (MOR) involves the recruitment of the transducer protein β-arrestin 2 to the receptor. In our assay, both β-arrestin 2 and MOR are linked to two inactive subunits of a split NanoLuc® luciferase, and receptor activation results in the structural complementation of the enzyme and therefore restoration of its ability to generate a luminescence signal in presence of the furimazine substrate, which can be measured using a luminometer. However, in the case of opioids, co-occurrence of opioid antagonists (such as the opioid 'antidote' naloxone) in a biological sample prevents receptor activation and hampers the implementation of the assay, resulting in samples which will be wrongly scored negative. In this thesis, we tried an improved screening method, which implied the additional injection of the opioid agonist hydromorphone in order to reveal whether an antagonist is present. To do so, we applied both the original and improved assay protocol to a set of blood samples, obtained from NMS Labs (Horsham, PA, USA) and we scored them independently as either "follow-up required" or "no follow-up required". The outcome was compared to the true content of the samples, as confirmed by bioanalytical techniques. Given the considerable increase in sensitivity (55.56% (40/72) with the original method *vs.* 98.61% (71/72) with the improved method), it is demonstrated that this "upgrade" results in fewer missed positive samples and therefore proves to be an added value to an already well-functioning screening test, bringing it another step closer to a possible future application in the clinical or forensic field as a first-line screening tool.

Secondly, two activity-based assays, monitoring either G protein coupling or β-arrestin 2 recruitment to MOR, were applied to a panel of 21 synthetic opioids, to evaluate if any of these compounds show a bias towards one of the two pathways. Although we were able to formulate some statements about their structure-activity-relationship, we did not find evidence on biased behaviour of the tested compounds.

Overall, this thesis demonstrates that the concept of activity-based assays is valuable in multiple areas of application, as demonstrated for screening and biochemical/pharmacological research.

SAMENVATTING

Nieuwe psychoactieve stoffen (NPS), een beruchte klasse aan stoffen, voornamelijk diverse structuuranalogen van bekende en verboden drugs, zijn een groeiend probleem. Naast de pijlsnelle opkomst van nieuwe stoffen op de drugmarkt zorgt hun structurele diversiteit er ook voor dat ze erin slagen de huidige detectiemethodes, zoals immunologische en massaspectrometrische technieken, met succes te omzeilen, aangezien deze vooraf bestaande kennis over de chemische structuur van de stof vereisen. Dit zorgt ervoor dat deze drugs niet worden gedetecteerd in afgenomen stalen in het kader van klinische en/of forensisch onderzoek en vormde de aanleiding tot de ontwikkeling van 'activiteits-gebaseerde' screeningsmethoden voor cannabinoïden. Aangezien opioïden een van de snelst groeiende klassen van NPS zijn en verantwoordelijk zijn voor een groot aantal (soms fatale) intoxicaties, werd een gelijkaardige assay voor deze drugs uitgedacht. Het concept steunt op de rekrutering van het signaaleiwit β-arrestine 2 naar de μ opioïde receptor (MOR) na activatie. β-arrestine 2 en MOR zijn beide gelinkt aan 2 inactieve Nanoluc® luciferase-subeenheden. Receptoractivatie resulteert in de structurele complementatie van het enzym en bijgevolg herstel van de enzymactiviteit, waardoor een luminescentie signaal wordt opgewekt in bijzijn van het substraat furimazine. In het geval van opioïden verhindert de simultane aanwezigheid van antagonisten (zoals naloxone) echter de activatie van de receptor, waardoor de assay niet naar behoren kan worden uitgevoerd, wat leidt tot het verkeerdelijk negatief scoren van stalen. In deze thesis werd een nieuwe screeningsmetode, die steunt op de extra injectie van de opioïde agonist hydromorfone, uitgeprobeerd. Op deze manier zou de aanwezigheid van antagonisten kunnen worden onthuld. Om dit te verifiëren werd een set bloedstalen, verkregen van een laboratorium in de Verenigde Staten, onderworpen aan beide assays (originele en verbeterde protocol) en werd ieder staal afzonderlijk gescoord als "verder opvolgen vereist" of "geen verdere opvolging vereist". Het resultaat werd vergeleken met de analytisch bevestigde inhoud van de stalen. Gezien de aanzienlijke toename in sensitiviteit (55.56% (40/72) met de originele methode versus 98.61% (71/72) met de verbeterde methode), is hiermee aangetoond dat invoeren van deze "upgrade" resulteert in minder gemiste positieve stalen, wat veelbelovend is met het oog op een mogelijke toepassing als eerstelijnsscreeningsmethode in het klinische en/of forensische kader.

Daarnaast werden 2 activiteits-gebaseerde assays, geschikt voor het onderzoeken van G proteïne koppeling aan of β-arrestine 2 rekrutering naar MOR, toegepast op een set van 21 synthetische opioïden, om na te gaan of een van deze componenten 'bias' vertonen voor signalisatie via een van bovenstaande pathways. Hoewel we erin slaagden enkele besluiten te formuleren wat betreft structuur-activiteits-relatie, kon er voor geen enkel van de geteste opioïden overtuigend bewijs gevonden worden voor signalisatie bias.

Kortom, deze thesis bewijst dat het principe van activiteits-gebaseerde assays waardevol is in verschillende toepassingsgebieden, zoals aangetoond voor screening en biochemisch/farmacologisch onderzoek.

ACKNOWLEDGEMENTS

During the past four months, I was granted the opportunity to perform experiments and write this thesis at the Laboratory of Toxicology and I've enjoyed every part of it. I would like to use this page to express my gratitude to the persons who have guided me through the whole process.

In particular, I would like to sincerely thank my promotor, Prof. Dr. C. Stove, for sharing his enthusiasm for and expertise in this particular subject. Thank you for arousing my interest in research. Thank you for empowering me and for making me want to aim higher. During my stay, I have learned much more than what is written in this dissertation.

I would also like to say a big 'Thank you!' to Dr. Annelies Cannaert, for her consistent willingness to answer my questions and to help me finish this thesis. Thank you for your endless tips and your good advice. Your enthusiasm for your research is contagious and I enjoyed every second of working with you.

To Lakshmi, thank you for the nice talks during our long hours in the lab and for our good collaboration. I wish you the best of luck in completing your PhD.
To every member of the team of the Laboratory of Toxicology, thank you for welcoming me with open arms and for the nice coffee (or tea) breaks. You always made me feel at home.

Finally, I would like to thank my parents for their infinite support and the heartfelt interest they kept showing when I kept rattling on about HEK 293T cells, 96 well plates and the opioid epidemic. To my mom, for always giving me the support and courage to carry on, in life and in my studies. To my dad, for reading my thesis and for supporting me. Thank you both for encouraging me to follow my dreams and to take the opportunities that are available.

TABLE OF CONTENTS

ABBREVIATIONS

4-ANPP	4-anilino-N-phenethylpiperidine
ADR	Adverse drug reaction
ANOVA	Analysis of variance
AP-2	Adaptor protein complex 2
APC	Allophycocyanin
Asn	Asparagine
AUC	Area under the curve
B2 adaptin	Beta-2-adaptin
cAMP	Cyclic adenosine monophosphate
CFSRE	Center for Forensic Science Research and Education
COPD	Chronic obstructive pulmonary disease
CYP	Cytochrome P450
DMEM	Dulbecco's modified Eagle's medium
DNA	Deoxyribonucleic acid
dNGFR	Truncated nerve growth factor receptor
DPD	Dihydropyrimidine dehydrogenase
DRP	Drug related problem
EC_{50}	Half maximal effective concentration
eGFP	Enhanced Green Fluorescent Protein
ELISA	Enzym-linked immuno sorbent assay
E_{max}	Maximal effect
EMCDDA	European Monitoring Centre for Drugs and Drug Addiction
ERK1/2	Extracellular signal-regulated kinase 1/2
FBS	Fetal bovine serum
FDA	Food and Drug Administration
GC	Gas chromatography
GDP	Guanosine diphosphate
GIRK	G protein-coupled inwardly-rectifying potassium channel
GPCR	G protein-coupled receptor
GRK	G protein-coupled receptor kinase
GTP	Guanosine triphosphate
HEK 293T	Human embryonic kidney 293T

His	Histidine
HM	Hydromorphone
HRMS	High-resolution mass spectrometry
ICS	Inhaled corticosteroids
IU	International unit
IV	Intravenous
JNK	c-Jun N-terminal kinase
kDa	Kilodalton
KO	Knock-out
LABA	Long-acting β-adrenoceptor agonist
LC	Liquid chromatography
LgBiT	Large BiT
M	Molar
MAPK	Mitogen-activated protein kinase
MOR	μ opioid receptor, mu opioid receptor
MS, MS/MS	Mass spectrometry, tandem mass spectrometry
NanoBiT	NanoLuc® Binary Technology
ND	Not determined
NPS	New psychoactive substances
PKA	Protein kinase A
PKC	Protein kinase C
QTOF	Quadrupole time-of-flight
RLU	Relative light units
R-PE	R-phycoerythrin
SAR	Structure-activity relationship
SEM	Standard error of the mean
SmBiT	Small BiT
SNP	Single nucleotide polymorphism
SPE	Solid phase extraction
THC	Tetrahydrocannabinol
TM	Transmembrane domain

Trp	Tryptophan
UK	United Kingdom
US, USA	United States (of America)

1. INTRODUCTION

1.1. NEW PSYCHOACTIVE SUBSTANCES: A NEVER-ENDING CAT-AND-MOUSE GAME

NPS (new psychoactive substances) are mostly synthetic chemicals, also referred to as "designer drugs" or "legal highs" (1). They are primarily synthesized in clandestine labs, are often cleverly altered structure analogues of traditional drugs (2) and mimic the psychoactive effects of their parent compounds, controlled substances such as heroin and cocaine (3). The United Nations Office on Drugs and Crime (UNODC) defines NPS as "individual drugs in pure form or in complex preparations that are not scheduled under the Single Convention on Narcotic Drugs (1961) or the Convention on Psychotropic Substances (1971), but which may pose similar threats to public health" (4).

Most NPS can be classified in one of the following categories: stimulants such as cathinones, opioids, cannabinoids or sedatives such as benzodiazepines (5). Since 2008, roughly 900 NPS have been identified (6). Even though international drug agencies try to combat the rapid emergence of new drug arrivals, a staggering assortment of NPS has been introduced to the public (7). Indeed, underground laboratories as well as large maleficent chemical companies (8) are capable of rapid production of these drug analogues, faster than these compounds can be controlled (9). Introduction of small alterations in the structure of previously controlled drugs provides a temporary "legal" status (10). Additionally, witty use of misleading labelling such as "bath salts" and "plant food" and delusional disclaimers like "not for human consumption", give them an unsuspicious allure and allows dealers to keep one step ahead of legal restrictions (11).

NPS are currently hard to put under legislation, yet over the last years, some progress has been made to increase the measures against drug use (12). Some European countries, for instance Belgium (13), have introduced a generic legislation, which focusses on the core molecular structure and prohibits all substances containing a wide diversity of chemical substituents on that basic scaffold (e.g. indole/indazole/benzodiazole derivatives for synthetic cannabinoids, fentanyl derivatives for synthetic opioids). This approach allows the control of groups of substances without the need to identify them individually. It therefore offers an advantage over individual listing of substances, where each substance has to be identified and specified separately in order to be put under legislation, an approach that proves to be insufficient when dealing with the rapid emergence of NPS (12, 14). Similarly, more recent laws in the UK (the Psychoactive Substances Act of 2016) now prohibit all substances with psychoactive properties (15), whereas the US (Synthetic Drug Abuse Prevention Act of 2012) now controls all substances with cannabimimetic properties. (16) (17)

Interestingly, a study from 2015 reported that once a substance is under legislative control, interest in that particular drug suddenly drops (18). While still legal, purchasing the drug online and having it delivered to a user's doorstep is a fairly easy procedure, but once controlled, sellers risk serious prison sentences and often decide to remove the product from their stock, thereby decreasing their availability (19).

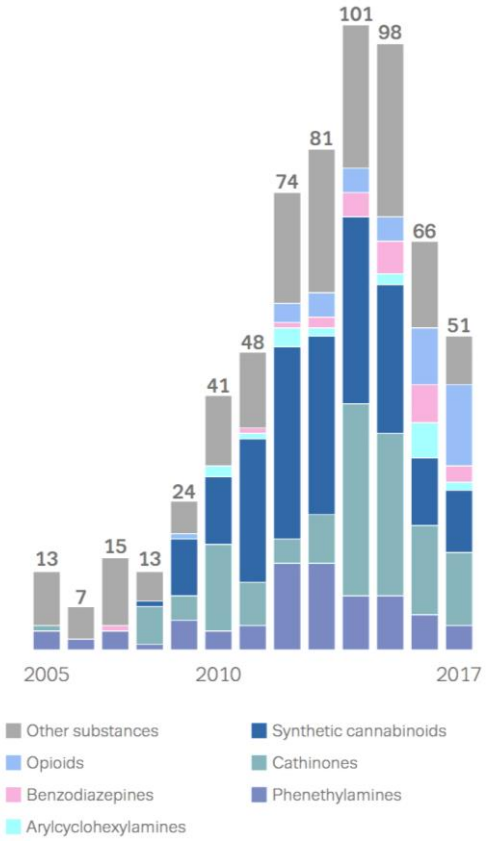

Figure 1.1: Number and categories of new psychoactive substances notified to the EU Early Warning System for the first time, 2005-2017.

Graphic from Statistical Bulletin EMCDDA, 2018

Despite the fact that synthetic cannabinoids and cathinones still dominate the NPS market (3), the European Monitoring Centre for Drugs and Drugs Addiction (EMCDDA) revealed novel synthetic opioids to be one of the fastest-growing groups within the NPS subclasses in the last couple of years (see Figure 1.1) (20).

Historically, the term opiate was used to indicate opium-derived drugs (21). Opium, typically the dried latex obtained from the *Papaver Somniferum* or Opium Poppy has been known for both its medicinal and "*dreamy reverie-inducing*" (22) properties. Opium or poppy use has been reported in ancient Greek, Egyptian, Indian, Roman and Chinese literature (23). Crude opium encompasses more than 40 alkaloids and their derivates, such as codeine, thebaine, noscapine and the well-known morphine (24). Morphine, initially extracted out of opium by the German pharmacist Sertürner in the early 19th century (23, 25), remains a commonly used treatment for moderate to severe malignant and non-malignant pain (23, 26). Nowadays, the term opioid is considered more fitting, since it includes both natural and synthetic variants of these drugs (21). Following the footsteps of other NPS, novel synthetic opioids (NSOs) have now become an undeniable pawn on the chessboard of illicit drugs.

In Europe for example, 38 new opioids made their entry since 2009, including 22 newly reported between 2016 and 2017. Most of these, 28 in particular, are highly potent derivatives of fentanyl (20).

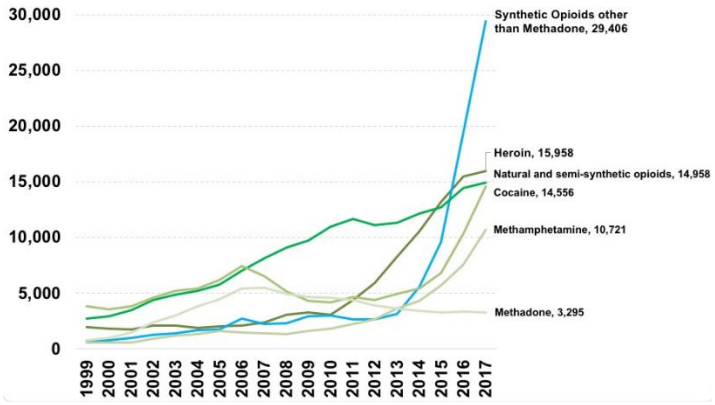

Figure 1.2: Drugs involved in U.S. Overdose Deaths (1999-2017) Light blue trend line represents fatalities caused by synthetic opioids other than methadone, thus including fentanyl analogues and other synthetic opioids such as U-47700. (27)

Fentanyl is a well-known analgesic, originally synthesized by Paul Janssen, (28) with the aim of developing a highly potent analgesic with a therapeutic index greater than that of morphine (29). Fentanyl analogues alfentanil, sufentanil and remifentanil have become widely used in human and veterinary medicine, more specifically in surgical procedures for anaesthesia and treatment of severe pain, while carfentanil and thiafentanyl find their application in immobilisation of large animals. (30). Pharmacological effects of fentanyl analogues, of which some are depicted in Figure 1.3, are similar to those of other opioids, with a potency depending on the substance. Some of these are extremely potent, for example ocfentanil and carfentanil which are reported to be respectively 200 and 10,000 times more potent than morphine (5, 31). Their high potency, rapid onset and short duration of action arise from their high lipophilicity and subsequently their ability to cross the blood-brain barrier (32). Apart from the therapeutic analgesic properties, fentanyls elicit other effects such as euphoria and relaxation (33, 34), making them attractive compounds on the illicit drug market. However, they also induce less desirable effects such as sedation, bradycardia, hypothermia, hypotension, nausea, vomiting and respiratory depression (34, 35), the latter usually being the cause of death in cases of drug overdose (32). Additionally, they are associated with behavioural effects such as anxiety and addiction (36). Unfortunately, in the past decade there is an increase in the distribution and use of illicitly manufactured fentanyl and fentanyl-related compounds, including carfentanil, ocfentanil, acetylfentanyl, and furanylfentanyl, resulting in over 250 deaths in Europe since 2016 (5, 8, 20) In the US, the situation is even more pronounced. As seen on Figure 1.2, at present, the US is experiencing a true epidemic of synthetic opioid-related overdose deaths (37).

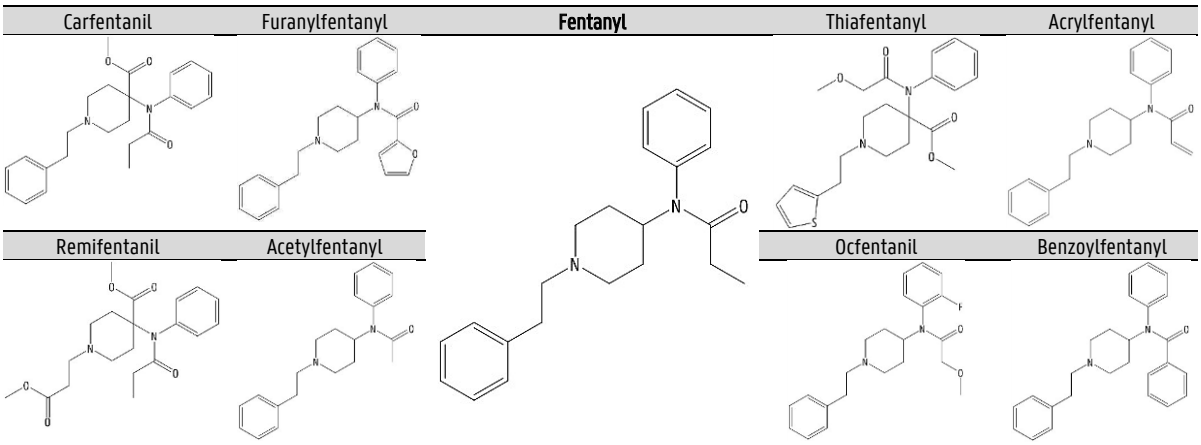

Figure 1.3: The chemical structure of fentanyl, surrounded by 8 fentanyl analogues. Clever chemists have succeeded in altering the fentanyl parent structure by adding various functional groups. Structures depicted include: carfentanil, furanylfentanyl, remifentanil, acetylfentanyl, thiafentanyl, acrylfentanyl, ocfentanil and benzoylfentanyl.

Production of these opioid substances is rather cheap and straightforward (38, 39). Given their highly potent properties, these fentanyl analogues pose a genuine threat, since users might be unaware of exposure to such powerful drugs (20, 40) as fentanyl and fentanyl-related compounds have been reported to be a component of speedball mixtures with cocaine (40), and are sometimes even mixed with heroin (32). Additionally, they can be present as a "contamination" in other fake street-purchased prescription drugs such as counterfeit Xanax pills (alprazolam) or preparations of oxycodone or hydrocodone (9, 39, 40). As with the majority of other NPS, their widespread availability on the "hidden web", the so-called dark net, (19, 31) substantially contributes to their popularity (3) and rise in number. Both buyers and sellers are attracted to the aspect of anonymity and the lack of face-to-face contact (41, 42) and buying substances of the Internet is perceived as safer then prowling across the illicit street market (41). Furthermore, a minimal amount of drug can be divided into an extensive amount of individual doses, which makes smuggling those small quantities and subsequent distribution to the public less burdensome (10, 20)

Another important source of fentanyls is the misuse of prescription fentanyl-containing medicines, such as transdermal patches, sublingual tablets and infusion solutions. These are "accessible" via over-prescribing doctors, collection from the waste of hospitals and sale of unused patches by patients (28). Additionally, new e-liquids for vaping and nasal sprays containing fentanyl, provide an easier and more attractive way to experience the desired psychoactive effects (8).

Apart from fentanyls, various other synthetic opioids have found their way into the black market. These substances include benzamide opioids such as U-47700 and AH-7921 and have been involved in drug overdoses as well (10).

Given increasing globalization of the recreational drug market, predicting future trends in an effort to prevent further outbreaks or restrain the growing crisis, is a complex matter (8). Likewise, it is difficult to anticipate which compounds would soon make an appearance and which substances would gain significant popularity amongst users (43).

1.2. THE μ OPIOID RECEPTOR

1.2.1. General

Novel synthetic opioids are μ opioid receptor (mu opioid receptor; MOR) agonists. MOR is a member of a family of opioid receptors, consisting of at least three major types, namely δ-, κ-and μ-subtypes. These subtypes share ±60% of their amino acid sequence, mainly intracellular regions. In contrast, extracellular regions are quite distinct (44). Located in multiple tissues such as several regions of the brain, spinal cord and digestive tract (45), opioid receptors are stimulated by both endogenous and exogenous ligands (46). Δ opioid receptors are associated with effects such as analgesia and constipation and are activated by enkephalins (46) whereas the κ opioid receptor, activated by endogenous dynorphin, plays an important role in the regulation of feeding. Additionally, κ opioid receptors are involved in nociception and gut motility and induce diuresis through inhibition of the release of antidiuretic hormone (44, 47, 48). In the light of the conducted experiments and topics discussed in this thesis, the μ opioid receptor will be discussed more elaborately.

The μ opioid receptor is distributed in different regions in the central and peripheral nervous system. It is associated with the transmission of nociceptive information (44) and is the main target of morphine (44). Likewise, beta endorphin and enkephalins are endogenous anti-nociceptive ligands for MOR (46). Like all opioid receptors, MOR is a member of the largest protein receptor superfamily in the body, the G protein-coupled receptors or GPCRs (49). GPCRs, which can generally be activated by a plethora of diverse stimuli such as photons, hormones, ions and neurotransmitters, (50, 51) all contain a common seven-transmembrane helical structure and play an important role in signal transduction to the cytosol of the cell. Upon binding with their respective agonists, GPCRs interact with proteins of a downstream signaling pathway to elicit the subsequent cascade of events, of which 2 distinct pathways will be discussed more thoroughly: the G protein-dependent and the β-arrestin-dependent signaling pathway.

The following sections (1.2.2 and 1.2.3) were added to this dissertation in the light of a review to which the author had the opportunity of contributing during her time at the Ghent University Laboratory of Toxicology.

1.2.2. Signaling through GPCR/MOR

1.2.2.1. G protein-dependent signaling

Activation of G proteins is considered as the major, classical signaling of GPCRs (52, 53). Ligand binding leads to contraction of the extracellular domain of the receptor, resulting in the opening of the intracellular transducer-binding site. These conformational changes allow the G_α subunit of the intracellular heterotrimeric G protein (G_α, G_β and G_γ) to enter and interact with the receptor, thereby disrupting the nucleotide binding pocket of the G protein (54-56). Subsequently, there is a release of the nucleotide guanosine diphosphate (GDP) from the G_α-subunit and occupancy by guanidine triphosphate (GTP), which is present at high concentrations. This binding results in conformational changes in the G_α subunit, that ultimately culminate in its dissociation from the $G_{\beta\gamma}$ dimer. G_α and $G_{\beta\gamma}$ can now each modulate different downstream pathways (55).

GPCRs can interact with different G protein isoforms (e.g. G_s, $G_{i/o}$, G_q), each isoform resulting in the recruitment of distinct secondary messenger molecules, thereby inducing specific effects (49). Various receptors can couple to the same G protein, however, the same receptor can also interact with multiple different G proteins (56). All opioid receptors activate inhibitory G-proteins ($G_{i/o}$) (36, 48). Receptor and subsequent $G_{i/o}$-protein activation leads to the inhibition of adenylyl cyclase, which results in the down-regulation of cAMP production (36), an effect found to be caused by the $G_{\alpha i}$ subunit as (see Figure 1.4). Signaling to the $G_{\alpha i}$ subunit is assumed to be required for antinociception provoked by morphine (36). After dissociation of the heterotrimeric G-protein, the released $G_{\beta\gamma}$ subunits aid in the opening of G protein gated inward rectifying potassium channels (GIRK or Kir3) (57, 58), causing a release of K^+ ions from the cell. This mechanism leads to hyperpolarization, inhibiting the excitability of neurons, which in turn inhibits spinal cord pain transmission (36). GIRK also have been thought to interact with the $G_{\alpha i/o}$ subunit, however this mechanism stays unclear (59). Additionally, the $G_{\beta\gamma}$ subunit also binds directly to the calcium channels, thereby further reducing Ca^{2+} currents, (see Figure 1.4) as cAMP-dependent influx is reduced following the inhibition of adenylyl cyclase (36). Inhibition of voltage dependent Ca^{2+} channels likewise contributes to decreasing neuronal excitability (44, 60).

The GTPase activity of the G_α subunit hydrolyses GTP to GDP, which results in the dissociation of the $G_{\beta\gamma}$ subunit from the channel to re-associate with the $G_{\alpha i/o}$ subunit (55).

1.2.2.2. β-arrestin-dependent signaling

Upon receptor stimulation, intracellular domains of the GPCR are quickly phosphorylated by G protein-coupled receptor kinases (GRK) (51), which enhances subsequent binding affinity for β-arrestins (61). These proteins couple to the intracellular loops and C-terminus of the GPCR by recognizing the phosphorylated regions in addition to the conformational changes induced by a specific ligand (36, 62). This results in desensitization of

the receptor by sterically preventing G protein coupling, thereby diminishing the signaling through the G protein. β-arrestins are also involved in the initiation of G protein-independent signal pathways, since some ligands can recruit arrestins without stimulating any detectable G protein signaling (62).

Different types of arrestins are known (63). The two isoforms β-arrestin 1 and β-arrestin 2 differentially mediate MOR regulation (36), MOR having a higher affinity for β-arrestin 2 (64). In the case of MOR, the C-terminal tail of the GPCR has been shown to be crucial for β-arrestin binding (36). Serine and threonine residues of the MOR are phosphorylated by GRK2 or GRK3 (36), which translocate towards the membrane as a result of interactions with the free $G_{\beta\gamma}$-subunits (65). The receptor can also be phosphorylated by other second-messenger-dependent protein kinases (such as protein kinase A or C (PKA or PKC)) which can directly impair G protein coupling (65). On the other hand, the phosphorylation by GRKs alone is not sufficient to have a significant effect on receptor-G protein coupling, but it does lead to an increased affinity to bind β-arrestins, which eventually leads to the desensitization of the receptor (65).

Following the recruitment of the β-arrestin, the GPCR can undergo internalization or endocytosis. β-arrestins act as docking sites for the endocytosis proteins such as clathrin and B2 adaptin of the AP-2 adaptor complex, which facilitate the formation of clathrin-coated pits (65). For MOR, the interaction with β-arrestin is rather transient as it rapidly dissociates from the receptor in the recycling endosomes (65, 66) where the receptor undergoes dephosphorylation and dissociation from its ligand, resulting in recycling the receptor back to the membrane (65).

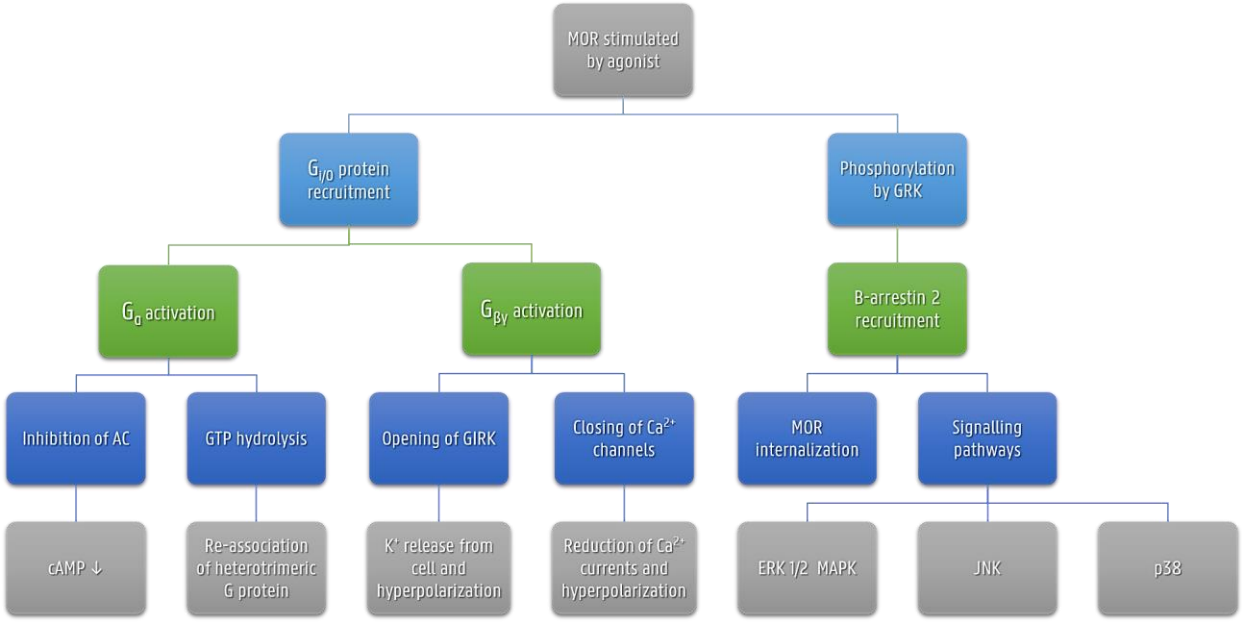

Figure 1.4: Schematic representation of different stages in MOR signaling.

Apart from its role in terminating G-protein dependent signals, β-arrestins can act as signal transducers as such when bound to the GPCR (36, 65). They can couple directly to Src family kinases, which results in several events (see Figure 1.4), for example the stimulation of Ras-dependent activation of the ERK1/2 MAP kinase pathway (65, 67), which is involved in cell proliferation, differentiation, protein scaffolding and apoptosis (36, 65). β-arrestins can serve as scaffolding proteins, thereby facilitating activation of one of the MAP kinase pathways, increasing signaling efficiency between the kinases of the MAPK cascade and targeting these kinases to specific locations within the cell (49, 65, 68, 69). Apart from that, MOR stimulation can also lead to induction of JNK and p38 pathways through β-arrestin (36). JNK pathways, although not elaborately studied for opioid receptors, are reported to be activated by stress, inflammation, neuropathic pain and cytokine activation (36, 68, 70, 71). p38 pathways are activated by similar stimuli (70) and it has been demonstrated that some MOR ligands cause receptor internalization by means of the p38 pathway (36, 72).

1.2.3. Biased signaling

It is assumed that small differences in the conformation of the intracellular loops and the C-terminus of the GPCR lead to a different interaction with intracellular signaling proteins (73). Additionally, it has been established that ligands are able to stabilize different (active) conformations of GPCRs, leading to differential interaction with cytosolic signaling proteins (74). This phenomenon has been described as functional selectivity, also called biased agonism or biased signaling. It defines the fact that different agonists stabilize specific active conformations of the same receptor, each inducing signals that are biased towards (a) specific pathway(s), eventually resulting in different outcomes (75, 76). This is possible for both endogenous and exogenous agonists (75, 76). Thus, a biased agonist is only capable of eliciting a subset of the signaling effects, present at its receptor (77). This mechanism has been described for activation of either G protein or β-arrestin-dependent pathways. Interestingly, it has been hypothesized for GPCRs that the conformation of a conserved motif within transmembrane domain 7 (TM7) contributes to the degree of arrestin coupling and activation, as shown by spectroscopy experiments with the β_2-adrenergic receptor: arrestin-biased ligands may only alter the TM7 conformation whereas ligands that mediate both G protein and arrestin signaling may change both the TM6 and TM7 conformation (56, 78). In addition to ligand-specific changes in receptor conformation, ligands are now also assumed to induce different receptor phosphorylation patterns, which influences arrestin interaction and the subsequent signal transduction (56, 79-86). Furthermore, receptor location within the cell and the environmental context can significantly contribute to the level of biased signaling, such as receptors localised in specific microdomains through interaction with membrane proteins and lipids. These microdomains can contain specific signal transducers, which can result in different responses to ligands (56, 87). This phenomenon of compartmentalization has been found to be important for MOR signaling as it explains the ligand dependent

spatiotemporal nature of the identified cellular responses (56, 88). Additionally, ligands can induce selective trafficking of the GPCR between different cellular compartments such as the Golgi apparatus, which may be a display of their biased nature (56, 89-94). Lastly, the potential assembly of GPCRs into signalosomes (multi-protein complexes (56)) through coupling to other GPCRs (forming dimers or oligomers (56)) or non-GPCR partners like proteins such as receptor-activity modifying proteins (RAMPs) (56, 95) can modulate the recruitment of different intracellular signaling proteins and the trafficking of the receptor, providing meticulous control of further signaling events (56, 96-104). Furthermore, the inclusion of GPCRs in these complexes supposedly modifies their conformation, which may influence (biased) ligand binding and interaction with downstream transducer molecules (56, 95).

Identifying true signaling bias is not straightforward, since plenty of different variables should be taken into consideration. It requires functional GPCR assays which monitor different signaling pathways to generate concentration-response curves, which can then be compared to verify whether a ligand preferably signals through one particular signaling pathway (56, 73). Although multiple cell-based assays are designed to monitor different signaling pathways quite accurately, some limitations remain. For example, β-arrestin recruitment assays are usually not capable of capturing the true refined nature of β-arrestin bias: additional differences in downstream signaling and receptor regulation are overlooked, since the available assays only monitor a specific part of the β-arrestin 2 signaling pathway (the recruitment of β-arrestin). Also the available G protein assays only evaluate single aspects of the G protein signaling (such as either the GTP binding in [^{35}S] GTPγS-based assays or the cAMP levels for example) and on top of that, to assume that all G protein biased ligands signal through the exact same downstream pathways is deceptive (105).

Since signaling bias is cell-dependent, predicting *in vivo* bias via *in vitro* assays is risky. Different cell types may contain varying levels of signal transducers, which complicates the determination of biased agonism (76). Therefore, both assays of interest should preferentially be conducted in the same cell type (106, 107). This would also avoid the influence of differences in cell receptor density (73). However, most assays monitoring the different pathways are often performed in different conditions, since conducting them in exactly identical settings is difficult (108). Moreover, possible *in vivo* phenomena, such as assembly of GPCRs into signalosomes, should be considered when identifying bias in *in vitro* cell-based assays, since the obtained results and suggested bias profile may not always be representative for *in vivo* profiles (56).

Biased agonism has been extensively documented for G protein and arrestin dependent signaling. However, bias can also occur between different G protein isoforms, different arrestin isoforms or even other downstream

pathways (73). For example, G protein assays, such as [^{35}S] GTPγS-based assays, usually do not allow differentiation between recruitment of different G protein isomers (108).

When encountering a signal imbalance which would suggest presence of a biased ligand, it is important to keep in mind that this can also be caused by a system or observational bias. System bias indicates differences in efficiency with which different pathways may be coupled to signal transducers, whereas observational bias refers to the sensitivity of the assays to measure signaling output (75). To circumvent this issue, the ligand bias is typically quantified by comparing the activity of the agonist to a common standard agonist, which will be affected by the same confounders as the ligand of interest. This allows cancelling out factors that are not solely determined by the signaling properties of the ligand and results in a relative activity, which can be compared to the relative activity in other assays (75, 109). However, choosing the proper reference ligand is a complicated matter. Selecting an unbiased ligand may sound easy but the assumption of the existence of such ligand is rather unrealistic because nearly every ligand displays a certain degree of bias. More importantly, the reference ligand should show activity in both pathways and should possess a signaling profile similar to (endogenous) ligands that target the specific receptor. The use of a reference ligand also complicates interpretation of bias since bias ascribed to a substance will change depending upon the selected reference ligand (76). Several approaches and methods have been proposed in an attempt to find the most appropriate way of calculating a defined numeric value, a so-called "bias factor" to quantify the ligand bias (75, 108). The fact that bias should also be considered in comparison with another ligand, makes it difficult to interpret the calculated numeric values and to compare between laboratories and even different assays.

Ligand bias has been extensively studied with respect to MOR, since studies have demonstrated greater antinociception after morphine treatment in β-arrestin knock-out (KO) mice *vs.* wild type (63). These β-arrestin KO mice also did not show a significant decline in breathing frequency, recovered rapidly from the morphine-induced constipation and did not develop antinociceptive tolerance to morphine (110). This implies that G protein biased ligands devoid of β-arrestin recruitment at MOR might exhibit a safer profile, with possibly increased analgesia and less side effects (111). More specifically, Schmid *et al.* described that β-arrestin-biased compounds are more likely to induce respiratory suppression at lower doses, while G protein signaling bias broadens the therapeutic window. However, it has not been directly proven that the β-arrestin pathway mediates the respiratory side effects in mice. Also the correlation with the induction of other opioid side effects remains to be investigated (107). Additionally, agonists such as fentanyl, which is reported to be β-arrestin biased, induced analgesia to the same extent in β-arrestin KO mice compared with wild-type mice. This discovery implied that the loss of β-arrestin 2 had no influence on the responsiveness to these substances (73, 112). Furthermore, endomorphins which are also indicated to be β-arrestin biased (113), showed analgesic properties without

eliciting side effects such as dependence (73, 114, 115). Additionally, the extent to which a ligand must preferably signal through a specific pathway compared to another to produce a relevant change in physiologic response is still undefined (116). This shows that the situation is clearly not that straightforward as originally assumed. Either way, regardless of some remaining challenges that require further more extensive research, biased agonism can definitely be considered an interesting and promising route to discover and pursue in the quest for better future drug development (75, 116, 117).

1.3. SCREENING FOR SYNTHETIC OPIOIDS

1.3.1. Slipping through the fingers of forensic toxicologists

Screening for NPS such as synthetic opioids can be a major challenge for toxicologists when identifying seized drugs or investigating intoxications possibly caused by these substances (9, 32, 118). When receiving biological samples from intoxicated patients or samples of seized drug batches, forensic toxicologists usually apply an approach which consists of 2 distinct steps. First, an initial screening step is performed, followed by confirmation of the positively screened samples where the true presence of (a) substance(s) can be ascertained by applying highly specific though more time-consuming techniques such as for example liquid chromatography coupled to (tandem) mass spectrometry (LC-MS(/MS))(119). Preliminary screening techniques should be highly sensitive, since the aim is to detect all suspicious samples, often containing very small amounts of the illicit substance. Therefore, at this point, some "false positives" are allowed. The major aim is to reduce work load and time of analysis and narrow down the number of samples requiring further, more elaborate analyses (119). Screening usually consists of the application of colorimetric techniques, immunoassays such as enzyme-linked immunosorbent assays (ELISA) or techniques based on liquid chromatography, which are all considered as "targeted" screening approaches (120). Although still commonly implemented (119), some considerations should be made concerning their applicability when it comes to the detection of NPS.

For example, one of the main limitations of immunoassays refers to the fact that the knowledge on the structure of the target compound is required for production of high affinity antibodies, which is a shortcoming regarding many NPS, as they are designed to circumvent detection (119). In the case of opioids, several immunoassays are available that often focus specifically on target opiate analytes with a structure related to morphine. Notable examples are the Immunalysis™ Opiates Direct kit, the Neogen™ Opiate Group kit, the Orasure OTI Opiates kit and the Randox Toxicology Opiates kit. Additionally, separate ELISA kits have been commercialized for the detection of oxycodone, such as the Immunalysis™ Oxycodone/Oxymorphone kit and the Neogen™ Oxycodone/Oxymorphone kit. Cross-reactivity towards different opioids can be quite variable though, and the ability of some opiate structure variants to bind opioid antibodies has often not been described (121). Also, due

to the limited structural analogy between substances such as fentanyls and opiates, the fentanyls typically go unnoticed (10). Despite the fact that ELISA kits for fentanyl and fentanyl analogues have been developed, not all analogues show equal cross-reactivity. The Immunalysis™ Fentanyl direct ELISA kit for instance, is not capable of detecting carfentanil, since the presence of a carbomethoxy group on the piperidine ring seemed to undo a possible interaction with the antibody in the assay. Additionally, cross-reactivity has shown to be reduced with increasing polarity of the substituents on the aniline ring (122). The development of new immunoassays is a time-consuming and rather difficult process (32) and the dynamic nature of the designer drug market therefore further complicates the use of immunoassays for the screening of new synthetic opioids. Additionally, detection via LC-MS(/MS) requires spectral information of the target analytes (119), thereby requiring spectral libraries which are often absent due to lack of reference materials (32, 118).

This describes the flaws of "targeted" screening: antecedent knowledge of the structure and identity of the substance to be detected is an essential prerequisite (123) and this is clearly not the case for the continuously emerging NPS. Given their rapid increase in number and variety, targeted detection techniques are constantly lagging behind, which makes NPS somewhat elusive.

More interest lies in untargeted techniques to detect unidentified illicit drug substances. Therefore, more specialized screening methods, such as liquid chromatography high resolution (tandem) mass spectrometry (LC-HRMS/MS) are warranted. LC-HRMS/MS allows very precise measuring of accurate masses and thereby prediction of a possible structural formula and provides a full scan mass spectrum which can easily be retrospectively re-examined upon detection of a new unknown analyte (124-126). However, due to complicated and tedious data processing software and the need for experienced laboratory operators, hassle-free implementation of LC-HRMS techniques is hampered (126). Furthermore, this sophisticated yet expensive technology is only scarcely available in clinical and forensic laboratories (9) resulting in poor estimation of the true extent of the illicit designer fentanyl use in the population (10).

Recently, a new and promising untargeted detection approach, which may be more interesting for easy first-line screening, has become available (118). The following section will describe a new alternative untargeted screening approach, which is used during the experiments reported in this thesis.

1.3.2. A promising screening method: Activity-based assays

In an effort to circumvent the screening issue concerning the requirement of structural information of the illicit substance of interest, in 2016, the Laboratory of Toxicology at Ghent University reported the successful development of cell-based screening assays which look exclusively at drug biological activity rather than structure. In the case of (new synthetic) opioids, biological activity implies GPCR activation, more specifically

MOR activation in the central and peripheral nervous system. With this knowledge in mind, a GPCR activation assay was designed, based on the ligand induced β-arrestin 2 recruitment (17). This approach was initially reported for the activity-based detection of (synthetic) cannabinoids in urine (17), followed by a slightly modified assay for the screening of synthetic cannabinoids in serum and blood (127). More recently, a MOR based approach was introduced to screen for opiates and opioids (118). These three screening assays use a similar approach and are based on the NanoLuc® Binary Technology (NanoBiT) by Promega, which comprises the functional complementation of a split NanoLuc luciferase enzyme to follow protein-protein interactions within living cells, (17) with the proteins of interest being the β-arrestin 2 and the GPCR (the cannabinoid receptors or μ opioid receptor).

NanoLuc luciferase is a 19.1 kDa luciferase enzyme that produces a high intensity luminescence signal after administration of its substrate furimazine. Upon the discovery of the enzyme in shrimp, the catalytic subunit was later mutated to a smaller size (compared to previously developed luciferases). Along with the creation of a specific substrate came the development of a new bioluminescent system with a more stable and longer lasting luminescence output, suitable for investigating protein interactions (128). In the NanoBiT® technology, the NanoLuc luciferase is split in two inactive sub-units. When coming into close proximity of each other (for example via the interaction of proteins to which these inactive subunits are fused), the subunits can functionally complement, thereby restoring the luciferase activity. In the screening assays, each subunit is attached to either the β-arrestin 2 or the GPCR. Following MOR stimulation by an opioid agonist, β-arrestin 2 is recruited to the receptor, causing structural and functional complementation of the luciferase enzyme. Since both MOR and β-arrestin 2 were fused to inactive subunits of a split luciferase, restoration of the enzyme's activity results in the generation of a bioluminescent signal when furimazine is administered and this signal can be monitored using a standard luminometer (17). More technical details will be given in the section Materials and Methods.

The main benefit of the described approach is that it allows for an untargeted detection of possibly unidentified opioids, since generation of a signal means presence of any substance with activity for MOR, irrespective of its structure. Given the fact that analyses are performed in 96 well plates, it is possible to screen multiple samples in one run, which allows faster analyses. Also, the assays do not require the use of complex and quite advanced appliances. In addition to these qualities, earlier test results revealed properties such as high sensitivity, since low to sub nanogram/mL agonist concentrations were picked up by the assay (17, 118, 127). One has to take into account that this approach remains a screening tool, therefore still a (mass spectrometry-based) confirmation is required: upon encountering a positive sample, this activity-based assay is unable to point out which opioid is present in particular. Moreover, it needs to be evaluated whether or not more than one substance is present

since the receptor picks up the "combined opioid activity". However, when dealing with acute opioid intoxications in a clinical setting, treatment of patients will be similar no matter which particular opioid is present (118).

1.3.3. Opioid antagonist: real lifesaver but villain in activity based bioassays

As this screening method is based on the activity of the (synthetic) opioids, an important restriction is that co-occurrence of opioid antagonists interferes with the principle of the assay (118). The best-known example in this context is naloxone.

Naloxone, considered the antidote for opioid overdose (129), is a competitive MOR antagonist that reverses symptoms of opioid intoxication such as respiratory depression, sedation and hypotension (130, 131). Since oral bioavailability is low due to extensive first-pass metabolism in the liver, naloxone is usually administered intravenously or intramuscularly (130). Since the end of 2015, the Food and Drug Administration (FDA) approved the first nasal spray version of naloxone (132), as intranasal administration is a valuable alternative to IV naloxone in the light of safety and comfort, avoiding painful injections and risks of exposure to blood borne pathogens when using needles (133, 134). Initially, naloxone administration mainly happened in an emergency room setting, to treat patients hospitalized with acute opioid intoxication. However, given the rapid increase in opioid overdoses the US has been experiencing, more overdose victims now receive an initial and possibly life-saving naloxone administration from police officers, friends or family. The administration of naloxone is relatively harmless. Treatment can induce signs of opioid withdrawal such as vomiting, diarrhoea, agitation, lacrimation, piloerection, yawning and rhinorrhoea; although unpleasant, these are usually not life-threatening and are clearly outweighed by the life-saving effect of opioid antagonists in case of an opioid intoxication (129, 135).

Typically, doses up to 2 mg are giving intravenously in case of overdose (130), however the need for multiple and possibly even higher doses has been proposed when dealing with highly potent substances such as fentanyls or very high doses of opioids. Additionally, multiple doses naloxone are often required in case of intoxication with opioids with longer duration of action, due to occurrence of 're-narcotization', since naloxone itself is rather short-acting and reoccurrence of opioid intoxication is possible when the opioid reoccupies the receptor (136).

Treatment with naloxone may be an effective rescue from death by overdose, but when performing activity-based screening, the presence of opioid antagonists is rather unwanted since it prevents receptor activation, therefore signal generation by possible agonists, resulting in a negatively scored sample (118). In other words, the antagonist in a way conceals the presence of opioid agonists, which is what we were initially looking for. This stresses the fact that the current assay protocol needs to be thought out more and that some slight

adaptations are in order. The ultimate goal is to build on the existing assay to achieve a nearly foul proof detection method that is not hampered by the presence of opioid antagonists.

2. OBJECTIVES

The rapid emergence of new (synthetic) opioid drugs and other NPS poses a threat to public health all around the globe. With every new substance making an entrance on the recreational drug market, drug agencies know even less how to cope with the ongoing situation. As mentioned before, currently used detection techniques, which are primarily based on targeted detection, are unable to keep up with the large influx of compounds with an unknown structure. Additionally, the arrival of highly potent substances, that often require very low doses to experience the (un)desired effects, further emphasises the need for highly sensitive screening approaches. However, the appliances suitable for this purpose (e.g. LC-HRMS) are often too expensive to be routinely available in forensic and clinical settings and the laborious operating procedure hampers high-throughput screening.

Recently, promising activity-based screening methods have been proposed for detecting the presence of cannabinoids as well as opioids in biological matrices. The rationale behind this approach is based on the structural and functional complementation of a split NanoLuc® luciferase enzyme in case of activation of the μ opioid receptor, which is expressed in a stable cell line. This event can be relatively easily monitored by luminescence. As reported by Cannaert *et al.* in 2018, the MOR reporter assay proved to be a useful untargeted first-line screening tool to reveal the presence of opioid activity in a biological matrix. However, the co-occurrence of naloxone or other opioid antagonists was found to be a limitation of the assay, as this prevents receptor activation and a subsequent rise in luminescence signal (118). When addressing the question "Is an opioid present in a given sample", co-occurrence of opioid antagonists will lead to a false negative result. In **Part I** of this thesis, we will try to circumvent this issue. We will apply the MOR reporter assay on a set of original blood samples using both the original method and an improved method (with additional application of hydromorphone while the assay is running). By adding a minimal amount of agonist during the assay, we hope to distinguish samples that are negatively scored due to the lack of opioids from the negatively scored samples due to the presence of an opioid antagonist, with the intention of reducing the amount of 'missed' or 'false negative' samples. Each sample will then be independently scored as either "requires follow-up" (samples containing opioid agonist or antagonist or both) or "no follow-up required" ("clean samples"). By carrying out both the readily existing method and this newly improved method on each sample, we will be able to compare the sensitivity and specificity of both methods and evaluate the applicability of the proposed improved method.

Furthermore, the concept of biased signaling at GPCRs has gained a lot of interest in the pharmacological field as it may possibly shed a new light on the question why different ligands for the same receptor elicit different effects. Ligands that only induce signaling towards (a) certain pathway(s) will most likely have an important role to play in future drug development, as they may possibly exhibit a more favourable adverse effect profile

with potentially enhanced therapeutic effects. These promising features of biased signaling have been explored for MOR in the light of the identification of new compounds with increased analgesic properties, devoid of detrimental side effects such as respiratory depression and the development of tolerance and dependence. Fentanyl itself has been reported to be β-arrestin biased (107), however little is known about the potentially biased behaviour of the numerous fentanyl analogues and other synthetic opioids. In **Part II** of this dissertation, we will test a set of 21 synthetic opioids and examine if any are significantly biased towards either β-arrestin or G protein signaling. To do so, separate activity-based assays for the β-arrestin 2 or G protein recruitment to the activated MOR will be executed for the 21 compounds, which will allow us to calculate efficacy (E_{max}) and potency (EC_{50}) and assess bias. Additionally, we will take a closer look at some structural features of the tested compounds and compare this with the acquired knowledge on their efficacy, potency and biased behaviour. In this way, by investigating if certain functional groups contribute to preferential signaling through one specific pathway, we would like to take the first step in the direction of determining a structure-activity-relationship of fentanyls and synthetic opioids in the context of biased signaling.

3. MATERIALS AND METHODS

3.1. DESIGN OF THE MOR REPORTER ASSAY

The described assay comprises an alternative cell-based untargeted approach for screening samples containing substances with opioid activity. By applying NanoLuc Binary Technology (NanoBiT®), which is based on structural and thereby functional complementation of a luciferase enzyme, the activation of MOR can be monitored. In the NanoBiT®, the NanoLuc® luciferase enzyme is split in two inactive subunits, a Large BiT (LgBiT) of 18 kDa and Small BiT (SmBiT) of 1.3 kDa (see Figure 3.1), and fused to specific target proteins, in this case MOR and β-arrestin 2 (138). Recruitment of β-arrestin 2 following activation of the receptor results in restored enzyme activity of the luciferase, which is marked by the generation of a bioluminescence signal in presence of furimazine, the enzyme's substrate. The development and set-up of the assay has been elaborately described in earlier publications by *Cannaert et al.* (118)

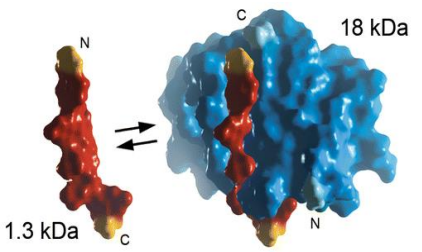

Figure 3.1: Illustration of the 2 NanoLuc luciferase subunits interlocking upon MOR activation, leading to functional complementation of the enzyme. Figure from Dixon, A.S., 2016 (137)

Briefly, expression vectors containing different combinations of MOR and β-arrestin 2 constructs fused via a flexible linker to the NanoLuc luciferase subunits (17) were generated. Upon development, all possible combinations of MOR and β-arrestin 2 and the luciferase subunits were tested in order to find the configuration that yields the largest increase in luminescence signal upon receptor activation. This turned out to be the MOR-LgBiT/SmBiT-βarr2 combination, i.e. LgBiT attached to the C-terminus of MOR and SmBiT attached to the N-terminus of β-arrestin 2. As mentioned earlier, β-arrestin 2 recruitment majorly depends on phosphorylation of the receptor. However, not all MOR agonists promote GRK-dependent phosphorylation to an equal extent (139) (Zhang, J. 1998), a finding which would undermine the sensitivity of the screening assay, since not all agonists would recruit β-arrestin 2 to the same extent. This led to the decision to also introduce co-expression of GRK2 into the cell system, an action that significantly increased sensitivity of the assay. Although human embryonic kidney (HEK) 293T cells were initially transiently transfected with the plasmids, the lab has now succeeded in obtaining stable cell lines expressing the MOR and β-arrestin 2 fusion proteins, combined with the co-expression of GRK2. This greatly reduces the workload and the inter-experiment variability.

This method was used for the above-mentioned opioid screening of original blood samples. In addition to the β-arrestin 2 recruitment assay, a second but quite similar cell line was established in the laboratory for the assessment of biased signaling amongst novel synthetic opioids. Instead of expressing the signal transduction protein β-arrestin 2 coupled to the SmBiT NanoLuc luciferase subunit together with MOR-LgBiT, this cell line

expresses the SmBiT linked to a protein designed to emulate the G protein. This protein, referred to as mini G_i, is in fact the GTPase domain of the G_α subunit of the heterotrimeric G protein coupled to MOR. These cells also expressed MOR-LgBiT but not GRK2, since the latter is not necessary for G protein recruitment. A schematic representation of the concept of both MOR bioassays is provided in Figure 3.2.

Expression of MOR, mini G_i, GRK2 and β-arrestin 2 in the established stable cell lines could be monitored using flow cytometry. For the β-arrestin 2 cell line, MOR-containing plasmids, used for transduction, also contained the enhanced Green Fluorescent Protein (eGFP), a protein that yields a bright green fluorescence when excited by light from the flow cytometer. On the other hand, β-arrestin 2 plasmid inserts were coexpressed with dNGFR, (truncated Nerve Growth Factor Receptor) which can be visualized with an APC-linked antibody (allophycocyanin). GRK2 expression could be monitored via co-expressed trunctated CD8, a protein of which the presence could be verified using the R-phycoerythrin-linked antibody (R-PE). Hence, detection of eGFP, APC and R-PE indicates the presence of both MOR, β-arrestin 2 and GRK2 respectively, and these triple-positive cells were then further kept in culture. (Cannaert, A. authentic urine samples using a stable cannabinoid reporter system) Checking the expression of the mini G_i cell line was done in a similar way by using eGFP (for MOR) and dNGFR (APC) for mini-G_i.

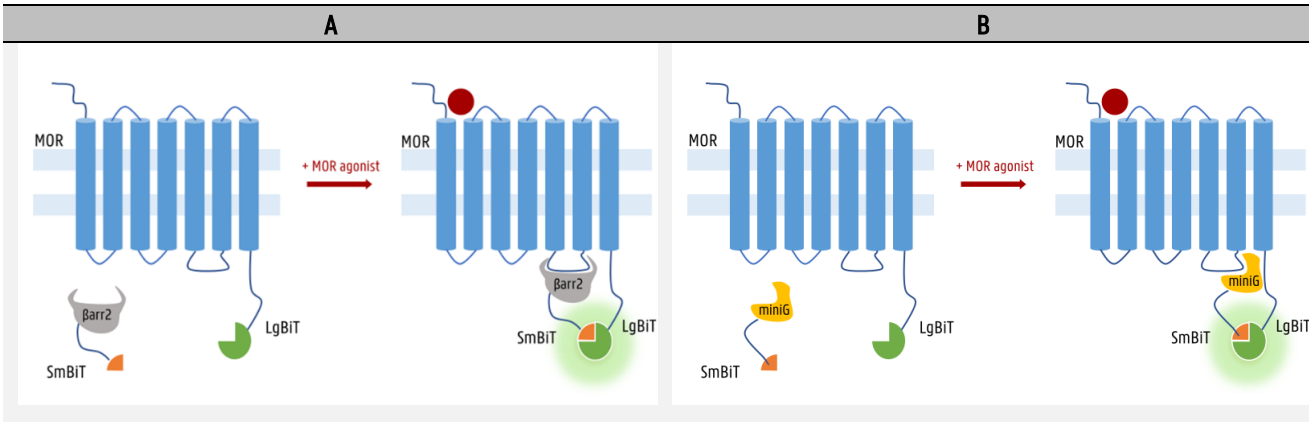

Figure 3.2: Schematic representation of the MOR activity-based bioassays. Once MOR is occupied by its agonist and therefore activated, either β-arrestin 2 (A) or mini-G_i (B), which are coupled to SmBiT, are recruited towards the receptor. This leads to complementation with the LgBiT and restores luciferase activity, which yields a luminescence signal.
Based on a figure from Cannaert, A. 2018 **(118)**

3.2. CELL CULTURE

HEK 293T cells were cultivated in an incubator (Sheldon Manufacturing, Cornelius, OR, USA) at 37 °C and 5% CO_2 under a humified atmosphere and were there maintained in Dulbecco's modified Eagle's medium (high glucose) (DMEM) (Thermo Fisher Scientific, Waltham, MA, USA). DMEM was enriched with 10% heat-inactivated fetal bovine serum (FBS, Sigma Aldrich, Darmstadt, Germany) to provide the required nutrients and growth factors for the cells to survive. Additionally, 2 mmol/L glutamine, 100 IU/mL penicillin, 100 µg/mL streptomycin and 0.25 µg/mL

amphotericin B (all from Thermo Fisher Scientific) were added to the medium. On the day before the experiment, cells were detached using trypsin (Thermo Fisher Scientific) counted and then plated at approximately $5x10^4$ cells/well on 96 well plates that were previously coated with a poly-D-lysine solution (Sigma Aldrich), which allows a more secure and stable attachment to the surface of the wells. The seeding process was then followed by overnight incubation.

3.3. SAMPLES AND CHEMICAL REAGENTS

Authentic blood samples were obtained from (post-mortem) case work from NMS Labs (Horsham, PA, USA). Sample preparation and analyses were performed externally at The Center for Forensic Science Research & Education (CFSRE) (Willow Grove, PA, USA) by means of GC-MS and, LC-MS/MS and LC-QTOF. The sample extracts (n= 150) were sent blind-coded to our laboratory.

Standards of fentanyl analogues (fentanyl, acetylfentanyl, furanylfentanyl hydrochloride, valerylfentanyl hydrochloride, tetramethylcyclopropylfentanyl hydrochloride, tetrahydrofuranylfentanyl, ocfentanil hydrochloride, methoxyacetylfentanyl hydrochloride, cyclopropylfentanyl, cyclopentylfentanyl hydrochloride, crotonylfentanyl, butyrylfentanyl hydrochloride, benzoylfentanyl, alfentanil hydrochloride, acrylfentanyl hydrochloride, 4-methoxybutyrfentanyl hydrochloride, 4-fluoroisobutyrylfentanyl hydrochloride, phenylpropionylfentanyl) and other synthetic opioids (U-47700 hydrochloride, U-49900 hydrochloride and AH-7921) were acquired from Chiron (Trondheim, Norway). A complete list of the acquired standards, as well as their structure, is provided in Appendix I.

3.4. IMPLEMENTATION OF THE MOR BIOASSAY

3.4.1. Part I: Screening of original blood samples

On the day of the experiment, after aspiration of the DMEM in the wells, the now-attached cells were washed twice with 150 µL of Opti-MEM I Reduced Serum Medium (Thermo Fisher) before adding 80 µL into each well. Washing steps were carried out to remove remaining FBS from the DMEM, in order to prevent potential serum protein binding of opioids. To prepare the furimazine substrate, the Nano-Glo® Live Cell reagent, a nonlytic cell permeable detection reagent, was diluted 20-fold with Nano-Glo® LCS Dilution buffer (both by Promega, Madison, WI, USA). Next, 25 µL substrate was added to each well. The plate was then placed in the TriStar^2 LB942 Multimode Reader luminometer (Berthold Technologies, Bad Wildbad, DE) and the luminescence signal was then monitored for 10-15 minutes until it had stabilized. In the meantime, samples were reconstituted as described in Section 3.5.1. Twenty µL of the reconstituted extract was added in each well. The plate was placed back in the luminometer and the signal was measured for 2 hours. For the improved protocol, an additional 10 µL of 0.5 ng/mL hydromorphone (13.5x concentrated) was injected on the 30-minute mark. All samples were run in

quadruplicate: two were run without the extra hydromorphone injection (original protocol) and two were run with the hydromorphone injection (improved protocol). Each plate was run with 2 predefined blank samples, which allowed correction for inter-well variability. Positive controls were taken along in the form of the HM injection in each well at the 30-minute mark.

3.4.2. Part II: Assessment of biased signaling of fentanyl analogues and other synthetic opioids

The applied protocol is rather similar to the previously described method (Section 3.4.1) . Cells of both cell lines (expressing mini G_i or β-arrestin 2), seeded in 96.well plates, were washed twice with 150 µL of Opti-MEM I Reduced Serum Medium (Thermo Fisher), now followed by the addition of 90 µL of Opti-MEM into each well. The Nano-Glo® Live Cell reagent was diluted 20-fold with Nano-Glo® LCS Dilution buffer (both by Promega) and 25 µL was added to each well. The plate was placed in the TriStar^2 LB942 Multimode Reader luminometer (Berthold Technologies), where the signal was monitored for 10-15 minutes until stabilisation. Next, 20 µL of test compound solution was added in each well, after which the signal was measured for 2 hours. Each compound was run in duplicate in 3 independent experiments and a concentration range of 10 pM-10µM (25µM) was tested. An appropriate blank (solvent control) with 0.5-5% methanol or acetonitrile in Opti-MEM I was taken alongside in every experiment. The same concentration range of hydromorphone was also run in duplicate on every plate, which is required for the subsequent bias calculation.

3.5. BLOOD SAMPLE PREPARATION AND BIOANALYSIS

3.5.1. Part I: Screening of original blood samples

Sample preparation was performed at the CFSRE, as previously described by Cannaert *et al.* (118) Briefly, blood samples were extracted by performing solid-phase extraction (SPE) with 130 mg of Clean Screen® DAU extraction columns, which allows both reverse (C8) and ion exchange (benzenesulfonic acid phase) SPE (140). The full-blood samples were first treated with 2 mL of phosphate buffer (at pH 6) and mixed, followed by a 5-minute-long centrifugation. Before extraction, the columns were consecutively conditioned with 3 mL of methanol, 3 mL of deionized water and 1 mL of phosphate buffer. Samples were then loaded on the column and unwanted blood matrix components were removed by washing the column with 1.5 mL of deionized water, 0.5 mL of 0.1 mol/L acetic acid and 1.5 mL of methanol, followed by drying the column under reduced pressure for 5 minutes. The samples were then eluted with 2 mL of ethyl acetate/acetonitrile/ammonium hydroxide (78:20:2) and the eluent was evaporated at 40°C (118). These dried extracts were sent to our laboratory. For the bioassay, the extracts were reconstituted in 100 µL Opti-MEM I Reduced Serum Medium (Thermo Fisher Scientific). For the bioanalysis, which was performed in the US, the same sample preparation was performed as above-mentioned. The residue was reconstituted in 60:40 mobile phase (0.1% formic acid in water: 0.1% formic acid in methanol) for LC-MS/MS

analysis. An improved version of a previously published validated opioid detection method (141) via LC-MS/MS was used and allowed determination of synthetic opioids such as U-47700, U-50488 and fentanyl analogues. Additionally, samples were evaluated for other therapeutic drugs and common drugs of abuse by gas chromatography coupled to mass spectrometry (GC-MS) and liquid chromatography coupled to quadrupole time-of-flight detection (LC-QTOF).

3.5.2. Part II: Assessment of biased signaling of fentanyl analogues and other synthetic opioids

For every test compound, a dilution series was calculated, which resulted in *in well* concentration ranges of 10 pM - 10 µM (25 µM). Considering the final *in well* volume of 135 µL, 6.75-fold concentrated solutions of the compounds were made in Opti-MEM via serial dilution. Compounds were provided in 100% methanol or acetonitrile and the methanol or acetonitrile percentage in each dilution was kept constant.

3.6. DATA PROCESSING AND STATISTICAL ANALYSIS

3.6.1. Part I: Screening for opioids in blood samples

Due to a slightly different cell count in each well, the light signal height may vary among the different wells. Raw data curves (Figure 3.3, A) were corrected for inter-well variability. This was done using the ratio of the average blank signal and the individual signal of the well at the last time point before the addition of the extract. This ratio was applied to the measured signals after extract addition. In essence, each data point from all wells was corrected using Equation (1), resulting in profiles corrected for the inter-well differences (see Figure 3.3, B).

$$Corrected\ profile = \left(\frac{Average\ signal\ of\ the\ blanks}{Individual\ signal\ of\ the\ well}\right)_{\substack{before\ extract\\addition}} x\ signal\ _{\substack{after\ extract\\addition}} \quad (1)$$

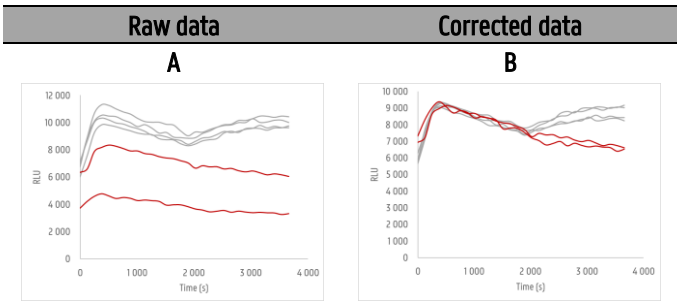

Figure 3.3: Example of correction for inter-well variability before (A) and after correction (B). x-axis, Time in seconds; y-axis, relative light units (RLU); red curve (n=2), sample signals; grey curves (n=4), blank signals

3.6.2. Part II: Assessment of biased signaling of fentanyl analogues and other synthetic opioids

Curve fitting and statistical analyses for the experiment were performed using the GraphPad Prism software (San Diego, CA, USA). Absolute luminescence signals were corrected for inter-well variability and the mean area under the curve (AUC) was calculated for each concentration of each test compound. A nonlinear regression model with Hill slope = 1 (three-parameter) was fitted to obtain a sigmoidal dose-response curve in order to obtain the pharmacological parameters (EC_{50} and E_{max}). The E_{max} of hydromorphone was arbitrarily set to 100% and each compound was normalized to this value and represented as a percentage. The data points were excluded for the highest concentration of agonists when the signal peak showed a reduction of more than 20% in comparison to the maximum signal obtained for the closest lower concentration (high concentration probably leading to cell toxicity). Each data point represents the mean and standard error of mean (SEM), stemming from three independent experiments, performed in duplicate. Statistical analyses were carried out by non-parametric one-way ANOVA (Kruskal-Wallis), followed by post hoc Dunn's multiple comparison test, both in order to verify statistically significant differences between the reference (HM) and the compounds.

Using the EC_{50} and E_{max} values determined earlier, pathway bias was calculated in accordance with the method described by Winpenny *et al.* (106). Equation (2) is used to calculate the Δlog (E_{max}/EC_{50}) value for both G protein coupling and β-arrestin 2 recruitment.

For one pathway (mini-G_i or β-arrestin 2):

$$\Delta\, log(\frac{E_{max}}{EC_{50}}) \;=\; log(\frac{E_{max,X}}{EC_{50,X}}) \;-\; log(\frac{E_{max,HM}}{EC_{50,HM}}) \qquad (2)$$

where X represents a test compound and HM represents hydromorphone.

For each compound, bias is then calculated as ΔΔlog (E_{max}/EC_{50}) using Equation (3):

$$\Delta\Delta\, log(\frac{E_{max}}{EC_{50}}) \;=\; \Delta\, log(\frac{E_{max}}{EC_{50}})_{pathway\ 1} \;-\; \Delta\, log(\frac{E_{max}}{EC_{50}})_{pathway\ 2} \qquad (3)$$

where pathway 1 is G protein coupling and pathway 2 is β-arrestin 2 recruitment. ΔΔlog (E_{max}/EC_{50}) has also been called 'bias factor'. A bias factor above 0 indicates a bias towards G protein-dependent signaling, whereas a negative result demonstrates bias towards β-arrestin 2 recruitment. For easier interpretation, the data will be

plotted with all the compounds shown at the x-axis and with the y-axis showing $\Delta\log (E_{max}/EC_{50})_{pathway\ 1}$ - $\Delta\log(E_{max}/EC_{50})_{pathway\ 2}$ ($\Delta\Delta\log (E_{max}/EC_{50})$). The different opioids will then be compared.

4. RESULTS AND DISCUSSION PART I

4.1. DEVELOPMENT OF AN 'OPIOID ANTAGONIST STRATEGY'

To address the issue of opioid antagonists (e.g. naloxone) interfering with the MOR activation assay, a specific strategy was thought out, which consists of adding a minimal amount of MOR agonist, in this case hydromorphone (HM), at a certain point during the experiment. Theoretically, the presence of an opioid antagonist would be revealed, as the antagonist would inhibit an increase in signal expected from the addition of agonist (118). Two key points still remained to be investigated: the ideal concentration as well as the optimal time point for adding the agonist.

A complete description of the development of the improved protocol, supplemented by curves generated during the experiments, is provided in Appendix II. As an introduction to the results sections below, the following section will briefly summarize the process.

The amount of HM to add is supposed to be kept small, in order not to generate a luminescence signal that is so high that it masks the possible presence of low levels of opioids in biological samples. Experiments were conducted to check the bioassay's sensitivity to low concentrations of HM (0.01 ng/mL to 1 ng/mL) and to assess the effect on the luminescence output of a HM injection at the 10-minute mark in presence of a low concentration range. In conclusion, injection with the lowest tested HM concentration resulted in clean curves that still allowed us to discern low levels of opioids and a final concentration of 0.5 ng/mL was determined. From that point on, injection now occurred after 30 minutes to more accurately estimate the initial opioid activity of a sample. The following experiments evaluated the effect of injecting 0.5 ng/mL HM in a solution of naloxone on the luminescence signal. Naloxone concentrations up to 4 ng/mL (corresponding to approximate plasma concentrations after administration of a common naloxone dose to patients) were tested and it was demonstrated that the rise in luminescence signal due to the additional 0.5 ngl/mL HM was inhibited by naloxone present at common plasma levels, which indicates that antagonist presence will theoretically be unveiled.

Subsequently, the impact of the HM injection on the luminescence results of different levels of opioid agonists was evaluated. Injection in wells with high opioid concentrations was found to result in a slight drop in signal, due to a slight dilution of the sample solution. On the other hand, injection in wells containing low opioid levels resulted in an increase in light signal, since the additional amount of agonist (HM) led to an extra MOR activation. Finally, assay conditions combining naloxone (4 ng/mL), different levels of opioids (HM, 0.1-1000 ng/mL) and the 0.5 ng/mL HM injection were created. These final experiments allowed for a prediction on which read-out profiles we could expect when screening original blood samples, which can be seen on Figure 4.1. High concentration of naloxone (with or without low concentrations of opioids) resulted in a signal that went straight

down, even upon HM injection (Figure 4.1, A). Luminescence signals generated from samples containing neither agonist nor antagonist would overlap with the blank signal (samples containing only medium), displaying a rise in signal upon HM injection (Figure 4.1, B). In contrast, presence of high levels of opioid agonists would result in profiles exhibiting (sometimes very) high signals (Figure 4.1, C).

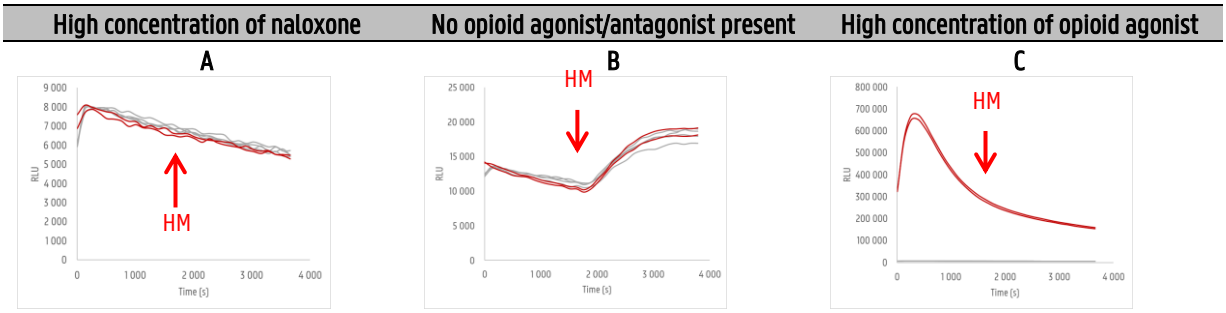

Figure 4.1: Representation of the expected profiles when applying the improved protocol. High concentration of naloxone will inhibit the additional HM injection (A), whereas injection would result in an increase in light signal in case of "blank" samples (B). High agonist concentrations would generate high luminescence signals (C). x-axis, Time in seconds; y-axis, relative light units (RLU); red curve (n=2), sample signals; grey curves (n=4), blank signals

Additionally, it was tested if reducing the assay time (from 2 hours to 1 hour) was feasible in the future. In case of opioid positive samples, it was observed that the significant rise in luminescence signal occurred during the first hour, which indicates that for screening purposes, the initial time period is the most valuable for detecting opioid agonist activity. Moreover, even the profiles that implicate antagonist presence were already noticeable before the 1-hour mark. This finding suggests that a one hour assay time may be equally suitable for detecting opioid agonists/antagonists in biological samples. This may be promising for further improvement of the assay, for instance by making it less time-consuming. For the experiments conducted in this thesis, it was decided to run the assay for the full 2 hours, just in case additional information turned out to be necessary. The initial scoring of the biological samples was based on the 1 hour graphs, but 2 hour graphs were also scored and the results were compared.

4.2. APPLICATION ON SAMPLES

4.2.1. Results of bioanalysis

A set of 94 blood extracts, supplemented with 42 duplicates and 14 disclosed blanks was provided for implementation of the MOR activity-based bioassay. As mentioned previously, a sample's content was bioanalytically determined in the US using LC-QTOF, LC-MS/MS and GC-MS. An extended list of the samples' contents can be found in Appendix III.

Amongst all 94 samples, 16 different compounds with opioid activity and 2 different antagonists were detected and are represented in Appendix IV. Ultimately, 72 out of 94 samples (76.60 %) contained either MOR agonist

compounds, MOR antagonist compounds or both. Presence of only agonist was found in 36 samples (38,30 %), whereas only antagonist was found in 15 (15.96 %) and co-occurrence of agonist and antagonist was determined in 21 samples (22,34 %). Naloxone was the most encountered antagonist, with naltrexone present to a lesser extent. Interestingly, naloxone without the co-occurrence of agonists was detected in 15/94 (15,96 %) samples, indicating unnecessary administration which presumably happened while being unsure about which substance caused a person's intoxication. Fentanyl followed by cyclopropylfentanyl and oxycodone were the most encountered opioid agonists, respectively detected in 15/94 (15,96 %), 13/94 (13,83 %) and 13/94 (13,83 %) samples.

In total, 94 individual compounds were determined. The most commonly detected compound was caffeine, present in 69/94 (73,40 %) samples. Evidence of alcohol use (presence of ethanol) was detected in 22 patients (23,40 %), whereas nicotine was found in 6 patients (6,38 %). Furthermore, apart from opioid-related substances, (traces of) other familiar drugs of abuse were identified in 50 (53,19 %) patients, with cocaine (n=12), benzoylecgonine (n=20), THC and/or its various metabolites (n=37), amphetamine (n=13), methamphetamine (11) and ketamine (n=1) the most well-known. These were detected in both presence and absence of opioids. Other (non-)prescription drugs, commonly not related to abuse, were for example antihistaminics, anti-depressants and anti-epileptics. Since a large number of these drugs were analytically confirmed in samples that were later scored 'negative', these substances do not interfere with our assay (and therefore MOR activation). A list of all compounds detected in correctly scored negative samples is given in Appendix V.

4.2.2. Scoring based on the MOR bioassay

4.2.2.1. 'Original Method'

The original protocol for activity-based screening for the presence of opioids in biological matrices, as reported in an earlier publication (118), does not involve the hydromorphone injection step during the assay. This approach only allows the distinction between "positive" samples i.e. samples containing opioid agonist substances, or "negative" samples, i.e. samples with no trace of substances with MOR activity, but potentially containing substances with MOR antagonistic properties. Scoring of the samples was done blind-coded and independently by two individuals, without pre-existing knowledge about the number of positives and duplicates. Scoring was mainly based upon corrected profiles of the raw read-outs, which were obtained by comparing the raw data to the average blank signal and allowed a correction for inter-well variability (see Material and Methods). In cases of uncertainty about whether samples should be scored positive or negative, raw data was used for confirmation. Samples were scored positive if a rise in luminescence signal, expressed as relative light units (RLU), is noticeable over time compared to a blank signal, measured on the same plate. An increase in signal, large or rather small,

was sufficient to ascribe opioid presence. Although higher signals may suggest higher agonist concentrations, such assumptions are not always easy to support since variable factors such as cell count in the wells or the co-occurrence of agonists and antagonists can considerably affect the signal height. Nevertheless, the extent of a signal usually somehow allows for a rough estimation of agonist levels and permits "labelling" samples as "strongly" or only "lightly" or "weakly" positive. Graphs that pretty much overlapped with the blank signals or showed an almost exact match in slope with the blanks, even when the signal was slightly elevated, were scored as "negative". By way of illustration, in Figure 4.2, an overview is given on the different read-outs that were encountered and how these samples were scored. Graph A shows a clear and large increase in RLU, whereas the increase in signal in Graph B is more subtle. Nevertheless, both samples would be scored positive for opioid activity. Graph C completely overlaps with the blank signal, which is why this sample is scored negative for opioid activity. Although a slight increase can be noticed in comparison to the blank signal for Graph D, the sample is scored negative since the slope of the curve entirely corresponds with the blank signal.

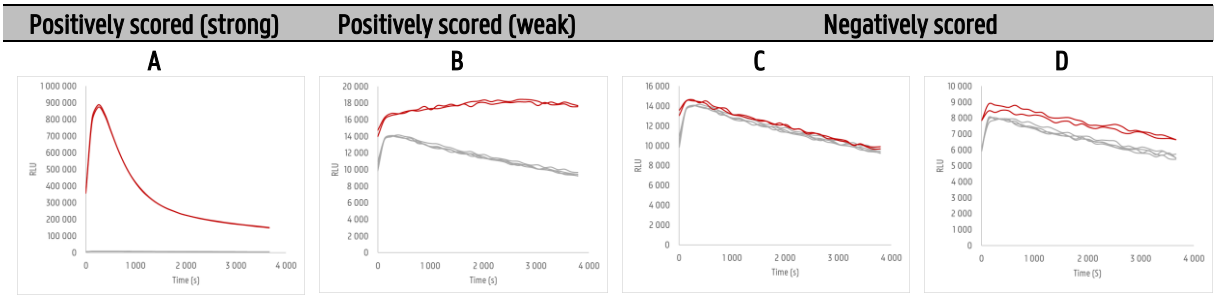

Figure 4.2: Representation of possible profiles generated through the MOR bioassay (original method). x-axis, Time in seconds; y-axis, relative light units (RLU); red curve (n=2), sample signals; grey curves (n=4), blank signals

4.2.2.2. Sensitivity and specificity when using the 'Original Method'

Table 4.1: Comparison of the results obtained by both analysis and our bioassay screening method.

		BIOANALYSIS	
		Follow-up	**No follow-up**
BIOASSAY	**Follow-up**	40	0
	No Follow-up	32	22
Total		**72**	**22**

In total, 94 unique samples were screened and 42 duplicates were included. All duplicate samples were ascribed the same scoring, demonstrating the robustness of the applied assay. By implementing the original method, 40 samples were scored positive with this screening, which would imply the initiation of a follow-up procedure. However, bioanalysis revealed the presence of opioid agonists in 57 of 94 samples, confirming that co-occurrence of antagonists hampers a reliable detection. Since the primary aim of a screening is to quickly designate samples that need follow-up, antagonist positive samples, which should also arouse suspicion, also need to be picked up, which is not possible with this approach.

From the 72 samples containing an opioid (agonist, antagonist or both), only 40 required follow-up according to this method, yielding a sensitivity of 55.56 %. The assay failed to pick up 17 opioid positive samples (all containing naloxone or naltrexone). The remaining 15 missed samples only contained antagonist, with or without other non-opioid compounds present. All 22 samples where follow-up was not mandatory were successfully scored negative, resulting in a specificity of 100%. An overview of the obtained results is provided in Table 4.1.

4.2.2.3. The 'New HM Method'

The improved protocol involves the injection step of HM at the 30 minute time point to allow the distinction between "real negative" samples and "negative" samples due to the presence of an opioid antagonist. In theory, the same conclusion from both methods should emerge from examination of the graphs as long as only the profiles before the 30-minute mark are taken into account. The entire graphs generated from the wells with HM injection were analysed in a similar manner (i.e. blind-coded, independently, using corrected curves). The scoring of this experiment was done separately and without knowing the results from previous scoring. In the new approach, a sample's identity could be unveiled more specifically: positive samples will already have an increase in signal from the start, whereas samples scored as "negative" for opioid activity would typically result in a signal increase upon injection of HM, while this signal will generally be inhibited in samples containing an antagonist. When encountering the latter situation, "negatively" scored samples will obtain a "antagonist positive" tag.

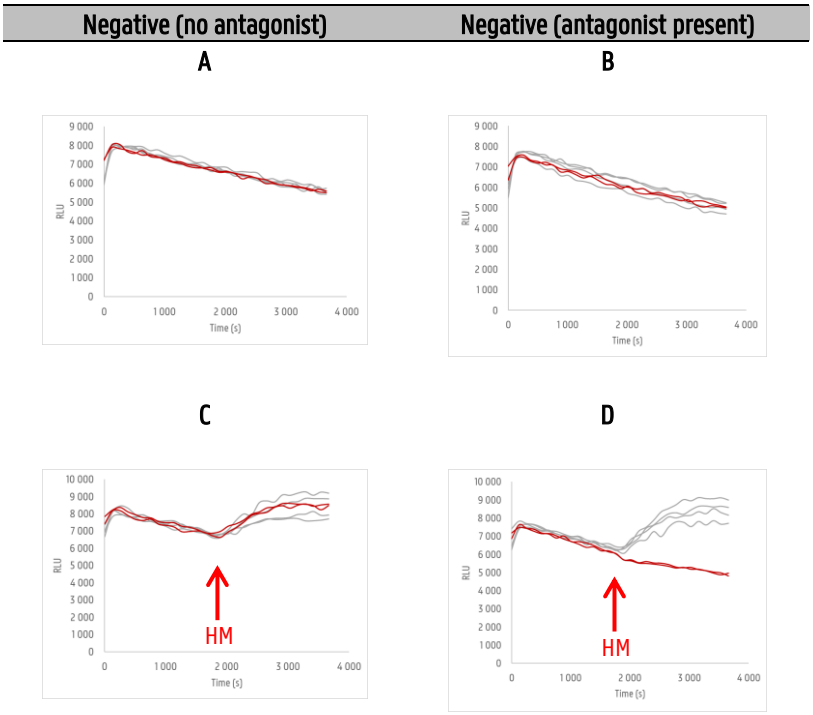

Figure 4.3 Comparison of the old (A and B) and new scoring method (C and D), applied to different samples. x-axis, Time in seconds; y-axis, relative light units (RLU); red curve (n=2), sample signals; grey curves (n=4), blank signals

Figure 4.3 demonstrates the two situations. Via the original protocol, both samples were scored negative (Graph A and B), but via the improved method, they are eventually scored differently (Graph C and D). In Graph C and D, it can be seen how an increase in signal is generated in the blanks (grey curves) after HM injection. With no opioid antagonist such as naloxone present, a sample's read-out exhibits the same specific pattern which can

also be seen on the blank signal (Graph C): the signal steadily goes down and then suddenly increases, followed by a second gradual signal decline, which is only noticeable after one hour. In presence of an antagonist, the signal stays down, even after HM injection: adding an additional amount of MOR agonist does not result in an increase in signal (Graph D).

Overall, the improved approach revealed the presence of an antagonist in 31 of the 54 samples that were scored "negative" in the original method. Two additional samples contained naloxone, however the concentration of agonists present in these samples was too high for naloxone to hamper receptor activation. All generated curves, arranged according their scoring, are provided in Appendix VI.

4.2.2.4. Sensitivity and specificity of the improved assay

Table 4.2: Comparison of the results obtained by both bioanalysis and the improved bioassay screening method (with HM injection).

		BIOANALYIS	
		Follow-up	**No follow-up**
BIOASSAY	**Follow-up**	71	1
	No Follow-up	1	21
Total		**72**	**22**

Parallel with the old method, all duplicates received the same scoring upon screening, demonstrating the robustness of the improved assay design. An overview which compares the profiles of the samples with their duplicates can be found in Appendix VII. Using the new and improved method, we screened 39 samples as positive for opioid activity and 35 samples as positive for opioid antagonists. In total, the assay picked up 72 samples which require further follow-up (2 samples were screened as both agonist and antagonist positive –see below in section 4.2.3.). A short overview of the results is given in Table 4.2. Out of 94 samples, 71 of the 72 samples that require follow-up procedures were correctly marked, which corresponds to a sensitivity of 98.61 %. The assay failed to pick up 1 opioid positive sample (bioanalysis revealed presence of hydrocodone, quantitated at 11 ng/mL). This was the only false negative sample (see Figure 4.4, A) . Twenty-one negative samples were correctly scored negative, contributing to a specificity of 95.45 % (21/22). One sample was mistakenly scored as suspicious, since the assay indicated presence of antagonist, which was not analytically confirmed, yielding only one false positive sample (Figure 4.4, B). The sample did contain ethanol, caffeine, metoclopramide, 11-nor-9-carboxy-THC, THC, amphetamine, methamphetamine and theophylline but no trace of an antagonist had been found. Both samples were afterwards reanalysed and screened for a second time using the bioassay, but the same results were obtained.

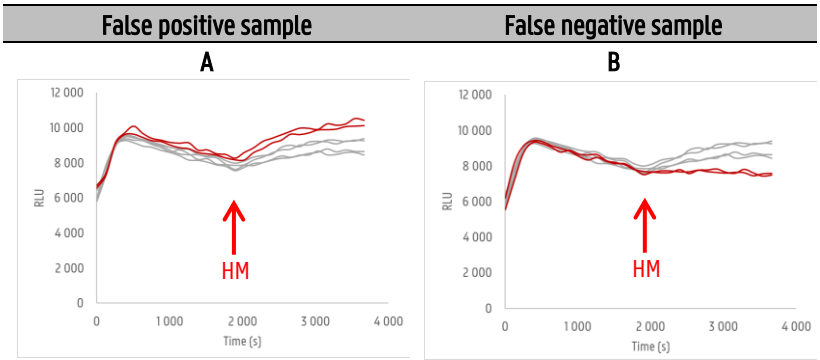

Figure 4.4: Depiction of the two falsely scored samples (only improved method is shown). Although the false negative sample (A) contained hydrocodone, the signal did not significantly exceed the blank signal. The false positive sample (B) was scored as positive for naloxone, since the signal did not rise to the same extent as the blank signal upon injection of HM, although no presence of antagonist was confirmed. x-axis, Time in seconds; y-axis, relative light units (RLU); red curve (n=2), sample signals; grey curves (n=4), blank signals

4.2.2.5. 1 hour assay time *vs.* 2 hour assay time

Finally, all samples were scored blind-coded, independently and without knowing results from previous scoring one last time, based on graphs generated after 2 hours. As expected, the same conclusions could be drawn from a longer assay time since every sample was ascribed the same scoring. This finding is promising in the light of further improving the assay, as mentioned before: reducing the assay time from 2 hours to 1 (30 minutes before and 30 minutes after the injection of hydromorphone) now appears to be a feasible plan. An overview of the read-out generated after a 2 hour assay time is provided in Appendix VIII.

4.2.3. New assay, new profiles

Performing a renewed assay protocol resulted in signal profiles which had not been encountered before. Apart from clearly opioid positive samples in which the signal was too extreme to be overpowered by a potentially present antagonist or samples where naloxone concentrations were sufficiently high to inhibit a rise in signal due to agonists that were also present, we came across a very particular signal profile, of which the only two examples are displayed in Figure 4.5. When using the original assay (Figure 4.5, A and B), these samples were more or less scored as weakly positive, suggesting lower levels of opioid agonist since the signal is only slightly elevated compared to the blank. Upon application of the new assay, the signal initially rose higher than the blank signal (which is expected in positive samples). However, it went straight down at the time of the HM injection,(Figure 4.5, C and D) instead of showing an additional increase (which is seen when an additional amount of hydromorphone is added to rather low concentrations of agonist), clearly indicating that there is also

an antagonist present in the samples. In short, the sample's signal first increases and then crosses the blank (+ HM injection) signal, clearly representing co-occurrence of both agonist and antagonist. In this fashion, these profiles allowed us to score a samples as "both agonist and antagonist present" or "double positive", a label that differs from the normal scoring and was only reserved for 2 out of 94 (2.13 %) screened samples. Nevertheless, both samples maintain their final "requires follow-up" tag anyway. Although samples containing both elements (agonist and antagonist) are quite common in the provided set of samples, the stated profiles are rather rare since it requires a specific ratio of agonist/antagonist. Antagonist concentrations should just be high enough to block the activity of the HM injection, but not so high to completely block the activity of other present agonists. Agonist concentrations should also not be too high to be inhibited by antagonists, therefore making it impossible to notice any traces of antagonists. Either way, with these profiles in mind, we were able to specify the contents of some samples even further, which is always a nice benefit. More specifically, Figure 4.5 (A and C) shows the read-out from a sample which contained both furanylfentanyl and naloxone, as well as caffeine, cotinine and nicotine. Graph B and D show data from a sample containing furanylfentanyl, naloxone, caffeine, temazepam, lorazepam, sertraline, desmethylsertraline and 4-anilino-N-phenethylpiperidine (4-ANPP).

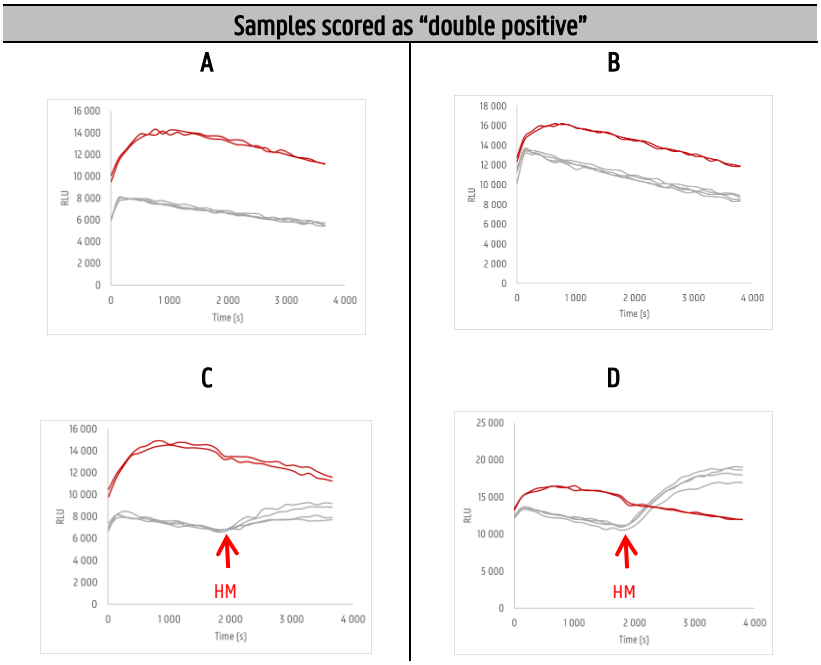

Figure 4.5: Depiction of the 2 samples (left and right column) specifically scored positive for both agonist and antagonist. When applying the original method (A and B), these samples were scored as weakly positive. Application of the improved method (C and D) also revealed presence of antagonists. x-axis, Time in seconds; y-axis, relative light units (RLU); red curve (n=2), sample signals; grey curves (n=4), blank signals

4.2.4. Considerations on the activity-based screening assay

Interestingly, when analysing the curves of positively-scored samples, different profiles became noticeable. Some curves showed a very prominent and rapid increase in luminescence signal, followed by a quick decline. Since high bioluminescence signals are considered to be the result of extensive MOR activation, these situations can occur when highly potent opioids or high concentrations are present. On the other hand, other profiles demonstrated a more gradual increase in signal that only steadily decreases over time. In general, the higher the overall signal, the more the profiles resembled the first-mentioned situation. We noticed a remarkable phenomenon: the higher and steeper the rise in luminescence signal, the quicker the signal decreased (see Figure 4.6). Upon first inspection of the curves, the assumption arose that maybe the presence of different compounds resulted in different profiles. However, subsequent comparison with the result sheet could not confirm this hypothesis, since the same compounds sometimes gave rise to very different signal profiles.

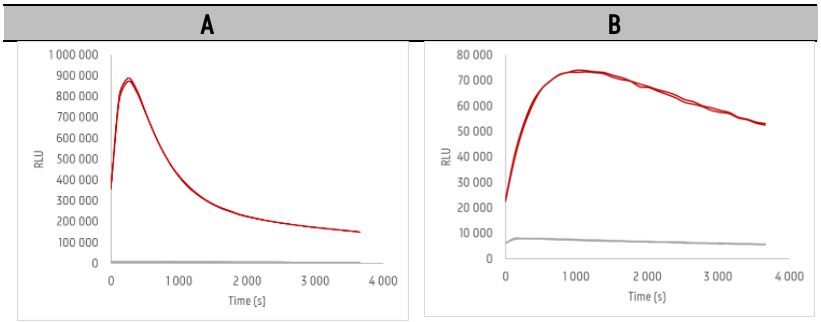

Figure 4.6: Comparison of different signal profiles. Very high signals (A) were found to decrease rapidly, whereas in the case of lower signals (B), the decrease occurs more gradually. x-axis, Time in seconds; y-axis, relative light units (RLU); red curve (n=2), sample signals; grey curves (n=4), blank signals

A potential explanation may be rapid receptor internalization in cases in which luminescence signals are particularly high. A study from 2018 (89) reported the finding that some opioid receptor ligands couple to the receptor in a cell's endosomes or the Golgi apparatus, with maximal endosomal activation occurring significantly later post agonist administration than activation of the membranous receptors, which is found to take place in seconds. Technically, this could explain the diversity of observed profiles, but it remains unclear to which extent signaling from endosomes is possible in the cells used for our assay.

Another key point that should be noted is that, when using the activity-based assay, a positive screen does not necessarily mean illicit drug abuse. Since this assay theoretically picks up all substances with activity at the μ opioid receptor, other compounds that possess this feature are also capable of generating a distinctive signal.
In this study, a large amount of samples contained common opioids typically used for therapeutic purposes e.g. morphine, oxymorphone, oxycodone and hydrocodone, instead of synthetic opioids such as fentanyl (and

analogues) and U-47700. However, claiming that all "therapeutic" opioid use is innocent is rather short-sighted, since these also have a potential for abuse (142, 143), potentially spark opioid addiction and are reported to probably facilitate the transition to heroin use (142, 144).

An interesting situation was encountered with one particular sample in which loperamide was present, a drug used to treat diarrhoea and available as a generic or under the name Imodium® (145, 146). Its effect is largely due to activation of opioid receptors in the mesenteric plexus in the gastrointestinal tract, which is also the mechanism underlying constipation, a well-known side effect of opioids (146). Therefore, loperamide detection cannot be equated to misuse of illegal drugs. However, the misuse and abuse potential has been called into question, with reports of overdose and misuse increasing (146). High doses of loperamide or co-ingestion with P-glycoprotein 1 (efflux pump) or CYP3A4 inhibitors are supposed to enhance passage through the blood brain barrier and are assumed to elicit euphoria or alleviate opioid withdrawal symptoms, hence its sonorous nickname "Poor Man's Methadone" (147, 148).

4.3. FUTURE PERSPECTIVES

Although the new protocol (with additional HM injection) was able to bypass former limitations of the screening assay, there is still room for further improvement with regards to high-throughput screening. Scoring based on luminescence read-out was done by two individuals and during this process, we often encountered certain profiles, mainly in case of a weak signal, which raised doubt as to the appropriate scoring of the sample. This emphasizes the fact that the ultimate scoring remains rather subjective and some samples may be scored differently by different individuals. Development of a software program that is capable of objectively scoring the samples may eliminate this issue and is planned to be completed in the near future.

Additionally, in the near future, a new project will launch in the Laboratory of Toxicology in Ghent. The concept of activity-based screening will be further exploited with the aim of simultaneous detection of multiple classes of psychoactive substances using only one screening assay. To achieve this, multiple reporter systems will be introduced to generate a cell line that expresses more than one receptor (e.g. cannabinoid receptor, μ opioid receptor) at the cell surface.

5. RESULTS AND DISCUSSION PART II

5.1. SCREENING OF SYNTHETIC OPIOIDS FOR MINI G_i AND β-ARRESTIN 2 RECRUITMENT

5.1.1. Potency and efficacy

A panel of 21 fentanyl analogues and other synthetic opioids were tested in both MOR reporter assays, monitoring the coupling of mini-G_i (G protein dependent signaling) and the recruitment of β-arrestin 2 (G protein independent pathway) to the receptor by means of the NanoBiT® principle in stable cell lines. The concentration-response curves for each compound at both β-arrestin 2 and mini-G_i platforms can be found in Appendix IX. In addition, the calculated E_{max} and $logEC_{50}$ values as well as their standard error of mean (SEM) can be found in Table 5.1. Figure 5.1 allows us to compare the obtained values for the tested opioids in both pathways.

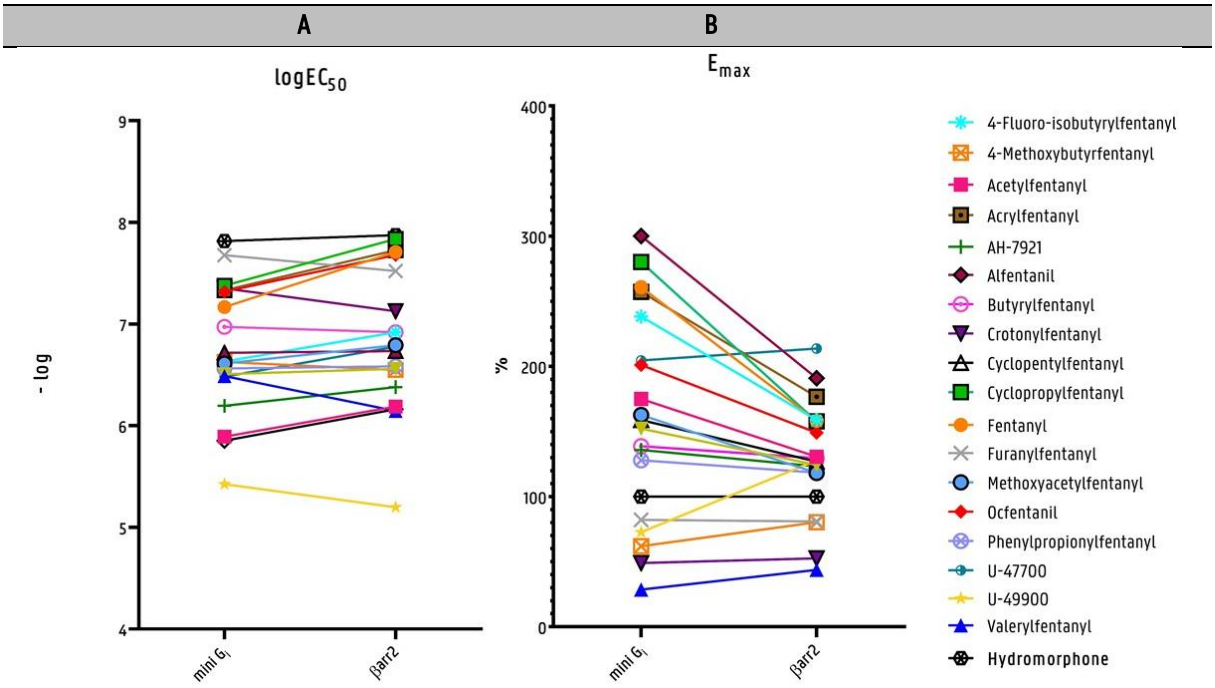

Figure 5.1: Comparison of the negative $logEC_{50}$ (A) and the E_{max} relative to that of hydromorphone (set at 100%) (B) of the 21 synthetic opioids tested with both reporter assays (βarr2 and mini G_i). x-axis shows the 2 pathways, y-axis shows either -$logEC_{50}$ values (A) or E_{max} (%) values (B)

The maximal efficacy (E_{max}) values of HM at both mini-G_i and β-arrestin 2 pathway were set to 100%. The compound showed a $logEC_{50}$ value of -7.816 in the mini-G_i and -7.873 in the β-arrestin 2 assay, which is consistent with a previous study performed in our laboratory (118). The fentanyls with the highest potency in the mini-G_i assay were furanylfentanyl with a $logEC_{50}$ value of -7.676, followed by cyclopropylfentanyl ($logEC_{50}$ of -7.376) and crotonylfentanyl ($logEC_{50}$ of -7.351). Similarly, we found that cyclopropylfentanyl, acrylfentanyl and fentanyl were found to be the most potent at the β-arrestin 2 platform, showing $logEC_{50}$ values of -7.837, -7.725 and -7.709 respectively. A comparison of the potencies (EC_{50} values) for the tested substances at both pathways is provided in Figure 5.1 (A).

Table 5.1: Overview of the obtained efficacies and potencies of the tested synthetic opioids in both β-arrestin 2 and mini-G_i pathways. E_{max} values are calculated relative to the E_{max} of the reference compound hydromorphone (E_{max} arbitrarily set at 100%). We observed no activity for tetramethylcyclopropylfentanyl hydrochloride and benzoylfentanyl in our assay, therefore, it was not possible to determine E_{max} and $logEC_{50}$ values.

Compound	Mini-G_i recruitment		B-arrestin 2 recruitment	
	E_{max} (%) ± SEM (n=3)	$LogEC_{50}$ ± SEM (n=3)	E_{max} (%) ± SEM (n=3)	$LogEC_{50}$ ± SEM (n=3)
Hydromorphone	**99.98 ± 2.77**	**- 7.816 ± 0.09**	**100.0 ± 2.16**	**-7.873 ± 0.06**
4-Fluoro-isobutyrylfentanyl	238.4 ± 4.61	- 6.631 ± 0.06	159.0 ± 2.27	- 6.920 ± 0.04
4-Methoxybutyrfentanyl	61.95 ± 3.21	- 6.626 ± 0.12	80.31 ± 3.55	- 6.548 ± 0.10
Acetylfentanyl	175.0 ± 3.32	- 5.892 ± 0.03	130.6 ± 2.43	- 6.188 ± 0.03
Acrylfentanyl	257.3 ± 4.15	- 7.332 ± 0.03	176.6 ± 3.84	- 7.725 ± 0.06
AH-7921	135.9 ± 2.41	- 6.196 ± 0.04	123.2 ± 2.35	- 6.379 ± 0.04
Alfentanil	300.2 ± 7.12	- 5.852 ± 0.06	190.9 ± 6.72	- 6.162 ± 0.09
Benzoylfentanyl	ND	ND	ND	ND
Butyrylfentanyl	138.7 ± 4.04	- 6.971 ± 0.07	129.6 ± 3.55	- 6.919 ± 0.06
Crotonylfentanyl	49.06 ± 2.44	- 7.351 ± 0.14	52.66 ± 1.10	- 7.125 ± 0.05
Cyclopentylfentanyl	158.8 ± 4.71	- 6.717 ± 0.07	126.9 ± 3.82	- 6.733 ± 0.07
Cyclopropylfentanyl	280.2 ± 4.56	- 7.376 ± 0.04	157.7 ± 1.48	- 7.837 ± 0.02
Fentanyl	260.9 ± 6.00	- 7.167 ± 0.06	158.2 ± 2.95	-7.709 ± 0.06
Furanylfentanyl	82.21 ± 1.74	- 7.676 ± 0.05	81.00 ± 1.98	- 7.522 ± 0.06
Methoxyacetylfentanyl	162.7 ± 2.29	- 6.612 ± 0.03	118.2 ± 1.31	- 6.791 ± 0.03
Ocfentanil	201.1 ± 5.18	- 7.318 ± 0.07	149.1 ± 1.70	- 7.679 ± 0.03
Phenylpropionylfentanyl	127.9 ± 5.98	- 6.562 ± 0.11	118.4 ± 3.69	- 6.584 ± 0.09
Tetrahydrofuranylfentanyl	152.2 ± 2.50	- 6.507 ± 0.04	124.3 ± 2.59	- 6.560 ± 0.05
Tetramethylcyclopropylfentanyl	ND	ND	ND	ND
U-47700	204.6 ± 3.75	- 6.482 ± 0.04	213.8 ± 6.35	- 6.776 ± 0.08
U-49900	72.67 ± 10.85	- 5.424 ± 0.2	127.9 ± 3.19	- 5.197 ± 0.03
Valerylfentanyl hydrochloride	28.65 ± 3.21	- 6.487 ± 0.27	43.72 ± 0.90	- 6.144 ± 0.04

ND, not determined

U-49900 was found to be the least potent compound in the mini-G_i and β-arrestin 2 assays, with a $logEC_{50}$ value of -5.424 and -5.197 respectively. Weakly potent fentanyls in the mini-G_i assay were alfentanil ($logEC_{50}$ of -5.852) and acetylfentanyl ($logEC_{50}$ of -5.892). These fentanyl analogues were also observed to be relatively weakly potent when considering the recruitment of β-arrestin 2, with $logEC_{50}$ values of -6.162 for alfentanil and -6.188 for acetylfentanyl. In addition, valerylfentanyl showed a rather low potency in β-arrestin 2 recruitment ($logEC_{50}$ of -6.144), although it was found to be slightly more potent in the mini-G_i assay ($logEC_{50}$ of -6.487). This proves that compounds with a certain potency in one pathway are not always equally potent in another. Overall, Figure 5.1 (A) shows that no distinct trend could be noticed: the potencies of the different compounds were found to be roughly clustered in a similar range of values for both pathways.

In terms of efficacy, with a few exceptions, all screened compounds turned out to be full agonists, exceeding the maximal efficacy (E_{max}) of HM (100%). The efficacy of the compounds in both assays can be compared using Figure 5.1 (B). According to our assay, valerylfentanyl, crotonylfentanyl, 4-methoxybutyrfentanyl and furanylfentanyl were found to be partial agonists, compared to HM, at both β-arrestin 2 and mini-G pathways with observed E_{max} values of 82.21 % for furanylfentanyl and lower values for the other three compounds. Interestingly, compared to HM, U-49900 was observed to be a partial agonist for mini-G_i (E_{max} value of 72.67 %) but a full agonist for β-arrestin 2 (E_{max} value of 127.9 %). The most efficacious substance observed at both pathways was alfentanil, showing an E_{max} of 300.2 % in the mini-G_i and 190.9 % in the β-arrestin 2 assay in comparison to HM. In the mini-G_i assay, cyclopropylfentanyl, fentanyl and acrylfentanyl also showed high efficacy, with E_{max} values of 280.2 %, 260.9 % and 257.3 % respectively. The other highly efficacious compounds in the β-arrestin-2 assay were acrylfentanyl, cyclopropylfentanyl and 4-fluoro-isobutyrylfentanyl, with E_{max} values of 176.6 %, 157.7 % and 159.0 % respectively. The two compounds that showed the least activity in both pathways were valerylfentanyl hydrochloride (28.65 % in the mini-G_i and 43.72 % in the β-arrestin 2 assay) and crotonylfentanyl (49.06 % in the mini-G_i and 52.66 % in the β-arrestin 2 assay).

Benzoylfentanyl and tetramethylcyclopropylfentanyl showed no activity in our assay, hence no valuable concentration-response curves could be generated and thus, calculation of EC_{50} and E_{max} was not possible.

We found that most of the screened opioids appeared to have a greater efficacy for the coupling of mini-G_i to the receptor than the recruitment of β-arrestin 2 (Figure 5.1 (B)). Only valerylfentanyl, crotonylfentanyl, 4-methoxybutyrfentanyl and U-49900 showed a higher efficacy in the β-arrestin 2 assay, but these were amongst the lower end (except U-49900) at both assays when compared to other opioids. Another interesting observation was that the compounds showed a diversity in their E_{max} values at the mini-G platform as compared to a more clustered distribution at the β-arrestin 2 assay. Finally, it's important to highlight that the most potent

substances were not necessarily the most efficacious. When comparing A and B of Figure 5.1, it could be noticed that alfentanil, which was very efficacious at both mini-G_i and β-arrestin 2 pathways, was one of the least potent substances screened. On the other hand, furanylfentanyl showed high potency at mini-G, but was found to be only weakly efficacious, compared to HM, at both signaling pathways.

5.1.2. Structure-activity relationship regarding both pathways

Upon correlation of the efficacy and potency with the synthetic opioid structures, we discovered some potentially interesting trends which could be the first step towards the establishment of a more in-depth structure-activity-relationship (SAR) with regard to β-arrestin 2 recruitment or G protein receptor coupling.

In general, only a limited amount of studies have reported a structure-activity relationship for fentanyls using molecular docking techniques. Before we discuss our findings, some interesting key elements will be outlined. Although fentanyls share some structural similarities with opioids such as morphine, e.g. an aromatic ring and protonated nitrogen atom, it is assumed that different mechanisms are involved in μ opioid receptor activation (149). Furthermore, several studies were able to characterize the fentanyl receptor binding pocket more thoroughly. For instance, it was revealed that mainly TM6, TM7 and the third extracellular loop of the receptor play a key role in fentanyl binding (150). Additionally, by means of site-directed mutagenesis, the negatively charged Asp147 (aspartic acid)residue at TM3 was pinpointed to be the primary binding site, since it serves as a counter ion for the protonated nitrogen, as found in many opioids (151). It is assumed that the unsubstituted phenylethyl group (see Figure 5.2) is crucial for receptor binding, since substitution on that location seemed to hamper receptor binding, resulting in an impotent compound (149). This group is assumed to engage a strong donor-acceptor interaction with the imidazole group of the His297 (histidine) residue at TM6. Substituents that alter the polarity or electron distribution of the phenylethyl group may therefore have a considerable damaging effect on the activity of a fentanyl analogue. Concerning the N-phenylpropanamide group (see Figure 5.2), it has been suggested that the ethyl group of propanamide is involved in non-polar (van der Waals) interactions with Trp318 (tryptophan) and situates in proximity to the rather polar Asn230 (asparagine) on TM5. Mutation of this amino acid to a more hydrophobic threonine or leucine increased the potency of fentanyl, which further strengthens the theory of hydrophobic interactions at this site (152). Finally, this study reports that all the other studied fentanyl analogues adopted similar alignments in the receptor binding pocket but emphasizes that multiple possible orientations within the binding pocket have been observed (149), which severely complicates SAR determination.

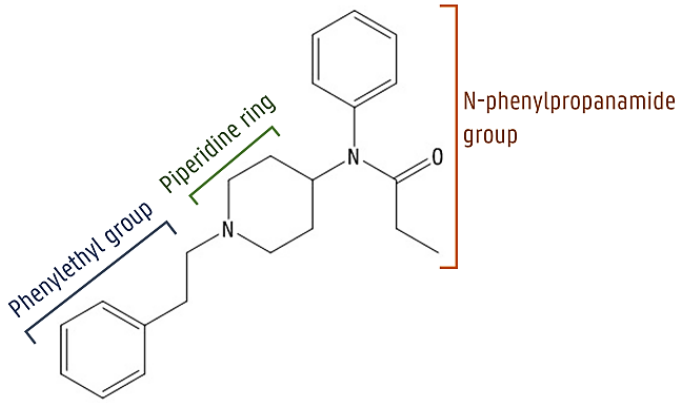

Figure 5.2: Structural elements of fentanyl.
Structure made with the ChemDraw 16 software.

It's important to note that the above-mentioned statements only describe general receptor binding. In the study reported here, we went more into detail about how different functional groups may contribute to different potencies/efficacies towards the β-arrestin 2 or G protein pathway.

Methoxyacetylfentanyl and acetylfentanyl showed similar efficacy at both signaling pathways, implying that the addition of a methoxy group did not result in a significant change in efficacy.

The ring structure at the R-group (see Figure 5.3) displayed a unique trend: as ring size increased from cyclopropylfentanyl (C3) to cyclopentylfentantyl (C5) to benzoylfentanyl (C6), potency and efficacy drastically decreased in both pathways, with benzoylfentanyl showing no activity. This finding suggests that steric hindrance, introduced by a ring structure at this location, could in some way affect the binding at the ligand binding pocket of MOR or the active conformation of the receptor. Insertion of a more flexible linker between the ring and the fentanyl structure, such as in the case of phenylpropionylfentanyl, results in a less rigid structure and was found to improve both potency ($\log EC_{50}$) and efficacy (E_{max}), in comparison to benzoylfentanyl. A similar trend can also be somewhat observed with open-chain aliphatic R-groups, with fentanyl being more efficacious than butyrylfentanyl, which was in turn more efficacious than valerylfentanyl. Similarly, extension of the R-group of acrylfentanyl with one methyl group yields crotonylfentanyl, resulting in lower potency values.

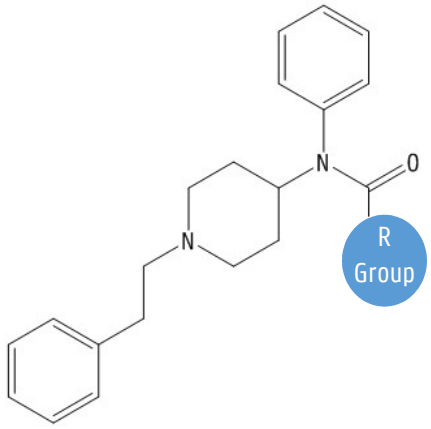

Figure 5.3. General structure of fentanyl analogues
Structure made with the ChemDraw 16 software.

Although being more flexible structures, fentanyls with longer aliphatic side chains were found to be less efficacious in our assay. In fact, crotonylfentanyl and valerylfentanyl, both containing an open-chained aliphatic functional group (R-group), were found to be partial agonists for the recruitment of β-arrestin 2 and coupling of the G protein to the receptor, compared to HM. Likewise, 4-methoxybutyrfentanyl, which also contains an aliphatic R-group but carries an additional substituent on the aromatic benzene ring of the N-phenylpropanamide group, also turned out to be a partial agonist. This finding suggests that a longer chain attached to the carbonyl group can have a negative impact on the functional effect mediated through the receptor. On the other hand, acetylfentanyl, the fentanyl analogue with the shortest R-group, was not found to be more efficacious than fentanyl, which may suggest that there could be additional factors in addition to chain length that may affect receptor activation.

5.2. LIGAND BIAS AT MOR

5.2.1. Calculated bias and potential association with structure-activity-relationship

Signaling bias has been studied quite extensively for MOR. However, we report for the first time an assessment of bias which focusses on synthetic opioids, including fentanyl and analogues. As mentioned before, hydromorphone was used as a reference compound, since it previously showed an almost identical potency ($logEC_{50}$ values) in both of our activity-based assays. Bias was calculated as described in Materials and Methods and a visual representation of the obtained values is provided in Figure 5.4. Values above the zero line reflect a preferential coupling to the G protein, whereas values below zero indicate a preference for β-arrestin 2 recruitment. A complete list of the calculated bias factors can be found in Appendix X. At first glance, no striking results could be observed, which was confirmed after applying the Kruskal-Wallis test, which indicated that none of the tested compounds showed a significant difference between G protein or β-arrestin 2 recruitment, when compared to hydromorphone. Although some assumptions about a "tendency towards either signaling pathway" could be made for some compounds, this should be done with caution, given the overall limited effects. Doing a similar analysis for a series of synthetic cannabinoids (PhD thesis Elise Wouters, unpublished) did result in more pronounced differences, indicating that the lack of observed clear bias is not intrinsic to the bio-assays used here.

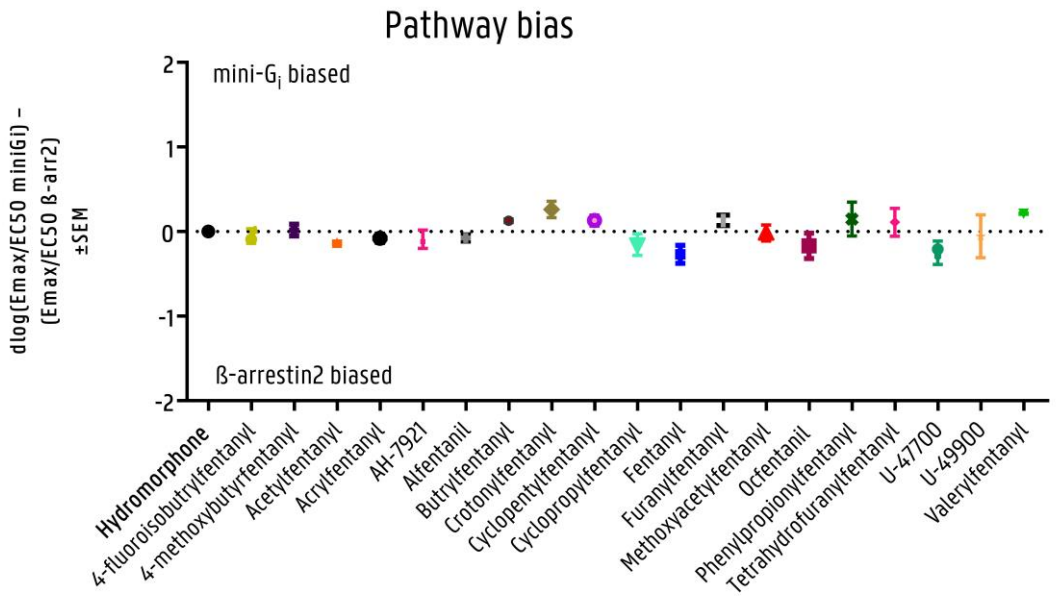

Figure 5.4 : Representation of the calculated pathway bias. Opioids with y-values above zero show a tendency towards G protein-coupling, values below zero indicate a tendency towards β-arrestin 2 recruitment. Error bars represent SEM (n=3). No compound showed a significant bias, when compared to the reference hydromorphone.

x-axis, listing of the tested compounds; y-axis, $\Delta\log(E_{max}/EC_{50})_{miniG}$-$\Delta\log(E_{max}/EC_{50})_{\beta\text{-}arr2}$ ± SEM (a measure of bias). Abbreviations: SEM, standard error of the mean.

Although we looked forward to formulating a somewhat unambiguous conclusion on biased behaviour in a set of novel synthetic opioids, we did not observe a definite bias in any of the procured compounds. We were thus unable to link their structural characteristics to a biased behaviour and could therefore not establish a set of widely applicable valid statements. A remarkable finding on our part is the fact that crotonylfentanyl showed a slight tendency towards the G protein assay, whereas acrylfentanyl was found to be unbiased, with a very subtle indication of a tendency towards β-arrestin 2 recruitment. Although none of these results were statistically significant, this is rather particular, especially when comparing their structure. As can be seen in Figure 5.5, the structures are identical except for one additional methyl group. Hence, it is somewhat surprising that they do not align better in terms of signaling through MOR. As mentioned before, although analogues of fentanyl take on similar conformations within the receptor, several different conformations are possible for each compound (149). It may be possible that each compound prefers a slightly different conformation in the receptor, which is in some way associated with a (slightly) different recruitment of signal transducers. Unfortunately, we are currently still lacking substantial knowledge on which orientation is preferably adopted by which compound and which variables (e.g. stereochemistry of the ligands, localisation of the receptor in microdomains) influence this phenomenon.

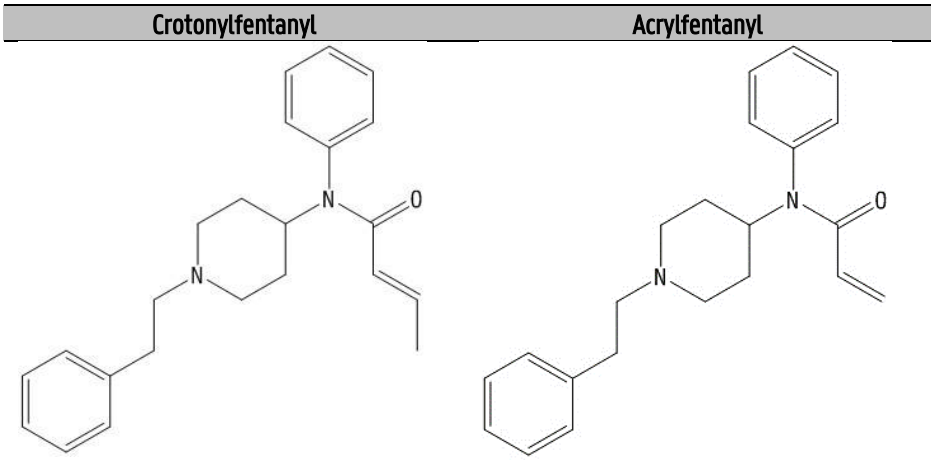

Figure 5.5 : Comparison of the structure of crotonylfentanyl (left) and acrylfentanyl hydrochloride (right). The only difference between both structures is the additional methyl group at the R group of crotonylfentanyl. Structures made with the ChemDraw 16 software.

5.2.2. Added-value of bias in the therapeutic field

As described earlier, the concept of signaling bias has gained significance over the past few years and has been studied for multiple GPCRs such as the angiotensin II receptor 1, the D_2 dopamine receptor, the β-adrenergic receptors (153) and the μ opioid receptor. In the case of MOR, several attempts have been made to develop biased ligands, which only stimulate a subset of the signaling pathways associated with the receptor. Some studies suggest that the β-arrestin pathway more likely leads to adverse effects, whereas tendency towards G protein signaling has been associated with a broader therapeutic window (63, 107). This mindset sparked the development G protein-biased agonists such as oliceridine (TRV130) and PZM21 (154), of which TRV130 has completed all three clinical trial phases (155). In mice, both ligands induced potent analgesia and appeared to cause less respiratory depression and constipation (153, 156, 157). However, more research is still required concerning the properties of these compounds and it is still unclear whether their benefit-risk ratio is in fact beneficial in humans (158-161).

Furthermore, it's important to keep in mind that these compounds (TRV130 and PZM21) were developed using either recombinant cell-based assays or *in silico* modelling and docking, although it has never been reported to which extent biased behaviour can be extrapolated to real living neurons (162). A recently published paper tackled this issue by designing a version of MOR of which the receptor trafficking could be easily visualized using fluorescence. Two systems were then set up: one involved extracted neurons from mice which expressed the altered MOR instead of the native receptor, the other involved HEK 293T cells which were also transfected with the altered MOR. The extent of ligand-dependent trafficking, which was considered to be characteristic of biased signaling, was monitored for a set of opioid agonists, including TRV130 and PZM21. Surprisingly, the degree of

receptor redistribution was strongly correlated in both assays, demonstrating that we may certainly translate recombinant cell responses to living neurons. This opens doors to future drug development in general (162).

Finally, although a promising correlation between recombinant cell-based assays and extracted neurons may be found, researchers still don't know which degree of bias is required to elicit a significant physiological response that differs from unbiased opioids (116). Schwienteck *et al.* theorized about the need for compounds that are even more G protein *vs.* β-arrestin biased, in order to attain the much sought-after "ideal opioid drug". Unfortunately, the currently achievable "bias" towards G protein in new compounds is probably insufficient that it remains to be seen whether a clinically relevant difference in pharmacology with the commonly used opioids can actually be expected (163).

5.3. FUTURE PERSPECTIVES

Although we did not find evidence for a significantly biased behaviour in our panel of synthetic opioids, there are still unanswered questions as to why different compounds, despite their sometimes striking structural similarity, showed disparities in potency and efficacy. Our results imply that the additional presence of structural elements as small as a single methyl group can have a great impact on a compound's pharmacological parameters. Since very few studies have been conducted on the receptor-ligand interaction of fentanyls (149), more binding experiments may contribute to a better fundamental understanding of how different synthetic opioids occupy MOR and how different functional groups contribute to signaling through G protein or β-arrestin dependent pathways. In addition, in the framework of drug development, more research is required on the extent of bias needed before a significant difference in physiologic effect is noticeable.

Moreover, although it has now been reported that the knowledge gained by means of recombinant cell-based assays is applicable to neuronal cells, the next great challenge will be to examine how these findings can be translated to whole organisms (162). Therefore, monitoring *in vivo* drug signaling in whole animals will gain importance and new emerging imaging techniques, such as *in vivo* calcium imaging using miniature microscopes (164), will become more widely applied (162).

6. CONCLUSIONS

The MOR reporter assay had already proven to be a promising, valuable tool for the screening for opioid substances in biological matrices, even allowing the detection of sub nanogram agonist concentrations without the need for highly advanced equipment (118). Since detection is based on activity of the substances rather than their structure, the assay is able to keep ahead of the currently applied screening techniques requiring prior knowledge on the identity of the analytes, which is the case for targeted approaches such as immunoassays and LC-MS(MS). One encountered weakness was that opioid antagonists hinder MOR activation and therefore generation of the luminescence signal evoked by agonists present in biological extracts. A new assay protocol which circumvents this issue was thought out and tested blind-coded by applying it to 94 blood samples containing both opioid and non-opioid substances, provided by NMS Labs (Horsham, PA, USA). We also applied the original method to the same samples in order to compare sensitivity and specificity of both screening assays. Based on the luminescence read-out, samples were ultimately scored as either "follow-up required" (samples containing opioid agonist or antagonist or both) or "no follow-up required" (no trace of opioid-related substances) and results were later compared to their actual contents, as confirmed by LC-MS and GC-MS analysis.

Out of 94 original blood samples, 71/72 samples were correctly scored as "follow-up required", which results in a sensitivity of 98.61 %. The assay failed to pick up one sample, which allegedly contained 11 ng/mL hydrocodone. Regarding specificity, 21/22 samples were correctly scored "negative", yielding a specificity of 95.45 %. Data profiles of one sample suggested the presence of an opioid antagonist, however this was not analytically confirmed. Remarkably, when implementing the original protocol without HM injection, a sensitivity of only 55.56 % was obtained, meaning that the improved method ensures a significant reduction in the amount of "false negatives". It is thereby demonstrated that the development and application of an assay which accounts for opioid antagonist presence by injecting a small amount of agonist can serve as the missing crucial piece of an important puzzle, since it not only results in a higher sensitivity but also often provides additional clues about a sample's content. Moreover, the plots generated during the experiments allowed the establishment of an easy visual model (Figure 6.1) which can be used during data analysis and scoring to identify the contents of the biological samples. This model gives an overview of the profiles which can be expected when performing the improved assay and also shows how to interpret them.

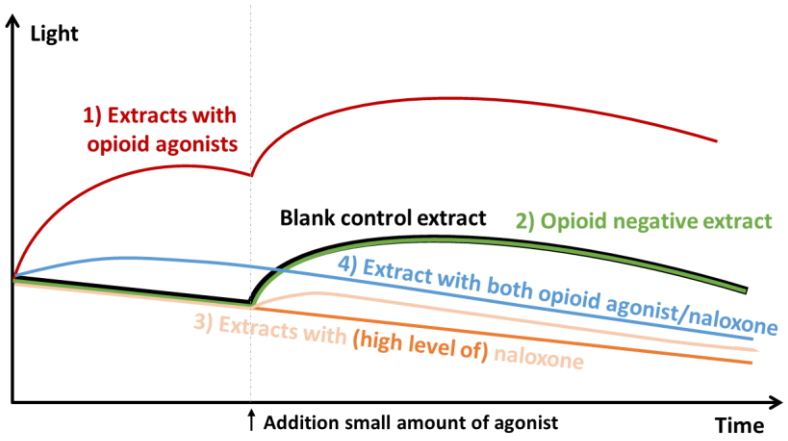

Figure 6.1: Model for scoring screened samples. The aim is to not only screen samples as "positive" or "negative" but to also assign a description which roughly predicts the contents of the sample.

Secondly, we used activity-based assays to test a panel of 21 synthetic opioids (including a large amount of fentanyl analogues) in order to assess if any of these substances displays biased behaviour at the μ opioid receptor. By means of the experiments performed in this dissertation, none of the tested compounds was found to be significantly biased towards one or another pathway. Although we were not able to find convincing evidence on the biased nature of the 21 screened compounds, the obtained data on their potency ($logEC_{50}$) and efficacy (E_{max}) allowed us to determine some correlations between some of their structural features and their potency/efficacy, as well as to make assumptions related to some structure-activity related trends.

Since this thesis describes the successful application of MOR bio-assays for two quite distinct purposes, it should be clear that the performed activity-based assays are appealing yet versatile tools in research. They allow us to gain fundamental insight into biochemical and pharmacological processes, as they support the monitoring of protein-protein interactions such as the mechanisms of receptor activation. In addition, although not routinely applied yet, their promising qualities such as high sensitivity suggest that they may earn their place in the clinical and forensic field in the future.

7. REFERENCES

1. Feng LY, Battulga A, Han E, Chung H, Li JH. New psychoactive substances of natural origin: A brief review. Journal of food and drug analysis. 2017;25(3):461-71.
2. Soussan C, Kjellgren A. The users of Novel Psychoactive Substances: Online survey about their characteristics, attitudes and motivations. The International journal on drug policy. 2016;32:77-84.
3. Lovrecic B, Lovrecic M, Gabrovec B, Carli M, Pacini M, Maremmani AGI, et al. Non-Medical Use of Novel Synthetic Opioids: A New Challenge to Public Health. International journal of environmental research and public health. 2019;16(2).
4. United Nations on Drugs and Crime. Early Warning Advisory on New Psychoactive Substances (March 13, 2019). Available from: https://www.unodc.org/LSS/Page/NPS.
5. Graddy R, Buresh ME, Rastegar DA. New and Emerging Illicit Psychoactive Substances. The Medical clinics of North America. 2018;102(4):697-714.
6. United Nations on Drugs and Crime. Current NPS Threats Volume I March 2019. 2019.
7. Taffe MA, Olive MF. Designer drugs - A continuing chemical (R)evolution. Neuropharmacology. 2018;134(Pt A):1-3.
8. Evans-Brown M, Sedefov R. Responding to New Psychoactive Substances in the European Union: Early Warning, Risk Assessment, and Control Measures. Handbook of experimental pharmacology. 2018;252:3-49.
9. Armenian P, Vo KT, Barr-Walker J, Lynch KL. Fentanyl, fentanyl analogs and novel synthetic opioids: A comprehensive review. Neuropharmacology. 2018;134(Pt A):121-32.
10. Suzuki J, El-Haddad S. A review: Fentanyl and non-pharmaceutical fentanyls. Drug and alcohol dependence. 2017;171:107-16.
11. Madras BK. The Growing Problem of New Psychoactive Substances (NPS). Current topics in behavioral neurosciences. 2017;32:1-18.
12. Van Amsterdam J, Nutt D, Van den Brink W. Generic legislation of new psychoactive drugs. Journal of Psychopharmacology. 2013;27(3):317-24.
13. Belgisch Staatsblad. Koninklijk Besluit houdende regeling van verdovende middelen, psychotrope stoffen (Federale overheidsdienst Volksgezondheid, Veiligheid van de voedselketen en leefmilieu)2017.
14. Commission on Narcotic Drugs. New psychoactive substances: overview of trends, challenges and legal approaches. 2016.
15. UK Parliament. Psychoactive Substances Act 2016. 2016. p. 1-57.
16. Food and Drug Administration Safety and Innovation Act (FDASIA): Synthetic Drug Abuse Prevention Act of 2012. Sect. 1151-1153 (2012).
17. Cannaert A, Storme J, Franz F, Auwarter V, Stove CP. Detection and Activity Profiling of Synthetic Cannabinoids and Their Metabolites with a Newly Developed Bioassay. Analytical chemistry. 2016;88(23):11476-85.
18. Ledberg A. The interest in eight new psychoactive substances before and after scheduling. Drug and alcohol dependence. 2015;152:73-8.
19. Wadsworth E, Drummond C, Kimergard A, Deluca P. A market on both "sides" of the law: The use of the hidden web for the sale of new psychoactive substances. Human psychopharmacology. 2017;32(3).
20. Fentanils and synthetic cannabinoids: driving greater complexity into the drug situation. An update from the EU Early Warning System (June 2018). Publications Office of the European Union, Luxembourg: European Monitoring Centre for Drugs and Drug Addiciton; 2018.
21. Ling W, Wesson DR. Drugs of abuse--opiates. The Western journal of medicine. 1990;152(5):565-72.
22. Lee P. Opium Culture: The Art and Ritual of the Chinese Tradition: Inner Traditions / Bear & Co; 2006. 232 p.
23. Brook K, Bennett J, Desai SP. The Chemical History of Morphine: An 8000-year Journey, from Resin to de-novo Synthesis. Journal of anesthesia history. 2017;3(2):50-5.
24. Dewick PM. Medicinal Natural Products: A Biosynthetic Approach, 3rd Edition: John Wiley & Sons, Ltd; 2009.
25. Krishnamurti C, Rao SC. The isolation of morphine by Serturner. Indian journal of anaesthesia. 2016;60(11):861-2.
26. Klepstad P, Kaasa S, Cherny N, Hanks G, de Conno F, Research Steering Committee of the E. Pain and pain treatments in European palliative care units. A cross sectional survey from the European Association for Palliative Care Research Network. Palliative medicine. 2005;19(6):477-84.
27. National Institute on Drug Abuse. Overdose Death Rates 2019 [Available from: https://www.drugabuse.gov/related-topics/trends-statistics/overdose-death-rates.
28. Mounteney J, Giraudon I, Denissov G, Griffiths P. Fentanyls: Are we missing the signs? Highly potent and on the rise in Europe. The International journal on drug policy. 2015;26(7):626-31.
29. Stanley TH. The history and development of the fentanyl series. Journal of pain and symptom management. 1992;7(3 Suppl):S3-7.
30. Ujvaŕy I, Jorge R, Christie R, Le Ruez T, Danielsson HV, Kronstrand R, et al. Acryloylfentanyl, a recently emerged new psychoactive substance:
a comprehensive review. Forensic Toxicology. 2017;35:232-43.
31. Zawilska JB. An Expanding World of Novel Psychoactive Substances: Opioids. Frontiers in psychiatry. 2017;8:110.

32. Prekupec MP, Mansky PA, Baumann MH. Misuse of Novel Synthetic Opioids: A Deadly New Trend. Journal of addiction medicine. 2017;11(4):256-65.
33. Wang S. Historical Review: Opiate Addiction and Opioid Receptors. Cell transplantation. 2018:963689718811060.
34. Frisoni P, Bacchio E, Bilel S, Talarico A, Gaudio RM, Barbieri M, et al. Novel Synthetic Opioids: The Pathologist's Point of View. Brain sciences. 2018;8(9).
35. Pattinson KT. Opioids and the control of respiration. British journal of anaesthesia. 2008;100(6):747-58.
36. Al-Hasani R, Bruchas MR. Molecular mechanisms of opioid receptor-dependent signaling and behavior. Anesthesiology. 2011;115(6):1363-81.
37. Jones CM, Einstein EB, Compton WM. Changes in Synthetic Opioid Involvement in Drug Overdose Deaths in the United States, 2010-2016. JAMA. 2018;319(17):1819-21.
38. Butler DC, Shanks K, Behonick GS, Smith D, Presnell SE, Tormos LM. Three Cases of Fatal Acrylfentanyl Toxicity in the United States and a Review of Literature. Journal of analytical toxicology. 2018;42(1):e6-e11.
39. Comer SD, Cahill CM. Fentanyl: Receptor pharmacology, abuse potential, and implications for treatment. Neuroscience and biobehavioral reviews. 2018.
40. Pichini S, Solimini R, Berretta P, Pacifici R, Busardo FP. Acute Intoxications and Fatalities From Illicit Fentanyl and Analogues: An Update. Therapeutic drug monitoring. 2018;40(1):38-51.
41. Van Hout MC, Bingham T. 'Silk Road', the virtual drug marketplace: a single case study of user experiences. The International journal on drug policy. 2013;24(5):385-91.
42. Wadsworth E, Drummond C, Deluca P. The Dynamic Environment of Crypto Markets: The Lifespan of New Psychoactive Substances (NPS) and Vendors Selling NPS. Brain sciences. 2018;8(3).
43. Sharma KK, Hales TG, Rao VJ, NicDaeid N, McKenzie C. The search for the "next" euphoric non-fentanil novel synthetic opioids on the illicit drugs market: current status and horizon scanning. Forensic toxicology. 2019;37(1):1-16.
44. Minami M, Satoh M. Molecular biology of the opioid receptors: structures, functions and distributions. Neuroscience research. 1995;23(2):121-45.
45. Shang Y, Filizola M. Opioid receptors: Structural and mechanistic insights into pharmacology and signaling. Eur J Pharmacol. 2015;763(Pt B):206-13.
46. Stein C. Opioid Receptors. Annual review of medicine. 2016;67:433-51.
47. Pradhan AA, Smith ML, Kieffer BL, Evans CJ. Ligand-directed signalling within the opioid receptor family. Brit J Pharmacol. 2012;167(5):960-9.
48. McDonald J, Lambert DG. Opioid mechanisms and opioid drugs. Pain 2016;17(9):464-8.
49. Defea K. Beta-arrestins and heterotrimeric G-proteins: collaborators and competitors in signal transduction. Brit J Pharmacol. 2008;153 Suppl 1:S298-309.
50. Gurevich VV, Gurevich EV. Molecular Mechanisms of GPCR Signaling: A Structural Perspective. International journal of molecular sciences. 2017;18(12).
51. Tan L, Yan W, McCorvy JD, Cheng J. Biased Ligands of G Protein-Coupled Receptors (GPCRs): Structure-Functional Selectivity Relationships (SFSRs) and Therapeutic Potential. Journal of medicinal chemistry. 2018;61(22):9841-78.
52. Zheng H, Loh HH, Law PY. Agonist-selective signaling of G protein-coupled receptor: mechanisms and implications. IUBMB life. 2010;62(2):112-9.
53. Wang W, Qiao Y, Li Z. New Insights into Modes of GPCR Activation. Trends in pharmacological sciences. 2018;39(4):367-86.
54. Ferguson SS, Barak LS, Zhang J, Caron MG. G-protein-coupled receptor regulation: role of G-protein-coupled receptor kinases and arrestins. Canadian journal of physiology and pharmacology. 1996;74(10):1095-110.
55. Mahoney JP, Sunahara RK. Mechanistic insights into GPCR-G protein interactions. Current opinion in structural biology. 2016;41:247-54.
56. Wootten D, Christopoulos A, Marti-Solano M, Babu MM, Sexton PM. Mechanisms of signalling and biased agonism in G protein-coupled receptors. Nature reviews Molecular cell biology. 2018;19(10):638-53.
57. Kahanovitch U, Tsemakhovich V, Berlin S, Rubinstein M, Styr B, Castel R, et al. Recruitment of Gbetagamma controls the basal activity of G-protein coupled inwardly rectifying potassium (GIRK) channels: crucial role of distal C terminus of GIRK1. The Journal of physiology. 2014;592(24):5373-90.
58. Lei Q, Jones MB, Talley EM, Garrison JC, Bayliss DA. Molecular mechanisms mediating inhibition of G protein-coupled inwardly-rectifying K+ channels. Molecules and cells. 2003;15(1):1-9.
59. Dascal N, Kahanovitch U. The Roles of Gbetagamma and Galpha in Gating and Regulation of GIRK Channels. Int Rev Neurobiol. 2015;123:27-85.
60. Berlin S, Keren-Raifman T, Castel R, Rubinstein M, Dessauer CW, Ivanina T, et al. G alpha(i) and G betagamma jointly regulate the conformations of a G betagamma effector, the neuronal G protein-activated K+ channel (GIRK). The Journal of biological chemistry. 2010;285(9):6179-85.
61. Zhou XE, He Y, de Waal PW, Gao X, Kang Y, Van Eps N, et al. Identification of Phosphorylation Codes for Arrestin Recruitment by G Protein-Coupled Receptors. Cell. 2017;170(3):457-69 e13.

62. Violin JD, Lefkowitz RJ. Beta-arrestin-biased ligands at seven-transmembrane receptors. Trends in pharmacological sciences. 2007;28(8):416-22.
63. Bohn LM, Lefkowitz RJ, Gainetdinov RR, Peppel K, Caron MG, Lin FT. Enhanced morphine analgesia in mice lacking beta-arrestin 2. Science (New York, NY). 1999;286(5449):2495-8.
64. Zuo Z. The role of opioid receptor internalization and beta-arrestins in the development of opioid tolerance. Anesthesia and analgesia. 2005;101(3):728-34, table of contents.
65. Luttrell LM, Lefkowitz RJ. The role of beta-arrestins in the termination and transduction of G-protein-coupled receptor signals. Journal of cell science. 2002;115(Pt 3):455-65.
66. Zhang J, Ferguson SS, Law PY, Barak LS, Caron MG. Agonist-specific regulation of delta-opioid receptor trafficking by G protein-coupled receptor kinase and beta-arrestin. Journal of receptor and signal transduction research. 1999;19(1-4):301-13.
67. Luttrell LM, Hawes BE, van Biesen T, Luttrell DK, Lansing TJ, Lefkowitz RJ. Role of c-Src tyrosine kinase in G protein-coupled receptor- and Gbetagamma subunit-mediated activation of mitogen-activated protein kinases. The Journal of biological chemistry. 1996;271(32):19443-50.
68. Pearson G, Robinson F, Beers Gibson T, Xu BE, Karandikar M, Berman K, et al. Mitogen-activated protein (MAP) kinase pathways: regulation and physiological functions. Endocrine reviews. 2001;22(2):153-83.
69. Burack WR, Shaw AS. Signal transduction: hanging on a scaffold. Current opinion in cell biology. 2000;12(2):211-6.
70. Minden A, Karin M. Regulation and function of the JNK subgroup of MAP kinases. Biochimica et biophysica acta. 1997;1333(2):F85-104.
71. Ji RR, Kawasaki Y, Zhuang ZY, Wen YR, Zhang YQ. Protein kinases as potential targets for the treatment of pathological pain. Handbook of experimental pharmacology. 2007(177):359-89.
72. Tan M, Walwyn WM, Evans CJ, Xie CW. p38 MAPK and beta-arrestin 2 mediate functional interactions between endogenous micro-opioid and alpha2A-adrenergic receptors in neurons. The Journal of biological chemistry. 2009;284(10):6270-81.
73. Kelly E. Ligand bias at the mu-opioid receptor. Biochemical Society transactions. 2013;41(1):218-24.
74. Kenakin T, Miller LJ. Seven transmembrane receptors as shapeshifting proteins: the impact of allosteric modulation and functional selectivity on new drug discovery. Pharmacological reviews. 2010;62(2):265-304.
75. Kenakin T, Christopoulos A. Signalling bias in new drug discovery: detection, quantification and therapeutic impact. Nature reviews Drug discovery. 2013;12(3):205-16.
76. Thompson GL, Kelly E, Christopoulos A, Canals M. Novel GPCR paradigms at the mu-opioid receptor. Brit J Pharmacol. 2015;172(2):287-96.
77. Whalen EJ, Rajagopal S, Lefkowitz RJ. Therapeutic potential of beta-arrestin- and G protein-biased agonists. Trends in molecular medicine. 2011;17(3):126-39.
78. Liu JJ, Horst R, Katritch V, Stevens RC, Wuthrich K. Biased signaling pathways in beta2-adrenergic receptor characterized by 19F-NMR. Science (New York, NY). 2012;335(6072):1106-10.
79. Smith JS, Lefkowitz RJ, Rajagopal S. Biased signalling: from simple switches to allosteric microprocessors. Nature reviews Drug discovery. 2018;17(4):243-60.
80. Busillo JM, Armando S, Sengupta R, Meucci O, Bouvier M, Benovic JL. Site-specific phosphorylation of CXCR4 is dynamically regulated by multiple kinases and results in differential modulation of CXCR4 signaling. The Journal of biological chemistry. 2010;285(10):7805-17.
81. Kim J, Ahn S, Ren XR, Whalen EJ, Reiter E, Wei H, et al. Functional antagonism of different G protein-coupled receptor kinases for beta-arrestin-mediated angiotensin II receptor signaling. Proceedings of the National Academy of Sciences of the United States of America. 2005;102(5):1442-7.
82. Zidar DA, Violin JD, Whalen EJ, Lefkowitz RJ. Selective engagement of G protein coupled receptor kinases (GRKs) encodes distinct functions of biased ligands. Proceedings of the National Academy of Sciences of the United States of America. 2009;106(24):9649-54.
83. Cahill TJ, 3rd, Thomsen AR, Tarrasch JT, Plouffe B, Nguyen AH, Yang F, et al. Distinct conformations of GPCR-beta-arrestin complexes mediate desensitization, signaling, and endocytosis. Proceedings of the National Academy of Sciences of the United States of America. 2017;114(10):2562-7.
84. Butcher AJ, Prihandoko R, Kong KC, McWilliams P, Edwards JM, Bottrill A, et al. Differential G-protein-coupled receptor phosphorylation provides evidence for a signaling bar code. The Journal of biological chemistry. 2011;286(13):11506-18.
85. Nobles KN, Xiao K, Ahn S, Shukla AK, Lam CM, Rajagopal S, et al. Distinct phosphorylation sites on the beta(2)-adrenergic receptor establish a barcode that encodes differential functions of beta-arrestin. Science signaling. 2011;4(185):ra51.
86. Shiraishi Y, Natsume M, Kofuku Y, Imai S, Nakata K, Mizukoshi T, et al. Phosphorylation-induced conformation of beta2-adrenoceptor related to arrestin recruitment revealed by NMR. Nature communications. 2018;9(1):194.
87. Parton RG, del Pozo MA. Caveolae as plasma membrane sensors, protectors and organizers. Nature reviews Molecular cell biology. 2013;14(2):98-112.
88. Halls ML, Yeatman HR, Nowell CJ, Thompson GL, Gondin AB, Civciristov S, et al. Plasma membrane localization of the mu-opioid receptor controls spatiotemporal signaling. Science signaling. 2016;9(414):ra16.

89. Stoeber M, Jullie D, Lobingier BT, Laeremans T, Steyaert J, Schiller PW, et al. A Genetically Encoded Biosensor Reveals Location Bias of Opioid Drug Action. Neuron. 2018;98(5):963-76 e5.
90. Bahouth SW, Nooh MM. Barcoding of GPCR trafficking and signaling through the various trafficking roadmaps by compartmentalized signaling networks. Cellular signalling. 2017;36:42-55.
91. Wang G, Wei Z, Wu G. Role of Rab GTPases in the export trafficking of G protein-coupled receptors. Small GTPases. 2018;9(1-2):130-5.
92. Irannejad R, Tsvetanova NG, Lobingier BT, von Zastrow M. Effects of endocytosis on receptor-mediated signaling. Current opinion in cell biology. 2015;35:137-43.
93. Wu G. Trafficking of GPCRs, 1st Edition: Academic Press; 2015. 328 p.
94. Shukla A. G Protein-Coupled Receptors, 1st Edition: Academic Press; 2016. 502 p.
95. Hay DL, Pioszak AA. Receptor Activity-Modifying Proteins (RAMPs): New Insights and Roles. Annu Rev Pharmacol Toxicol. 2016;56:469-87.
96. Navarro G, Cordomi A, Casado-Anguera V, Moreno E, Cai NS, Cortes A, et al. Evidence for functional pre-coupled complexes of receptor heteromers and adenylyl cyclase. Nature communications. 2018;9(1):1242.
97. Frangaj A, Fan QR. Structural biology of GABAB receptor. Neuropharmacology. 2018;136(Pt A):68-79.
98. Siljee JE, Wang Y, Bernard AA, Ersoy BA, Zhang S, Marley A, et al. Subcellular localization of MC4R with ADCY3 at neuronal primary cilia underlies a common pathway for genetic predisposition to obesity. Nature genetics. 2018;50(2):180-5.
99. Guinzberg R, Diaz-Cruz A, Acosta-Trujillo C, Vilchis-Landeros MM, Vazquez-Meza H, Lozano-Flores C, et al. Newly synthesized cAMP is integrated at a membrane protein complex signalosome to ensure receptor response specificity. The FEBS journal. 2017;284(2):258-76.
100. Nikolaev VO, Moshkov A, Lyon AR, Miragoli M, Novak P, Paur H, et al. Beta2-adrenergic receptor redistribution in heart failure changes cAMP compartmentation. Science. 2010;327(5973):1653-7.
101. Lyon AR, Nikolaev VO, Miragoli M, Sikkel MB, Paur H, Benard L, et al. Plasticity of surface structures and beta(2)-adrenergic receptor localization in failing ventricular cardiomyocytes during recovery from heart failure. Circulation Heart failure. 2012;5(3):357-65.
102. Jensen DD, Halls ML, Murphy JE, Canals M, Cattaruzza F, Poole DP, et al. Endothelin-converting enzyme 1 and beta-arrestins exert spatiotemporal control of substance P-induced inflammatory signals. The Journal of biological chemistry. 2014;289(29):20283-94.
103. Ayling LJ, Briddon SJ, Halls ML, Hammond GR, Vaca L, Pacheco J, et al. Adenylyl cyclase AC8 directly controls its micro-environment by recruiting the actin cytoskeleton in a cholesterol-rich milieu. Journal of cell science. 2012;125(Pt 4):869-86.
104. Halls ML, Cooper DM. Sub-picomolar relaxin signalling by a pre-assembled RXFP1, AKAP79, AC2, beta-arrestin 2, PDE4D3 complex. EMBO J. 2010;29(16):2772-87.
105. Emery MA, Eitan S. Members of the same pharmacological family are not alike: Different opioids, different consequences, hope for the opioid crisis? Prog Neuropsychopharmacol Biol Psychiatry. 2019;92:428-49.
106. Winpenny D, Clark M, Cawkill D. Biased ligand quantification in drug discovery: from theory to high throughput screening to identify new biased mu opioid receptor agonists. Brit J Pharmacol. 2016;173(8):1393-403.
107. Schmid CL, Kennedy NM, Ross NC, Lovell KM, Yue Z, Morgenweck J, et al. Bias Factor and Therapeutic Window Correlate to Predict Safer Opioid Analgesics. Cell. 2017;171(5):1165-75 e13.
108. Galandrin S, Onfroy L, Poirot MC, Senard JM, Gales C. Delineating biased ligand efficacy at 7TM receptors from an experimental perspective. The international journal of biochemistry & cell biology. 2016;77(Pt B):251-63.
109. Nagi K, Pineyro G. Practical guide for calculating and representing biased signaling by GPCR ligands: A stepwise approach. Methods (San Diego, Calif). 2016;92:78-86.
110. Raehal KM, Walker JK, Bohn LM. Morphine side effects in beta-arrestin 2 knockout mice. The Journal of pharmacology and experimental therapeutics. 2005;314(3):1195-201.
111. Violin JD, Crombie AL, Soergel DG, Lark MW. Biased ligands at G-protein-coupled receptors: promise and progress. Trends in pharmacological sciences. 2014;35(7):308-16.
112. Bohn LM, Dykstra LA, Lefkowitz RJ, Caron MG, Barak LS. Relative opioid efficacy is determined by the complements of the G protein-coupled receptor desensitization machinery. Molecular pharmacology. 2004;66(1):106-12.
113. Rivero G, Llorente J, McPherson J, Cooke A, Mundell SJ, McArdle CA, et al. Endomorphin-2: a biased agonist at the mu-opioid receptor. Molecular pharmacology. 2012;82(2):178-88.
114. Wilson AM, Soignier RD, Zadina JE, Kastin AJ, Nores WL, Olson RD, et al. Dissociation of analgesic and rewarding effects of endomorphin-1 in rats. Peptides. 2000;21(12):1871-4.
115. Varamini P, Mansfeld FM, Blanchfield JT, Wyse BD, Smith MT, Toth I. Lipo-endomorphin-1 derivatives with systemic activity against neuropathic pain without producing constipation. PloS one. 2012;7(8):e41909.
116. Luttrell LM, Maudsley S, Bohn LM. Fulfilling the Promise of "Biased" G Protein-Coupled Receptor Agonism. Molecular pharmacology. 2015;88(3):579-88.
117. Rankovic Z, Brust TF, Bohn LM. Biased agonism: An emerging paradigm in GPCR drug discovery. Bioorganic & medicinal chemistry letters. 2016;26(2):241-50.

118. Cannaert A, Vasudevan L, Friscia M, Mohr ALA, Wille SMR, Stove CP. Activity-Based Concept to Screen Biological Matrices for Opiates and (Synthetic) Opioids. Clinical chemistry. 2018;64(8):1221-9.
119. Favretto D, Pascali JP, Tagliaro F. New challenges and innovation in forensic toxicology: focus on the "New Psychoactive Substances". Journal of chromatography A. 2013;1287:84-95.
120. Graziano S, Anzillotti L, Mannocchi G, Pichini S, Busardo FP. Screening methods for rapid determination of new psychoactive substances (NPS) in conventional and non-conventional biological matrices. Journal of pharmaceutical and biomedical analysis. 2019;163:170-9.
121. Winborn J, Kerrigan S. Desomorphine Screening Using Commercial Enzyme-Linked Immunosorbent Assays. Journal of analytical toxicology. 2017;41(5):455-60.
122. Guerrieri D, Kjellqvist F, Kronstrand R, Green H. Validation and Cross-Reactivity Data for Fentanyl Analogs With the Immunalysis Fentanyl ELISA. Journal of analytical toxicology. 2019;43(1):18-24.
123. Brandt SD, Kavanagh PV. Addressing the challenges in forensic drug chemistry. Drug testing and analysis. 2017;9(3):342-6.
124. Pasin D, Cawley A, Bidny S, Fu S. Current applications of high-resolution mass spectrometry for the analysis of new psychoactive substances: a critical review. Analytical and bioanalytical chemistry. 2017;409(25):5821-36.
125. Remane D, Wissenbach DK, Peters FT. Recent advances of liquid chromatography-(tandem) mass spectrometry in clinical and forensic toxicology - An update. Clinical biochemistry. 2016;49(13-14):1051-71.
126. Maurer HH, Meyer MR. High-resolution mass spectrometry in toxicology: current status and future perspectives. Archives of toxicology. 2016;90(9):2161-72.
127. Cannaert A, Storme J, Hess C, Auwarter V, Wille SMR, Stove CP. Activity-Based Detection of Cannabinoids in Serum and Plasma Samples. Clinical chemistry. 2018;64(6):918-26.
128. England CG, Ehlerding EB, Cai W. NanoLuc: A Small Luciferase Is Brightening Up the Field of Bioluminescence. Bioconjugate chemistry. 2016;27(5):1175-87.
129. Boyer EW. Management of opioid analgesic overdose. The New England journal of medicine. 2012;367(2):146-55.
130. Lobmaier P, Gossop M, Waal H, Bramness J. The pharmacological treatment of opioid addiction--a clinical perspective. European journal of clinical pharmacology. 2010;66(6):537-45.
131. Handal KA, Schauben JL, Salamone FR. Naloxone. Annals of emergency medicine. 1983;12(7):438-45.
132. FDA News Release: FDA moves quickly to approve easy-to-use nasal spray to treat opioid overdose [press release]. 2015.
133. Merlin MA, Saybolt M, Kapitanyan R, Alter SM, Jeges J, Liu J, et al. Intranasal naloxone delivery is an alternative to intravenous naloxone for opioid overdoses. The American journal of emergency medicine. 2010;28(3):296-303.
134. Wermeling DP. A response to the opioid overdose epidemic: naloxone nasal spray. Drug delivery and translational research. 2013;3(1):63-74.
135. Clarke SF, Dargan PI, Jones AL. Naloxone in opioid poisoning: walking the tightrope. Emergency medicine journal : EMJ. 2005;22(9):612-6.
136. Moss RB, Carlo DJ. Higher doses of naloxone are needed in the synthetic opiod era. Substance abuse treatment, prevention, and policy. 2019;14(1):6.
137. Dixon AS, Schwinn MK, Hall MP, Zimmerman K, Otto P, Lubben TH, et al. NanoLuc Complementation Reporter Optimized for Accurate Measurement of Protein Interactions in Cells. Acs Chem Biol. 2016;11(2):400-8.
138. Promega. NanoBiT® PPI Starter Systems: Protein Interaction Assays that Reflect Natural Cellular Biology 2019 [Available from: https://be.promega.com/products/protein-interactions/live-cell-protein-interactions/nanobit-ppi-starter-systems/?catNum=N2014.
139. Zhang J, Ferguson SS, Barak LS, Bodduluri SR, Laporte SA, Law PY, et al. Role for G protein-coupled receptor kinase in agonist-specific regulation of mu-opioid receptor responsiveness. Proceedings of the National Academy of Sciences of the United States of America. 1998;95(12):7157-62.
140. United Chemical Technologies (UCT). Sample Preparation - Clean Screen DAU 2018 [Available from: https://sampleprep.unitedchem.com/clean-screen-dau.
141. Mohr AL, Friscia M, Papsun D, Kacinko SL, Buzby D, Logan BK. Analysis of Novel Synthetic Opioids U-47700, U-50488 and Furanyl Fentanyl by LC-MS/MS in Postmortem Casework. J Anal Toxicol. 2016;40(9):709-17.
142. Kolodny A, Courtwright DT, Hwang CS, Kreiner P, Eadie JL, Clark TW, et al. The prescription opioid and heroin crisis: a public health approach to an epidemic of addiction. Annu Rev Public Health. 2015;36:559-74.
143. Compton WM, Jones CM, Baldwin GT. Relationship between Nonmedical Prescription-Opioid Use and Heroin Use. N Engl J Med. 2016;374(2):154-63.
144. Mars SG, Bourgois P, Karandinos G, Montero F, Ciccarone D. "Every 'never' I ever said came true": transitions from opioid pills to heroin injecting. Int J Drug Policy. 2014;25(2):257-66.
145. Jaffe JH, Kanzler M, Green J. Abuse potential of loperamide. Clin Pharmacol Ther. 1980;28(6):812-9.
146. Miller H, Panahi L, Tapia D, Tran A, Bowman JD. Loperamide misuse and abuse. J Am Pharm Assoc (2003). 2017;57(2S):S45-S50.
147. Dierksen J, Gonsoulin M, Walterscheid JP. Poor Man's Methadone: A Case Report of Loperamide Toxicity. Am J Forensic Med Pathol. 2015;36(4):268-70.

148. Di Rosa E, Di Rosa AE. Loperamide overdose-induced catatonia: potential role of brain opioid system and P-glycoprotein. Acta Neuropsychiatr. 2014;26(1):58-60.
149. Dosen-Micovic L, Ivanovic M, Micovic V. Steric interactions and the activity of fentanyl analogs at the mu-opioid receptor. Bioorganic & medicinal chemistry. 2006;14(9):2887-95.
150. Van Bever WF, Niemegeers CJ, Janssen PA. Synthetic analgesics. Synthesis and pharmacology of the diastereoisomers of N-(3-methyl-1-(2-phenylethyl)-4-piperidyl)-N-phenylpropanamide and N-(3-methyl-1-(1-methyl-2-phenylethyl)-4-piperidyl)-N-phenylpropanamide. J Med Chem. 1974;17(10):1047-51.
151. Surratt CK, Johnson PS, Moriwaki A, Seidleck BK, Blaschak CJ, Wang JB, et al. -mu opiate receptor. Charged transmembrane domain amino acids are critical for agonist recognition and intrinsic activity. J Biol Chem. 1994;269(32):20548-53.
152. Dosen-Micovic L, Ivanovic M, Micovic V. Steric interactions and the activity of fentanyl analogs at the mu-opioid receptor. Bioorg Med Chem. 2006;14(9):2887-95.
153. Siuda ER, Carr R, 3rd, Rominger DH, Violin JD. Biased mu-opioid receptor ligands: a promising new generation of pain therapeutics. Curr Opin Pharmacol. 2017;32:77-84.
154. Madariaga-Mazon A, Marmolejo-Valencia AF, Li Y, Toll L, Houghten RA, Martinez-Mayorga K. Mu-Opioid receptor biased ligands: A safer and painless discovery of analgesics? Drug Discov Today. 2017;22(11):1719-29.
155. Mores KL, Cummins BR, Cassell RJ, van Rijn RM. A Review of the Therapeutic Potential of Recently Developed G Protein-Biased Kappa Agonists. Front Pharmacol. 2019;10:407.
156. DeWire SM, Yamashita DS, Rominger DH, Liu G, Cowan CL, Graczyk TM, et al. A G protein-biased ligand at the mu-opioid receptor is potently analgesic with reduced gastrointestinal and respiratory dysfunction compared with morphine. J Pharmacol Exp Ther. 2013;344(3):708-17.
157. Manglik A, Lin H, Aryal DK, McCorvy JD, Dengler D, Corder G, et al. Structure-based discovery of opioid analgesics with reduced side effects. Nature. 2016;537(7619):185-90.
158. Kliewer A, Schmiedel F, Sianati S, Bailey A, Bateman JT, Levitt ES, et al. Phosphorylation-deficient G-protein-biased mu-opioid receptors improve analgesia and diminish tolerance but worsen opioid side effects. Nat Commun. 2019;10(1):367.
159. Altarifi AA, David B, Muchhala KH, Blough BE, Akbarali H, Negus SS. Effects of acute and repeated treatment with the biased mu opioid receptor agonist TRV130 (oliceridine) on measures of antinociception, gastrointestinal function, and abuse liability in rodents. J Psychopharmacol. 2017;31(6):730-9.
160. Austin Zamarripa C, Edwards SR, Qureshi HN, Yi JN, Blough BE, Freeman KB. The G-protein biased mu-opioid agonist, TRV130, produces reinforcing and antinociceptive effects that are comparable to oxycodone in rats. Drug Alcohol Depend. 2018;192:158-62.
161. Hill R, Disney A, Conibear A, Sutcliffe K, Dewey W, Husbands S, et al. The novel mu-opioid receptor agonist PZM21 depresses respiration and induces tolerance to antinociception. Br J Pharmacol. 2018;175(13):2653-61.
162. Ehrlich AT, Semache M, Gross F, Da Fonte DF, Runtz L, Colley C, et al. Biased Signaling of the Mu Opioid Receptor Revealed in Native Neurons. iScience. 2019;14:47-57.
163. Schwienteck KL, Faunce KE, Rice KC, Obeng S, Zhang Y, Blough BE, et al. Effectiveness comparisons of G-protein biased and unbiased mu opioid receptor ligands in warm water tail-withdrawal and drug discrimination in male and female rats. Neuropharmacology. 2019;150:200-9.
164. Girven KS, Sparta DR. Probing Deep Brain Circuitry: New Advances in in Vivo Calcium Measurement Strategies. ACS Chem Neurosci. 2017;8(2):243-51.

8. APPENDICES

8.1. APPENDIX I: ACQUIRED STANDARDS OF SYNTHETIC OPIOIDS AND THEIR STRUCTURES

Structures: Fentanyl analogues and synthetic opioids

4-Fluoro-isobutyrylfentanyl

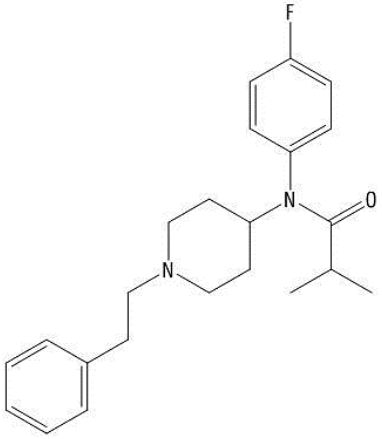

4-Methoxybutyrfentanyl

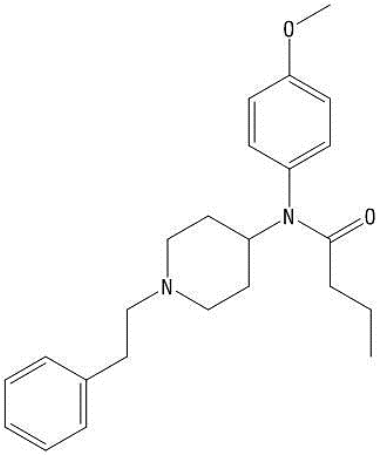

Acetylfentanyl

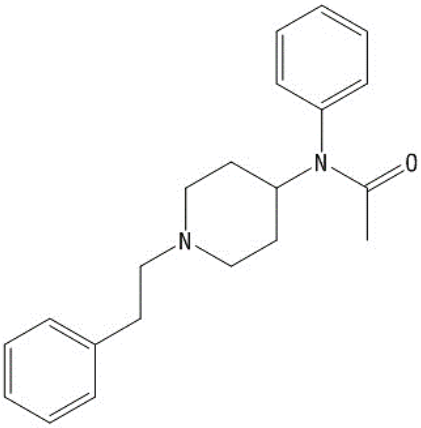

Acrylfentanyl

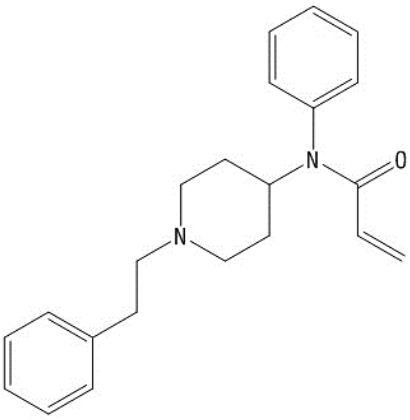

Alfentanil

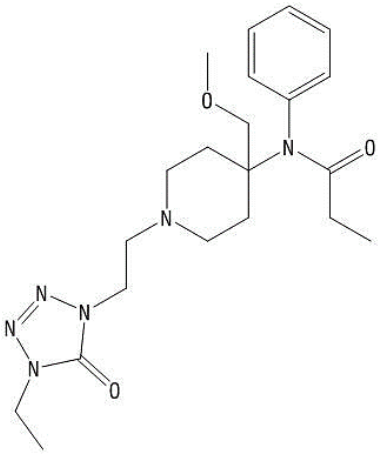

Benzoylfentanyl

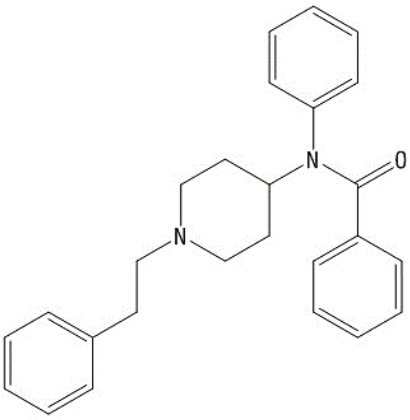

Butyrylfentanyl

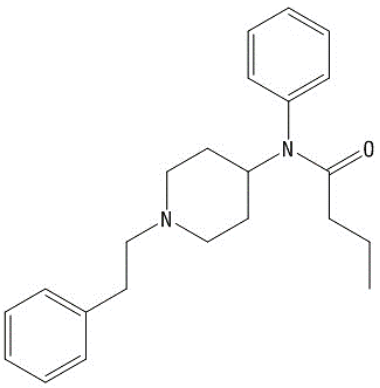

Crotonylfentanyl

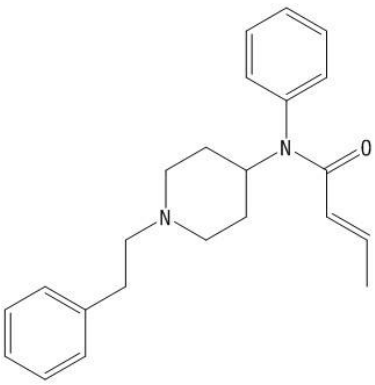

Cyclopentylfentanyl

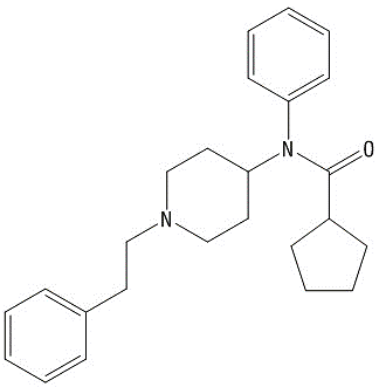

Structures: Fentanyl analogues and synthetic opioids (continued)

Cyclopropylfentanyl

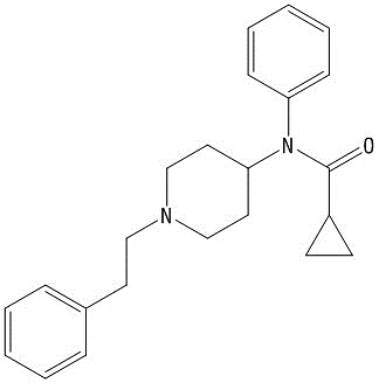

Fentanyl

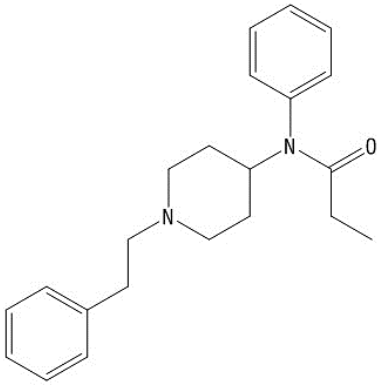

Furanylfentanyl

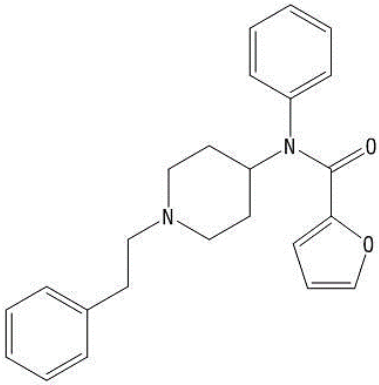

Methoxyacetylfentanyl

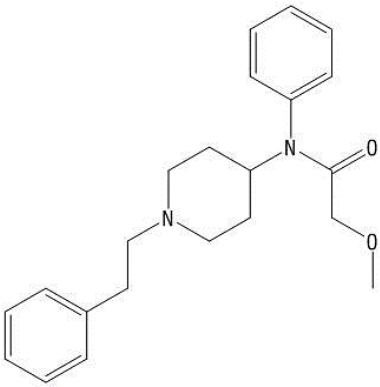

Phenylpropionylfentanyl

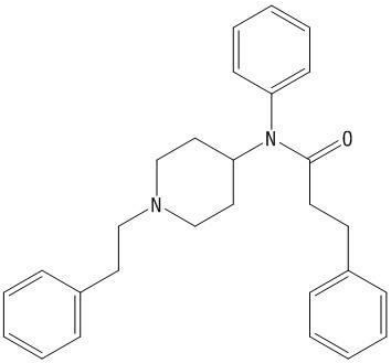

Ocfentanil

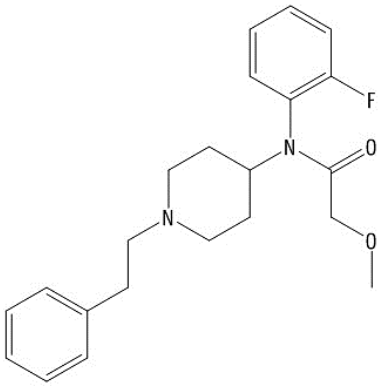

Tetrahydrofuranylfentanyl

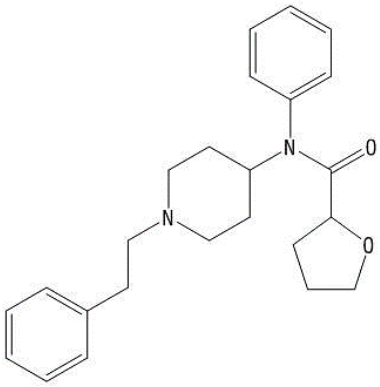

Tetramethylcyclopropylfentanyl

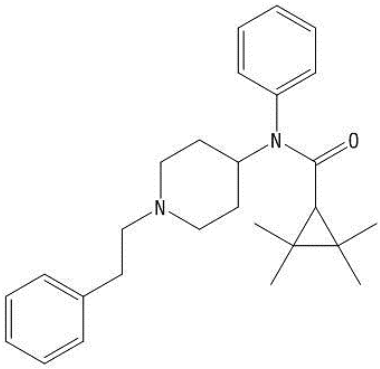

Valerylfentanyl

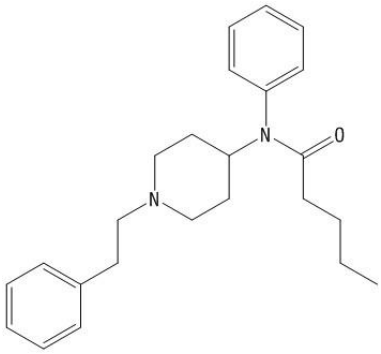

AH-7921

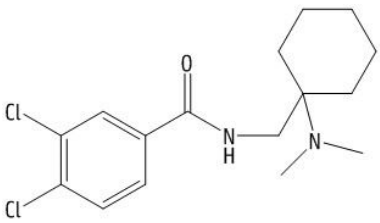

U-47700

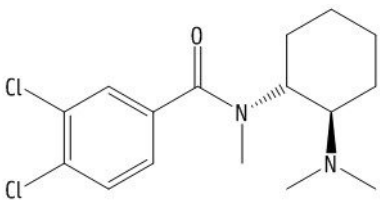

U-49900

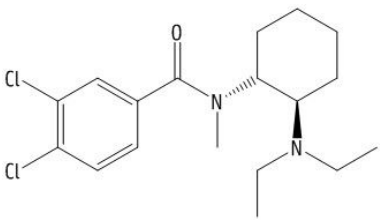

All compounds were acquired from Chiron (Trondheim, Norway).

8.2 APPENDIX II: DEVELOPMENT OF AN 'OPIOID ANTAGONIST STRATEGY': DESCRIPTION OF THE PROCESS

Co-occurrence of opioid antagonists remains a restriction in the designed activity-based assay. To tackle the problem of substances, such as naloxone, interfering with MOR activation, a specific strategy was thought out, which consists of adding a minimal amount of MOR agonist at a certain point during the experiment. Theoretically, the presence of an opioid antagonist would be revealed as the antagonist would inhibit an increase in signal expected from the addition of agonist (Cannaert, A. 2018). Two key points still remained to be investigated: the ideal concentration, as well as the optimal time point for adding the agonist. Hydromorphone (HM) was selected to serve as the MOR agonist, since this substance is a more water-soluble variant of morphine and therefore easy to work with. Additionally, HM is easy to obtain and has been previously used in the lab as a reference standard.

First, experiments were run to determine the amount of hydromorphone to add. The concentration of HM should be sufficiently high to be able to either induce a signal increase or to be blocked by naloxone but has to be low enough to still be able to distinguish biological samples with possibly low quantities of opioids from samples in which opioids are absolutely absent ("blank" samples). Initially, 1 ng/mL and 1 nM (which is about 0.3 ng/mL) HM were selected as concentrations of agonist used for injection. Several low concentrations of HM (0.01-1 ng/mL) were tested without the extra HM injection, with the aim of checking the sensitivity of the bioassay when working with such low HM concentrations. Luminescence results revealed that even concentrations as low as 0.1 ng/mL (light green line in Figure 8.1, B) could still be properly distinguished from the blank signal (black line in Figure 8.1, B), so the selected concentrations could be a viable pick.

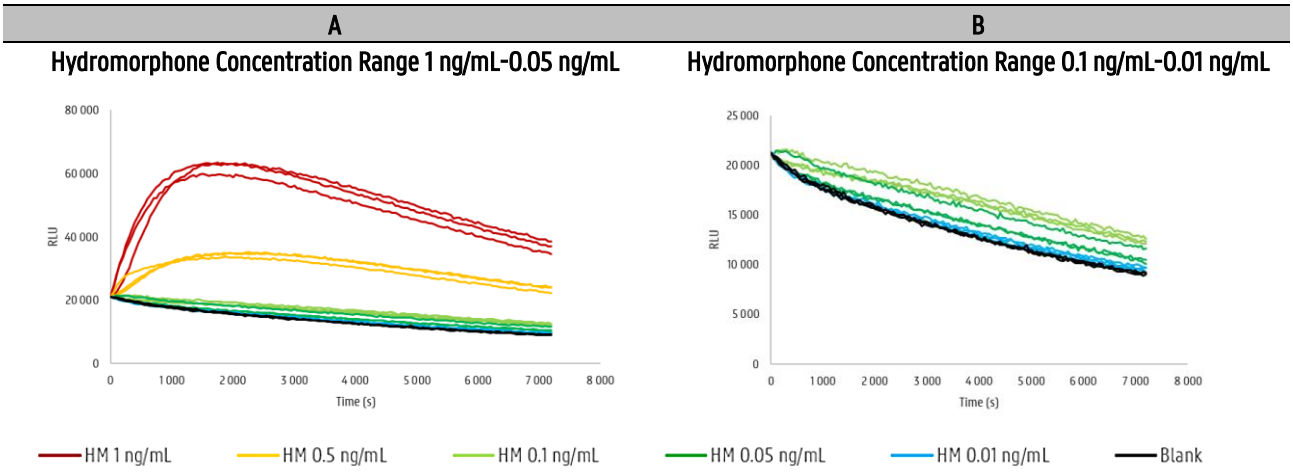

Figure 8.1: Result curves obtained from initial runs with only hydromorphone (HM, concentration range: 0.01 ng/mL-1 ng/mL). As seen on plot A, 1 ng/mL (red) and 0.5 ng/mL (yellow) concentrations yield an evident increase in luminescence signal, picked up by the luminometer. Plot B, which shows a more zoomed view of the curve, demonstrates that a HM concentration as low as 0.1 ng/mL (light green) was still able to elicit a signal, sufficient to be picked up by the assay. x-axis: time in seconds, y-axis: relative light units (RLU)

Second, the effect of 1 ng/mL and 1 nM HM injections after 10 min in the presence of the same concentration range of HM (0.01-1 ng/mL) as in the previous experiment (which simulated opioids in biological samples) was assessed. Both experiments resulted in decent plots but when focussing on lower concentrations, as depicted in Figure 8.2, injection with the higher (1 ng/mL) concentration of HM resulted in overlapping curves (Figure 8.2, A), indicating that the increased opioid activity of the added 1 ng/mL HM may mask the activity from opioids present in low concentrations in the sample. No distinction could be made between the curves from a blank with injection of 1 ng/mL HM injection at 10 minutes (blank + HM injection, black line in Figure 8.2) and the low concentration levels of HM already present at the start with 1 ng/mL HM injection at 10 minutes ((light)green and blue lines in Figure 8.2). Injection with a lower amount of HM (1 nM) still allowed a more distinct detection of low opioid activity (Figure 8.2, B), which is an interesting property when analysing biological samples with lower concentrations of opioids. As a result, for the following experiments, an injection concentration of 0.5 ng/mL, which resembles the 1 nM HM, was selected to preserve the sensitivity of the assay.

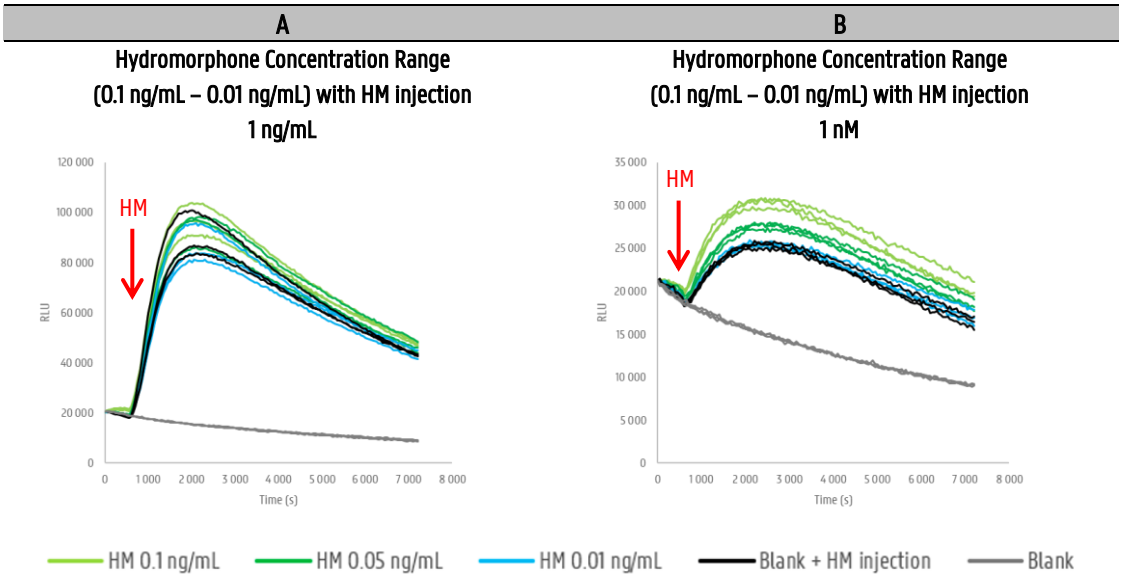

Figure 8.2: Comparison between injection of 1 ng/mL hydromorphone (A) **and 1 nM hydromorphone** (B) **in assay conditions containing low levels of hydromorphone (HM). Injection of 1 ng/mL HM (A) results in overlapping curves that cannot be used for screening samples. Lower concentration (1 nM) HM (B) allows better discrimination in case of opioids present in low concentrations.** x-axis, time in seconds; y-axis, relative light units (RLU); red arrow, injection of hydromorphone

Additionally, from this point onward, the hydromorphone injection was delayed to 30 minutes. When injecting at the 10-minute mark, the increase in signal is abruptly interrupted (see Figure 8.2), which does not allow to assess the initial opioid activity of a sample, complicating the following result analysis. Injection after 30 minutes will still allow the evaluation of a potential opioid-evoked rise in signal.

A new set of experiments was set up where various combinations of naloxone and HM were tested to reflect real samples containing mixtures of both. In an effort to reduce analysis time, results of a 2 hour assay time were

compared to those of only 1 hour of total assay time to evaluate if the same conclusion could be made in both experiments.

Several different assay conditions were created, one involving naloxone concentrations ranging up to 4 ng/mL, which resemble naloxone plasma concentrations after administration of a commonly used dose of naloxone in case of intoxication. As seen in Figure 8.3, analysis of the results revealed that injection of 0.5 ng/mL HM did not result in a signal increase in the presence of 0.4 ng/mL of naloxone (yellow line in Figure 8.3) or higher, indicating that naloxone, in the absence of other compounds with opioid activity, was able to block MOR activation, which is less -or not- the case with lower concentrations of naloxone (green, blue and purple line in Figure 8.3). If naloxone is present in a biological sample at common plasma concentrations, the signal originating from the additional HM injection will be inhibited and the antagonist presence will theoretically be unveiled.

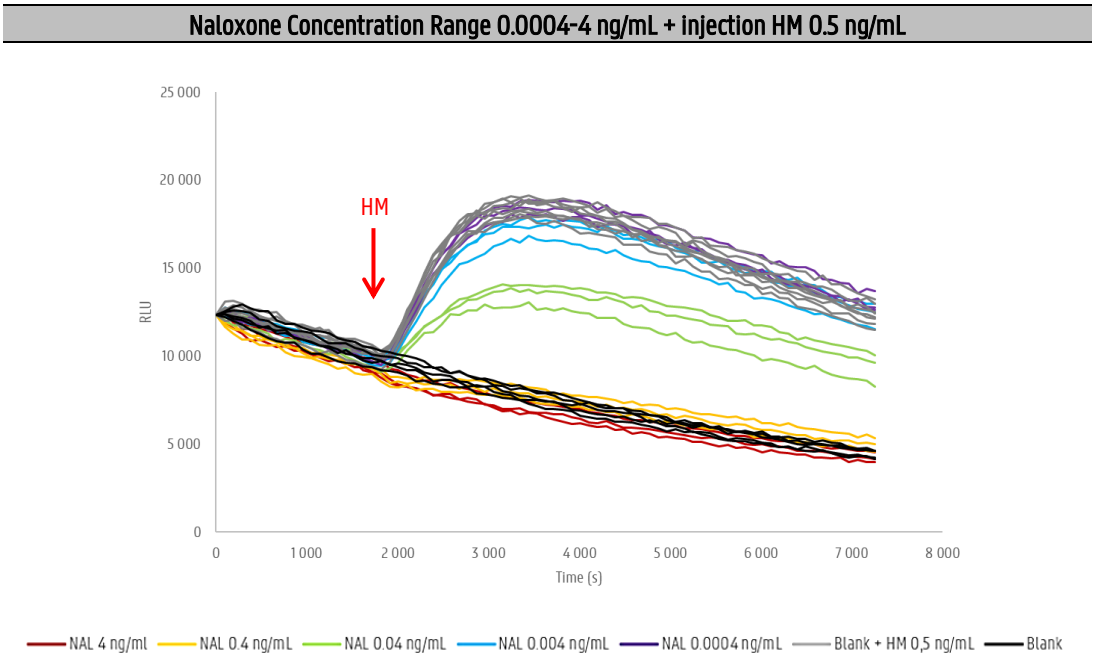

Figure 8.3: Naloxone Concentration Range (0.004 – 4 ng/mL) + injection of 0.5 ng/mL hydromorphone (HM). Naloxone concentrations starting at 0.4 ng/mL are able to completely reduce opioid activity provoked by the 0.5 ng/mL HM injection at 30 minutes. x-axis, time in seconds; y-axis, relative light units (RLU); red arrow, injection of hydromorphone

The next experiment was conducted where 0.5 ng/mL HM was injected after 30 minutes in the presence of a wide range of HM concentrations (0.01-1000 ng/mL) to verify the impact of the HM injection on the luminescence results of different levels of opioids. Upon HM injection at 30 minutes, a small but sudden drop of the signal could be noticed at the high concentrations, which can be explained by the fact that injection involved the addition of a small volume, which results in a small dilution of the sample solution in the wells. (see Figure 8.4) At the lower concentrations, an increase of light (corresponding to receptor activation) was seen, which is expected upon addition of an extra amount of HM, which can be seen on Figure 8.5. Just as previous experiments

without injection (Figure 8.1, light green), the start concentration of 0.1 ng/mL HM (Figure 8.5, light blue), can just be distinguished from the blank profiles which also received an HM injection (Figure 8.5, grey).

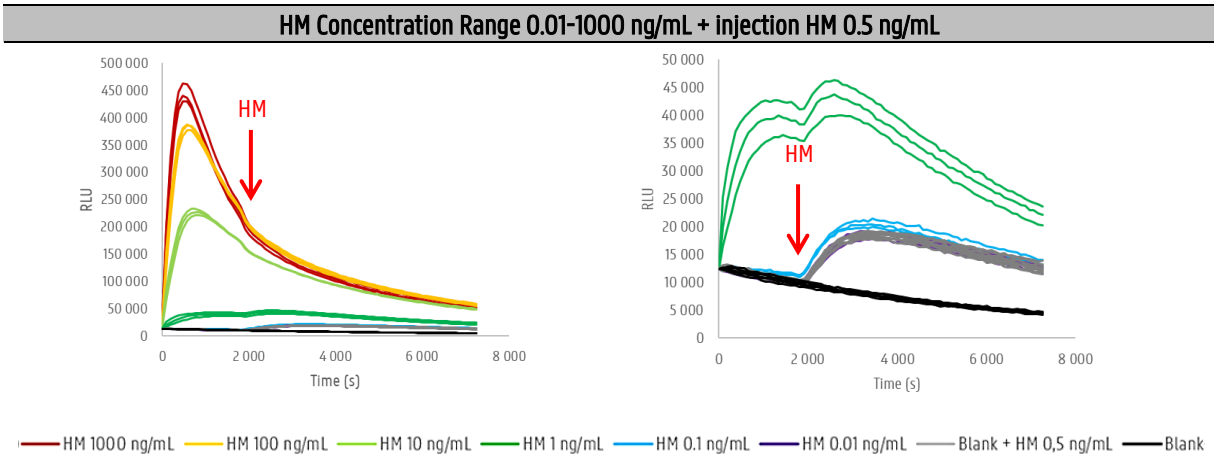

Figure 8.4: HM Concentration Range (0.01-1000 ng/mL with injection of 0.5 ng/mL HM after 30 minutes. Higher concentrations of HM generate a luminescence signals that hardly seem to be affected by additional HM injection. A small drop in signal is noticeable after adding HM, due to a slight dilution of the sample.
x-axis, time in seconds; y-axis, relative light units (RLU); red arrow, injection of hydromorphone

Figure 8.5: Zoomed view of figure Y. At lower concentrations (1 ng/mL, dark green), addition of HM results in a noticeable increase in signal.
x-axis, time in second; y-axis, relative light units (RLU); red arrow, injection of hydromorphone

The final set of experiments monitored the combined presence of naloxone (4 ng/mL) and HM (concentration range 0.1-1000 ng/mL) along with a HM (0.5 ng/mL) injection at the 30 minute point. As can be seen in Figure 8.6 (B), a concentration of 1000 ng/mL HM in the presence of 4 ng/mL naloxone still yields an apparent increase in luminescence signal, comparable to what can be noticed in absence of naloxone (Figure 8.6, A). It is possible that a HM concentration as high as 1000 ng/mL is too extreme to be blocked by the inhibitory behaviour of naloxone at MOR. When looking at lower concentrations, a strong reduction in signal can be observed in the presence of naloxone (Figure 8.6, A and B). For example, 10 ng/mL HM (light green) of which the signal reached almost 250 000 RLU in the absence of naloxone (Figure 8.6, A, light green), only faintly yields a signal in the presence of naloxone (Figure 8.6, D, light green). The signal of lower concentrations of HM are even completely blocked (Figure 8.6, D, dark green and light blue).

The conclusion is that the presence of opioids (both agonists and antagonists) will be revealed with our improved assay with the additional HM injection. The presence of opioid agonists will be detected via the increased luminescence, while the presence of opioid antagonists, which is in any case suspicious since it indicates a possible opioid overdose and requires further investigation, will be detected via the additional HM injection, as this allows to distinguish between “real negative” samples and “negative” samples due to the presence of an antagonist.

HM Concentration Range 0.01-1000 ng/mL + injection HM 0.5 ng/mL WITHOUT 4 ng/mL naloxone	HM Concentration Range 0.01-1000 ng/mL + injection HM 0.5 ng/mL WITH 4 ng/mL naloxone

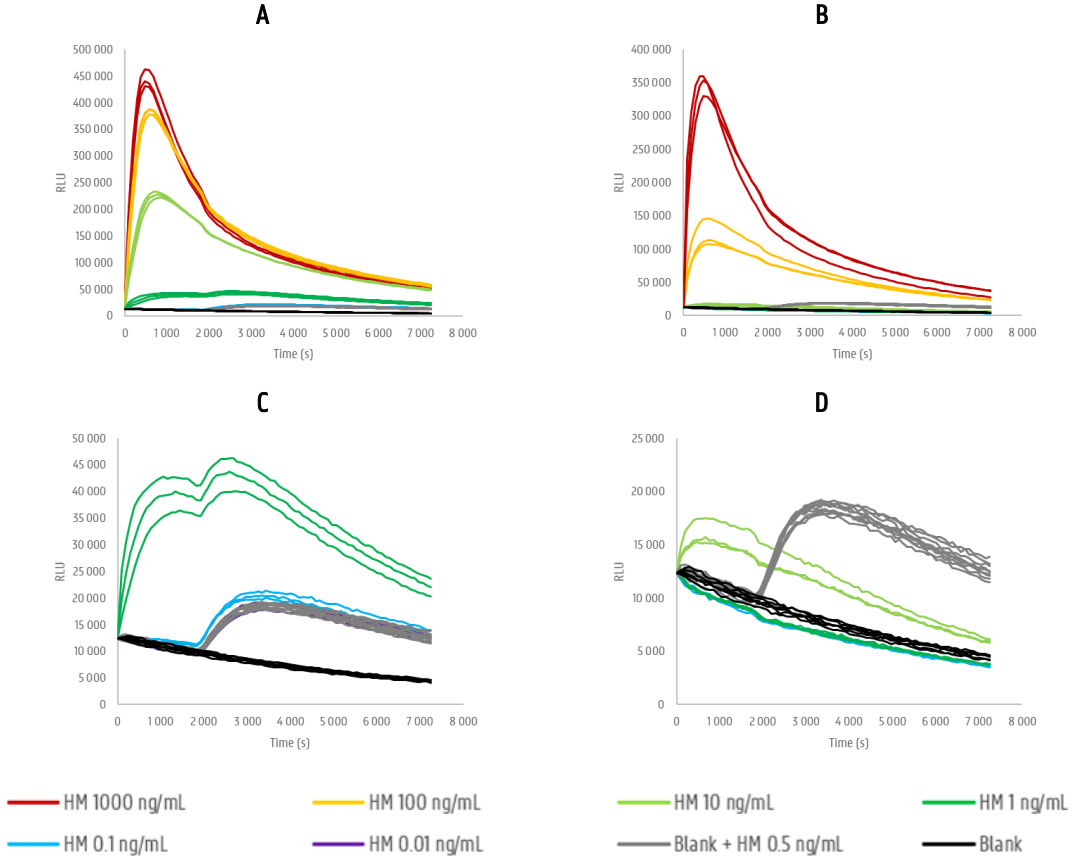

Figure 8.6 : Comparison of sensitivity in absence (A and C) or presence (B and D) of 4 ng/mL naloxone. C and D provide a zoomed view of graphs A and B. In presence of naloxone, luminescence signals provoked by MOR activation are greatly reduced when comparing equal concentrations of opioid agonist (equal colours).
x-axis, time in seconds; y-axis, relative light units (RLU)

Finally, a 2 hour assay time was compared to a 1 hour assay time in the light of reducing analysis times. Results revealed that a total assay time of 1h proved to be equally viable for evaluating the composition of the samples, since all clues that would give away the sample's content were already noticeable after 1 hour. High opioid concentrations yield a rapid and clear rise in signal, making assaying for 2 full hours unnecessary. Furthermore, even low concentrations generated signals that were already distinguishable from blank signals before the 1-hour mark, which can be seen in Figure 8.7. This finding is promising for the future improvement of the assay's protocol, which would make this detection method less time-consuming and would allow us to screen more samples in a shorter amount of time.

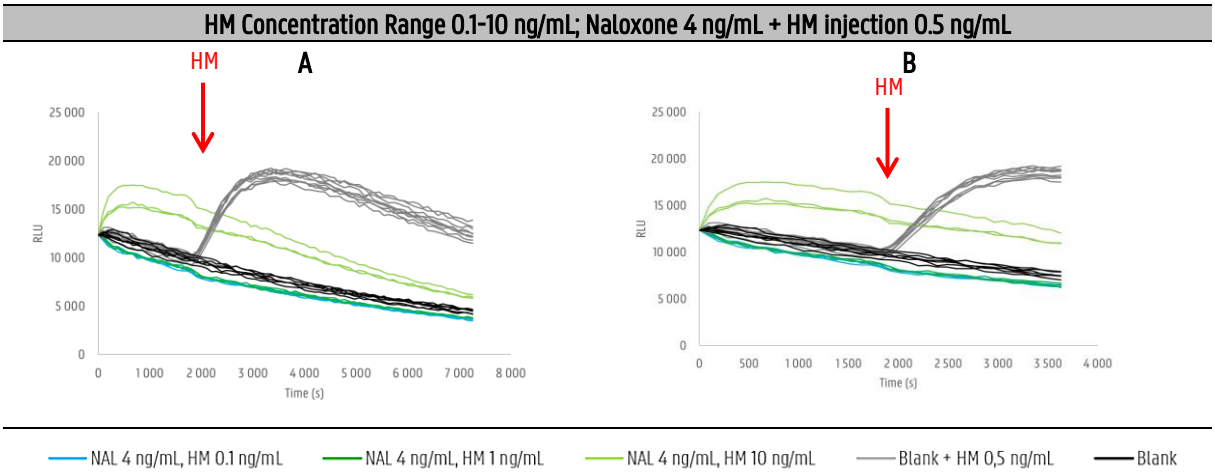

Figure 8.7: Comparison between a 2h assay time (A) and a 1h assay time (B). Even with lower opioid concentrations present, no additional information was obtained after one supplementary hour, which may be promising for future improved and less time-consuming experiments. x-axis, time in seconds; y-axis, relative light units (RLU); red arrow, injection of hydromorphone

8.3 APPENDIX III: LISTING OF THE ANALYTICAL FINDINGS IN THE 94 OBTAINED BLOOD SAMPLES

Sample N°	Detected opioid agonists	Detected opioid antagonists	Other findings	Additional information
1	Cyclopropylfentanyl		Caffeine, cotinine, cyclobenzaprine	
2	Cyclopropylfentanyl		Ethanol, caffeine, cotinine, cocaine, 7-aminoclonazepam, BZE, hydroxyzine, cyclobenzaprine	
3	Loperamide		Caffeine, cotinine, diazepam, nordiazepam, alprazolam, 11-OH-THC, 11-COOH-THC, THC, citalopram/escitalopram, desmethylloperamide	
4	Fentanyl		Caffeine, cotinine, alprazolam, buproprion, hydroxybupropion, citalopram/escitalopram, amphetamine	
5	Furanylfentanyl		Ethanol, caffeine, 7-aminoclonazepam, 4-ANPP	
6	Fentanyl		Ethanol, caffeine, cotinine, Nicotine, acetaminophen, BZE, citalopram/escitalopram, norfentanyl, methamphetamine	
7	Cyclopropylfentanyl Oxycodone Fentanyl		Caffeine, cotinine, diazepam, nordiazepam, BZE, 11-COOH-THC, diphenhydramine, norfentanyl	
8	Oxycodone Oxymorphone		Caffeine, carisoprodol, meprobamate, cyclobenzaprine	
9	U-47700		Nicotine, mirtazapine	
10	Oxycodone Oxymorphone		Caffeine, alprazolam, duloxetine, eszopiclone/zopiclone, chlorpheniramine, buspirone	
11	Methadone		Carboxyhemoglobin, EDDP, quetiapine, desmethylsertraline, amphetamine, aripirazole, caffeine, sertraline	
12	Oxycodone Oxymorphone		Caffeine, acetaminophen, cotinine, mescaline, methamphetamine, nicotine	Oxycodone detected at 1181% of the cut-off (10 ng/mL) and oxymorphone detected at 270% of the cut-off (2 ng/mL)
13	Oxymorphone Oxycodone		Caffeine, cotinine, alprazolam, midazolam, ketamine, norketamine, 11-OH-THC11-COOH-THC, citalopram/escitalopram, 11-hydroxymidazolam, acetaminophen, amphetamine, etomidate,	Oxycodone detected at 73% of the cut-off (10 ng/mL) and oxymorphone detected at 9% of the cut-off (2 ng/mL)
14	Morphine		Ethanol, caffeine, alprazolam	
15	Furanylfentanyl		Ethanol, alprazolam, THC, 4-ANPP	
16	Fentanyl		Caffeine, BZE, norfentanyl	
17	Cyclopropylfentanyl		Caffeine, cocaine, BZE, hydroxyzine	
18	Buprenorphine Norbuprenorphine	Naloxone	Caffeine, cotinine	
19	Furanylfentanyl		Caffeine, 4-ANPP	
20	Cyclopropylfentanyl		Caffeine, cotinine, cocaine, BZE	
21	Fentanyl		Cotinine, quinine, BZE, norfentanyl	
22	Buprenorphine Norbuprenorphine	Naloxone	Isopropanol, acetone, hydroxyzine	

Analytical findings in the 94 obtained blood samples (continued)

Sample N°	Detected opioid agonists	Detected opioid antagonists	Other findings	Additional information
23	Oxycodone Oxymorphone		Caffeine, cotinine, diphenhydramine	
24	Buprenorphine Dextro/levo methorphan		7-aminoclonazepam, THC and metablites, amphetamine, methamphetamine, clonazepam, cotinine	Buprenorphine detected at 34% of the cut-off (1 ng/mL) and dextro/levomethrophan detected at 23.5% of the cut-off (50 ng/mL)
25	Furanylfentanyl	Naloxone	Ethanol, tadalafil, diphenhydramine, 4-ANPP, 3-MeO-PCP	
26	Oxycodone Oxymorphone		Caffeine, diazepam, nordiazepam	
27	Fentanyl		Ethanol, cotinine, BZE, amphetamine, methamphetamine	
28	Furanylfentanyl		7-aminoclonazepam, THC and metabolites, 4-ANPP	
29	U-47700		Ethanol, caffeine, diphenhydramine, methoxphenidine	
30	Oxycodone Methoxyacetylfentanyl		Ethanol, caffeine, cotinine	
31	U-47700 Cyclopropylfentanyl		Caffeine, cotinine, THC and metabolites, citalopram	
32	Fluoro-isobutyrylfentanyl Morphine Fentanyl Acetylfentanyl		4-ANPP, caffeine, cotinine, alprazolam, cocaine, BZE, norfentanyl	
33	Fentanyl Cyclopropylfentanyl		Cotinine, alprazolam	
34	Methoxyacetylfentanyl		Cotinine	
35	Cyclopropylfentanyl		Caffeine, cotinine, BZE, olanzapine	
36	Cyclopropylfentanyl		Caffeine, cocaine, BZE, hydroxyzine	
37	Codeine Morphine		Amphetamine, methamphetamine	
38				Completely blank sample
39			Caffeine, cotinine, 11-OH-THC, THC, diphenhydramine	
40			Ethanol, caffeine, cotinine, cocaine, cocaethylene, nortriptyline	
41			Caffeine, bupropion, hydroxybupropion, amitriptyline, nortriptyline	
42			Caffeine	
43			Citalopram/escitalopram	
44			Ethanol, caffeine, cotinine, nicotine	
45			Ethanol, caffeine, cocaethylene, BZE	
46			Caffeine, clonazepam, 7-aminoclonazepam, quetiapine, amitriptyline, nortriptyline, 11-COOH-THC, THC, cyclobenzaprine	

Analytical findings in the 94 obtained blood samples (continued)

Sample N°	Detected opioid agonists	Detected opioid antagonists	Other findings	Additional information
47			Ethanol, caffeine, cotinine, diazepam, 7-aminoclonazepam, 11-COOH-THC, THC	
48			Bupropion, hydroxybupropion, olanzapine, benztropine	
49			Ethanol, caffeine, cotinine, 11-OH-THC, 11-COOH-THC, THC	
50			Cotinine, 11-COOH-THC, THC, amphetamine, methamphetamine	
51			Caffeine, acetaminophen, amphetamine, methamphetamine	
52			Ethanol, caffeine, cotinine, alprazolam, quetiapine, fluoxetine, norfluoxetine, diphenhydramine	
53			Diazepam, nordiazepam, chlordiazepoxide, levetiracetam	
54			Caffeine, pseudoephedrine, norpseudoephedrine	
55			Caffeine, cotinine, nicotine, methamphetamine, amphetamine	
56			Caffeine	
57			Caffeine	
58			Caffeine	
59	Morphine (free) Hydrocodone (free) Fentanyl	Naloxone	Caffeine, cotinine, levamisole, butalbital, 7-aminoclonazepam, cocaine, BZE, amphetamine, norfentanyl	
60	Hydrocodone (free) Fentanyl	Naloxone	Caffeine, lidocaine, MEGX, 11-COOH-THC, THC	
61		Naloxone	Ethanol, caffeine	
62	Methoxyacetylfentanyl Cyclopropylfentanyl	Naloxone	Cotinine, 11-COOH-THC, THC	
63	Cyclopropylfentanyl Morphine (free) Fentanyl	Naloxone	Caffeine, alprazolam, levetiracetam, quetiapine, norfentanyl	
64	Furanylfentanyl	Naloxone	Ethanol, phenylpropanolamine, amphetamine, 4-ANPP	
65	Oxymorphone	Naloxone	Caffeine, alprazolam	
66		Naloxone	Caffeine, cotinine	
67	Morphine Hydrocodone Oxycodone	Naloxone	Caffeine, sertraline, desmethylsertraline, THC, diphenydramine, hydroxyzine	
68		Naltrexone 6-β-naltrexol	Ethanol, caffeine, alprazolam, sertraline, desmethylsertraline, risperidone, 9-hydroxyrisperidone, diphenydramine,	
69	Methoxyacetylfentanyl	Naloxone	Caffeine, cotinine, 7-aminoclonazepam, alprazolam, midazolam, amphetamine, methamphetamine	
70		Naloxone	Caffeine, cotinine, THC	
71		Naloxone	Caffeine, cocaine, BZE	
72		Naloxone	Ethanol, caffeine, diphenhydramine	
73	Oxycodone Furanylfentanyl	Naloxone	Caffeine, lidocaine, alprazolam	

Analytical findings in the 94 obtained blood samples (continued)

Sample N°	Detected opioid agonists	Detected opioid antagonists	Other findings	Additional information
74		Naloxone	Caffeine	
75		Naloxone	Caffeine, cotinine, THC	
76	Fentanyl U-47700	Naloxone	10-hydroxycarbazepine, sertraline, desmethylsertraline, cyclobenzaprine	
77	Fentanyl Acetylfentanyl	Naloxone	Caffeine, metoclopramide, clonazepam, 7-aminoclonazepam, sertraline, desmethylsertraline, 11-COOH-THC, THC, amphetamine, methamphetamine	
78	Dihydrocodeine/hydrocodol Morphine Hydrocodone Oxycodone	Naloxone	Caffeine, citalopram/escitalopram	
79		Naloxone	Caffeine, acetaminophen, diphenhydramine	
80	Hydrocodone Oxycodone	Naloxone	Caffeine, cotinine	
81		Naloxone	Caffeine	
82	Fentanyl	Naloxone		
83		Naloxone Naltrexone 6-β-naltrexol	Ethanol, cotinine, levamisole, cocaine, cocaethylene, BZE, quetiapine, diphenhydramine	
84		Naloxone	Caffeine	
85		Naloxone	Cotinine, cocaine, BZE, THC and metabolites	
86		Naloxone	Cotinine, levamisole, cocaine, BZE	
87		Naloxone	Caffeine, ethanol	
88	Morphine Oxymorphone Fentanyl	Naloxone	Alprazolam, cocaine, BZE, citalopram/escitalopram, norfentanyl	
89	Cyclopropylfentanyl	Naloxone	Caffeine, cotinine, THC	
90			Ethanol, caffeine, metoclopramide, amphetamine, metamphetamine, theophylline, 11-COOH-THC, THC	
91	Hydrocodone		Caffeine, cotinine, 11-COOH-THC, THC	Hydrocodone quantitated at 11 ng/mL
92	Buprenorphine Norbuprenorphine		Alprazolam, BZE	
93	Furanylfentanyl	Naloxone	Caffeine, nicotine, cotinine	
94	Furanylfentanyl	Naloxone	Caffeine, temazepam, lorazepam, sertraline, desmethylsertraline, 4-ANPP	

Abbreviations: BZE, benzoylecgonine; **11-OH-THC**, 11-hydroxy-Δ^9-tetrahydrocannabinol; **THC**, tetrahydrocannabinol; **MEGX**, monoethylglycinexylidide; **11-COOH-THC**, 11-nor-9-carboxy-Δ^9-tetrahydrocannabinol; **4-ANPP**, 4-anilino-N-phenethylpiperidine; **EDDP**, 2-ethylidene-1,5-dimethyl-3,3-diphenylpyrrolidine; **3-MeO-PCP**, 3-methoxyphencyclidine

8.4 APPENDIX IV: LISTING OF THE ANALYTICALLY CONFIRMED MOR RELATED COMPOUNDS

Overview of the analytically detected opioid-related substances in the 94 unique blood samples, along with their overall number of detections.

MOR agonists		
Compound name		Number
Acetylfentanyl		2
Buprenorphine		4
Codeine		1
Cyclopropylfentanyl		13
Dextro/Levomethorphan*		1
Dihydrocodeine		1
Fentanyl		15
Fluoro-isobutyrylfentanyl		1
Furanylfentanyl		9
Hydrocodone		6
Loperamide		1
Methadone		1
Methoxyacetylfentanyl		4
Morphine		8
Oxycodone		13
Oxymorphone		8
U-47700		4
MOR antagonists		
Compound Name		Number
Naloxone		35
Naltrexone		2
Metabolites or by-products of MOR agonists or antagonists		
Compound Name	Parent Compound	Number
Desmethyl Loperamide	Loperamide	1
Norfentanyl	Fentanyl	9
4-ANPP** *(4-Anilino-N-phenethylpiperidine)*	**	8
6-β-Naltrexol	Naltrexone	2
Norbuprenorphine	Buprenorphine	4

* occasionally occurs as racemic mixture of stereoisomers dextromethorphan and levomethorphan.

** precursor in the production process of fentanyls, occasionally present as a contamination in fentanyl preparations

8.5 APPENDIX V: LIST OF COMPOUNDS DETECTED IN CORRECTLY SCORED SAMPLES

Analgesics
Acetaminophen (paracetamol)
Antidepressants
Tricyclic antidepressants
Amitriptyline
Nortriptyline
Selective Serotonin Reuptake Inhibitors
Citalopram/escitalopram
Fluoxetine
Norfluoxetine (metabolite of fluoxetine)
Atypical
Bupropion (atypical)
Hydoxybupropion (metabolite of bupropion)
Antihistaminics
Diphenhydramine
Antipsychotics
Olanzapine
Quetiapine
Depressants
Ethanol
Cannabinoids
11-hydroxy THC (metabolite of THC)
11-nor-9-carboxy-THC (metabolite of THC)
Tetrahydrocannabinol (THC)
Sedatives or hypnotics
Benzodiazepines
7-aminoclonazepam (metabolite of clonazepam)
Alprazolam
Clonazepam
Chlordiazepoxide
Diazepam
Nordiazepam
Stimulants
Benzoic acid esters
Benzoylecgonine (metabolite of cocaine)
Cocaethylene (by-product of co-occurrent cocaine and ethanol)
Phenylethylamines
Amphetamine
Methamphetamine
Norpseudoephedrine (commonly used as a decongestant)
Pseudoephedrine
Pyrrolidinylpyridines
Cotinine (metabolite of nicotine)
Nicotine
Xanthines
Caffeine
Other
Benztropine (antimuscarinic agent, used in treatment of Parkinsonian syndrome)
Cyclobenzaprine (muscle relaxant, used for musculoskeletal conditions)

During our experiments, these compounds were not found to contribute to/interfere with MOR activation.

8.6 APPENDIX VI: OVERVIEW OF THE SCORED SAMPLES

8.6.1. Overview of the correctly scored positive samples (original and improved method)

Samples screened positive for opioid agonists

Sample 1

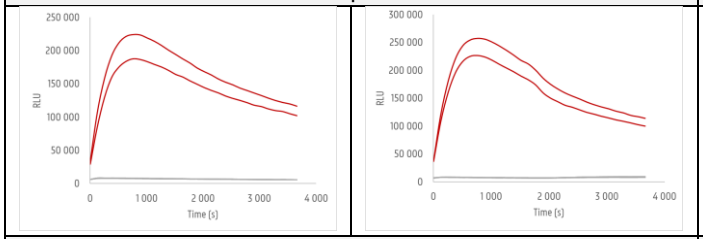

Sample 2

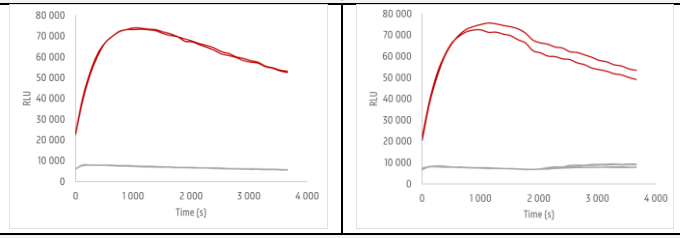

Sample 3

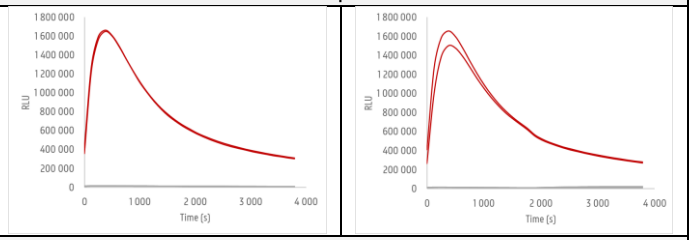

Sample 4

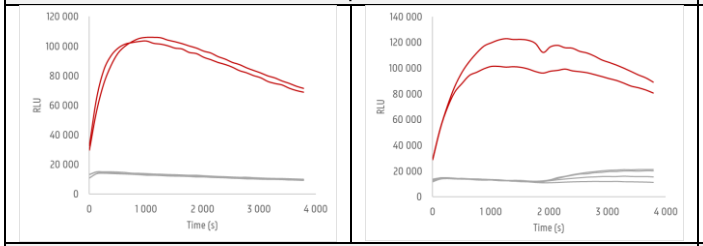

Sample 5

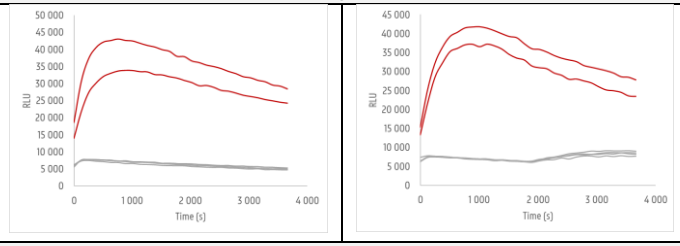

Sample 6

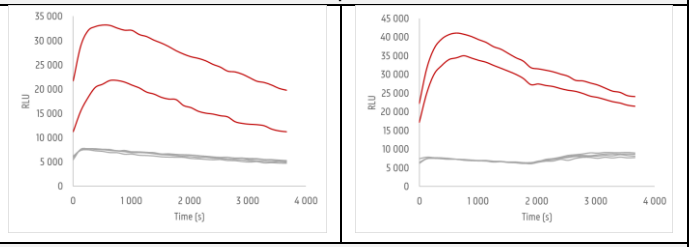

Sample 7

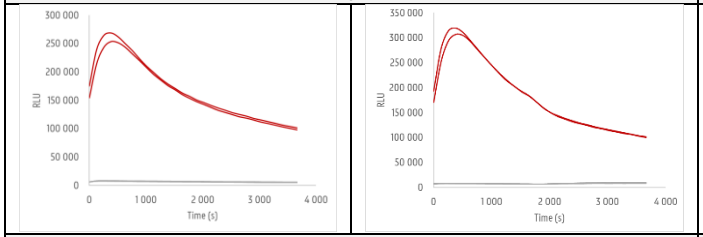

Sample 8

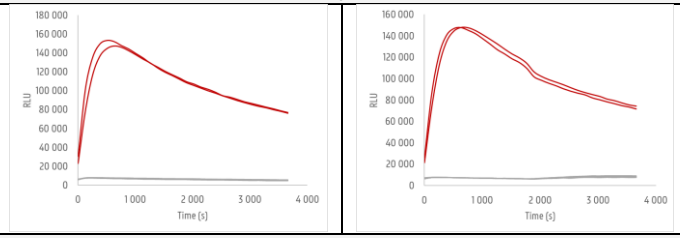

Sample 9

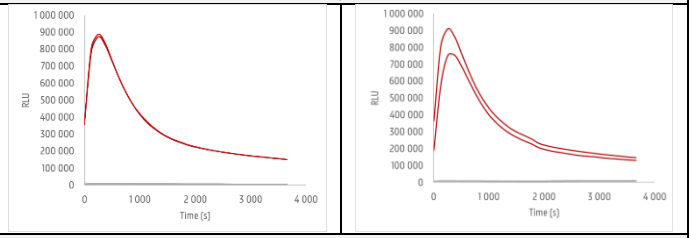

Sample 10

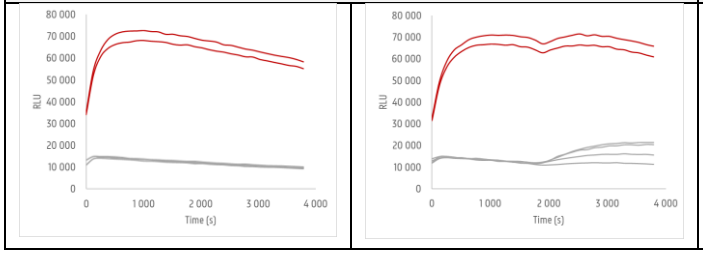

Sample 11

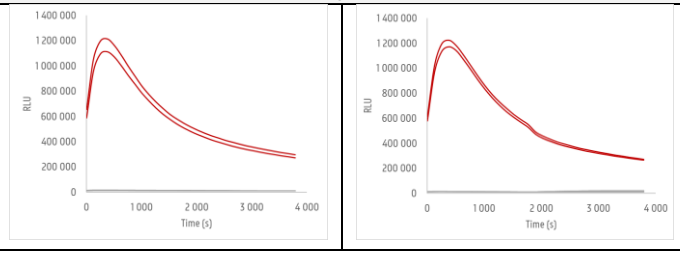

Sample 12

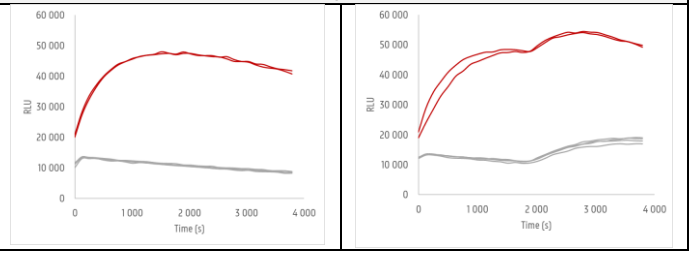

Samples screened positive for opioid agonists (continued)

Sample 13

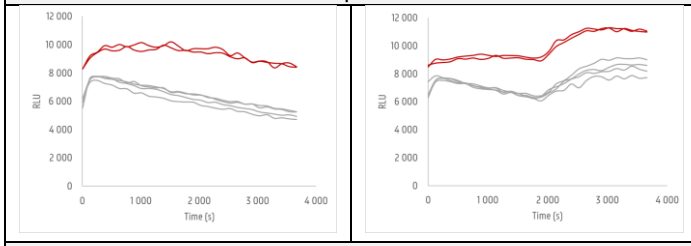

Sample 14

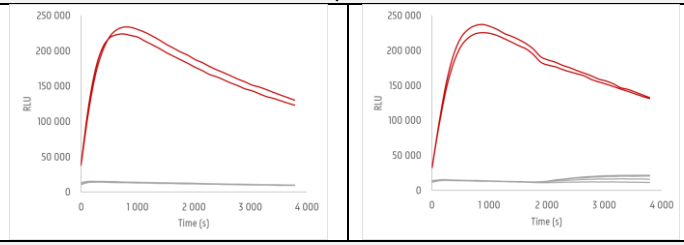

Sample 15

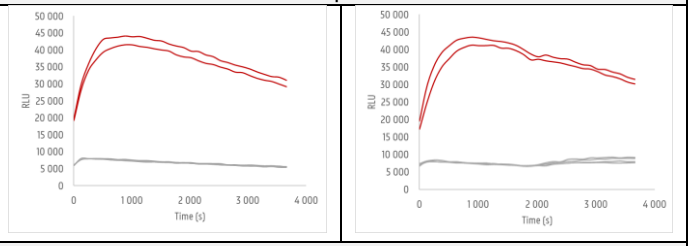

Sample 16

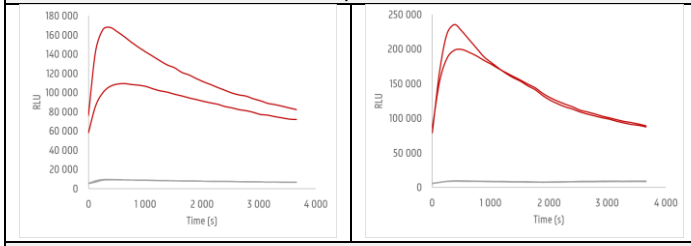

Sample 17

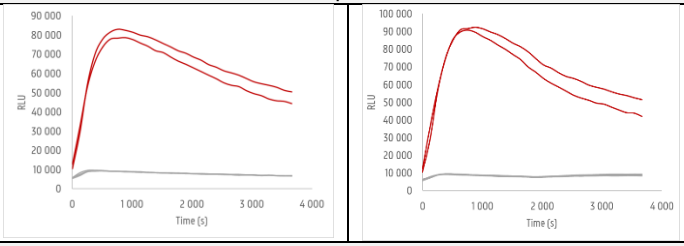

Sample 18

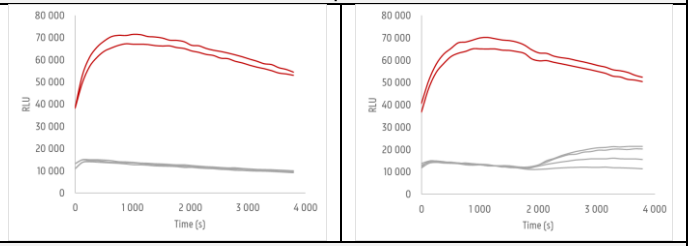

Sample 19

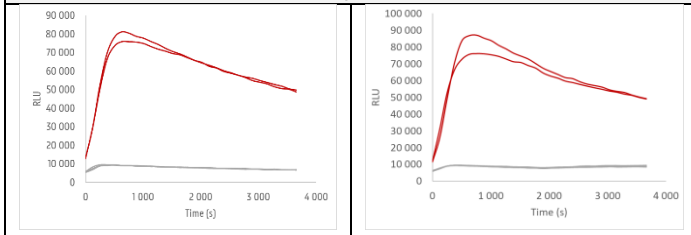

Sample 20

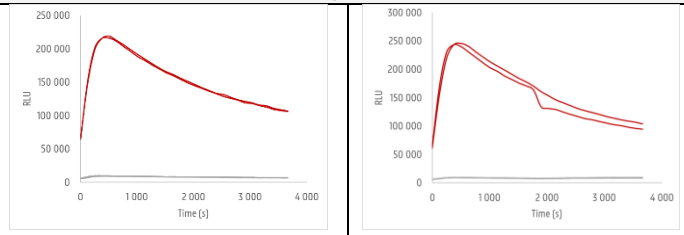

Sample 21

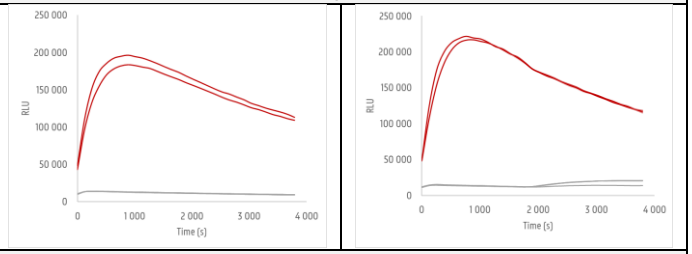

Sample 22

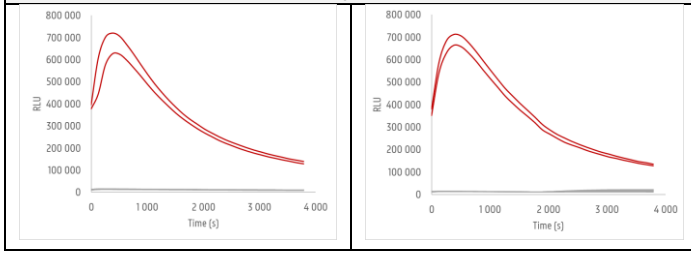

Sample 23

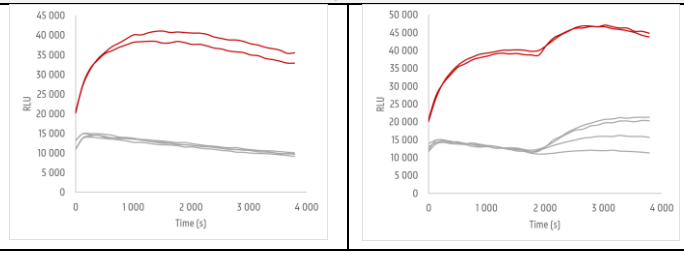

Sample 24

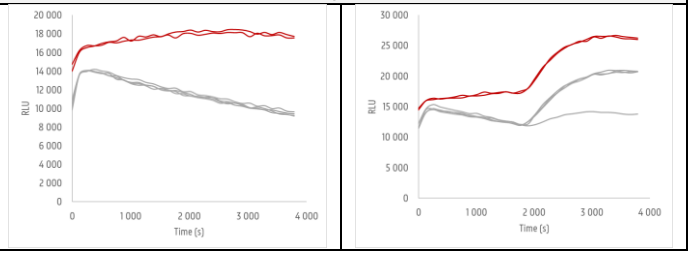

Samples screened positive for opioid agonists (continued)

Sample 25

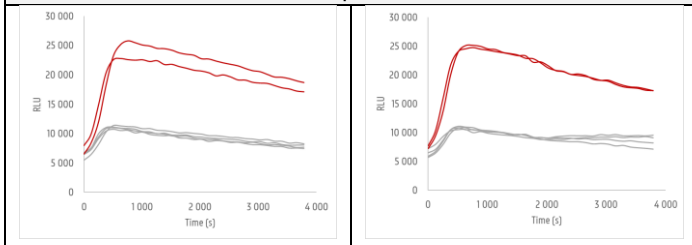

Sample 26

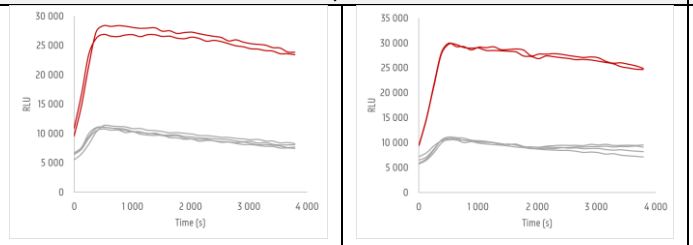

Sample 27

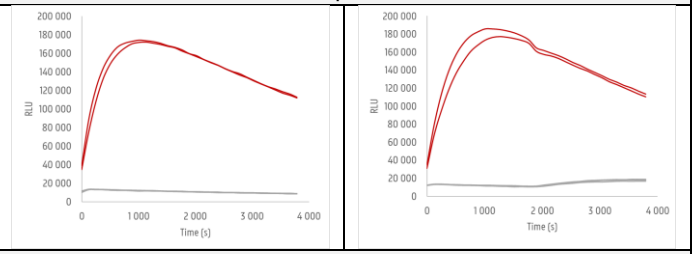

Sample 28

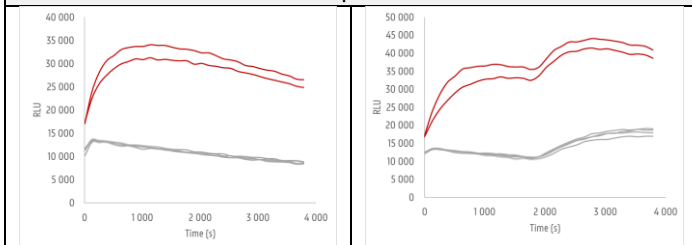

Sample 29

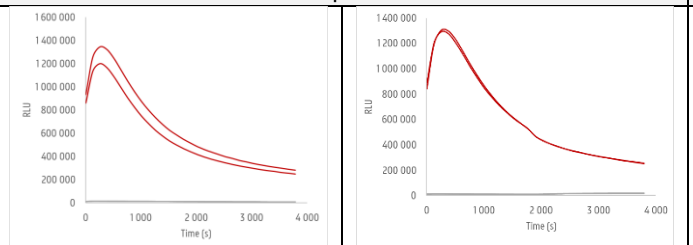

Sample 30

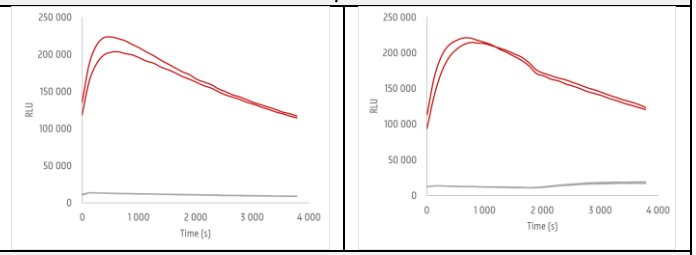

Sample 31

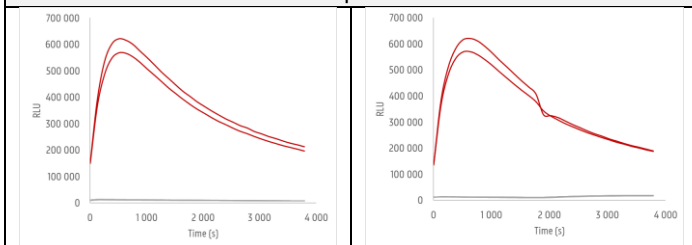

Sample 32

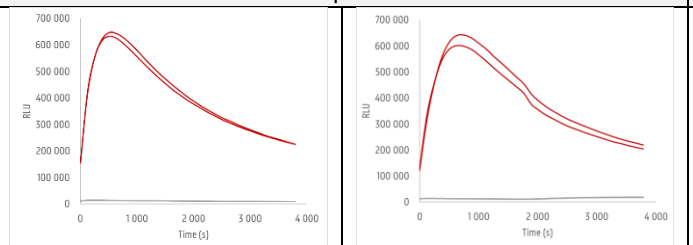

Sample 33

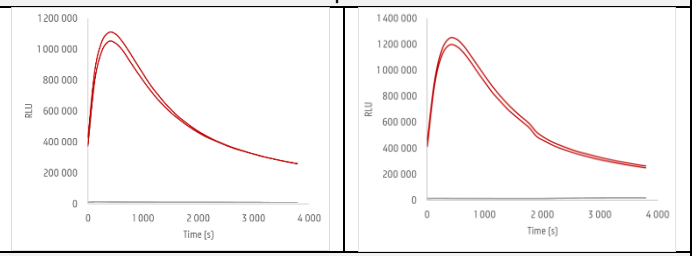

Sample 34

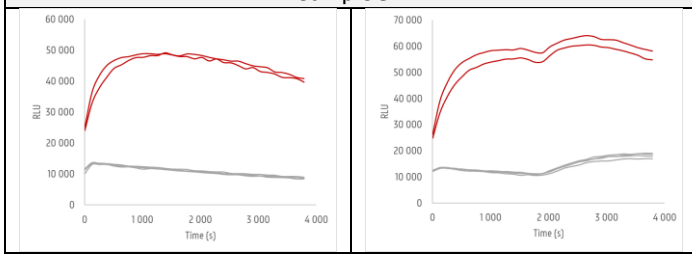

Sample 35

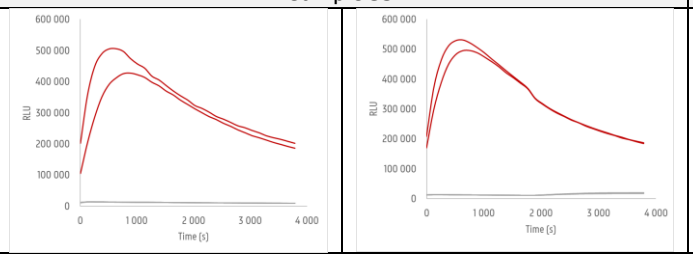

Sample 36

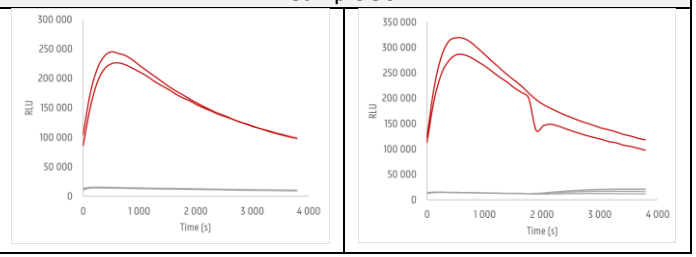

Samples screened positive for opioid agonists (continued)
Sample 37

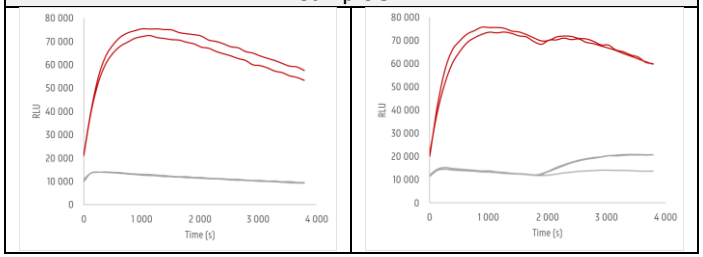

The profiles represent corrected data from the MOR bioassay (1 hour assay time). Each sample is depicted twice, indicating both the original method and the improved method (+ HM injection). x-axis, time in seconds; y-axis, relative light units (RLU) **Legend: Red lines**, sample data (n = 2); **grey lines**, independent blanks (n = 4).

8.6.2. Overview of the correctly scored negative samples (original and improved method)

Samples screened negative for opioid agonists		
Sample 38	Sample 39	Sample 40
Sample 41	Sample 42	Sample 43
Sample 44	Sample 45	Sample 46

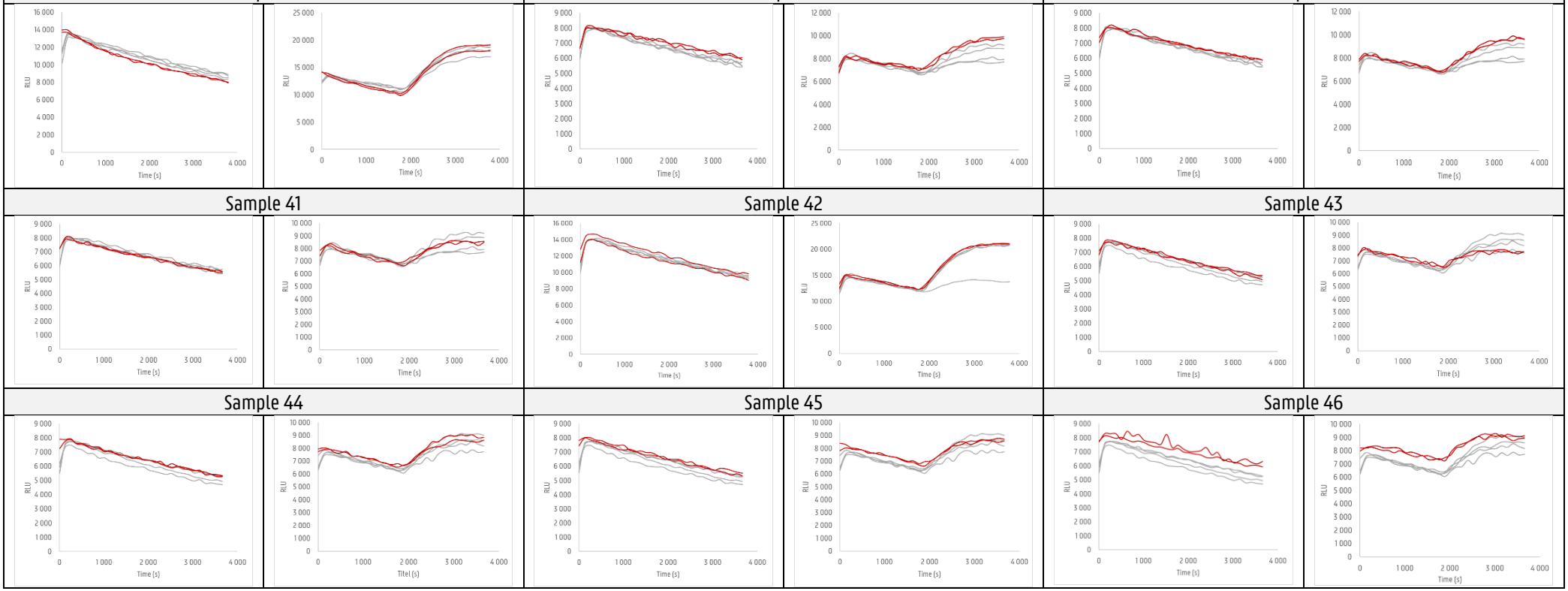

Samples screened negative for opioid agonists (continued)

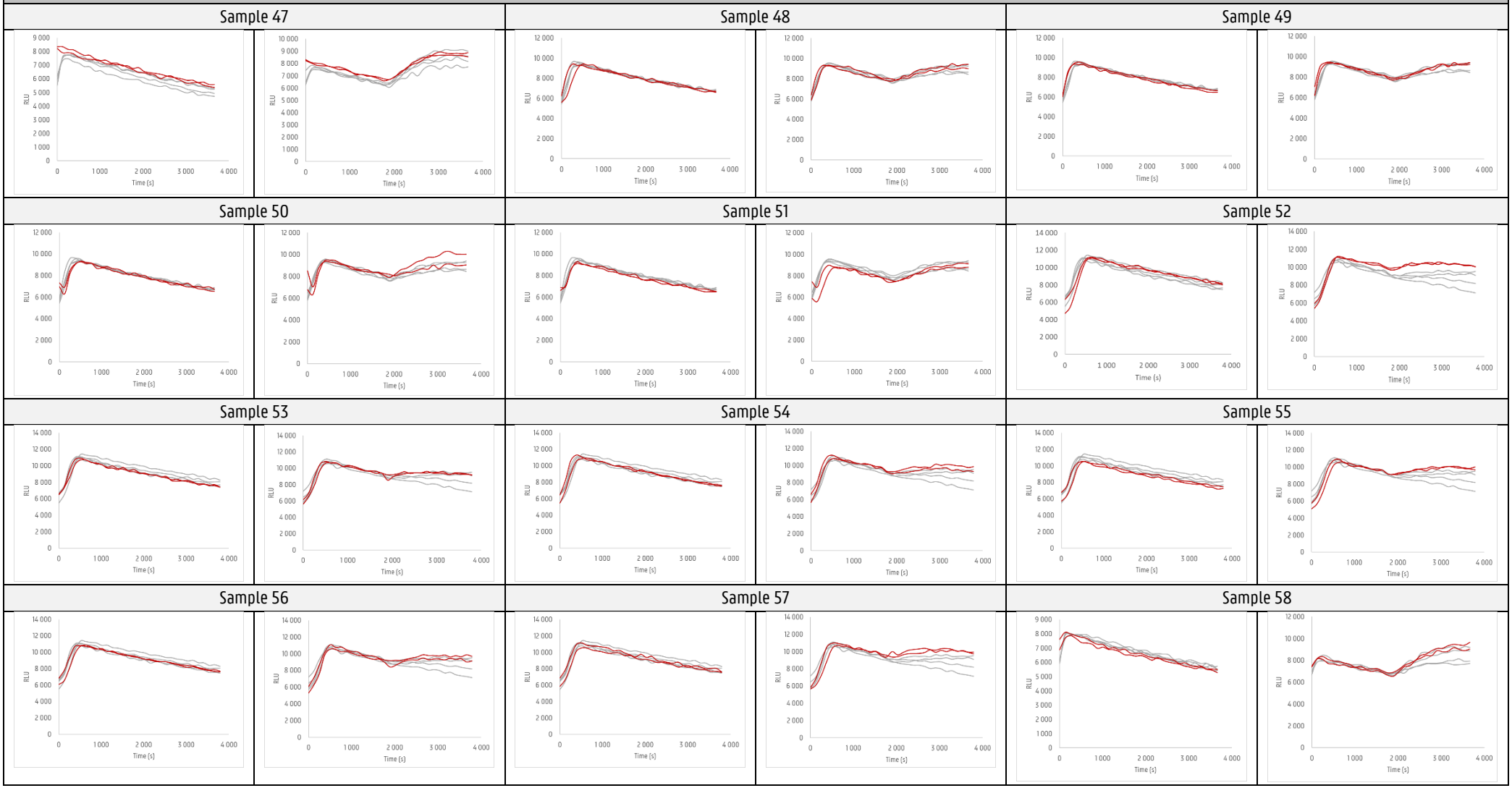

The profiles represent corrected data from the MOR bioassay (1 hour assay time). Each sample is depicted twice, indicating both the original method and the improved method (+ HM injection). x-axis, time in seconds; y-axis, relative light units (RLU) **Legend: Red lines**, sample data (n = 2); **grey lines**, independent blanks (n = 4).

8.6.3. Overview of the correctly scored positive samples for opioid antagonist (original and improved method)

Samples screened positive for opioid antagonists		
Sample 59	Sample 60	Sample 61
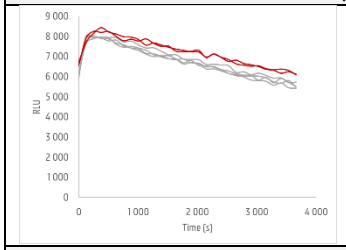 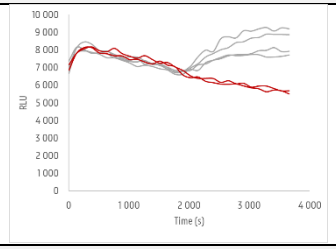	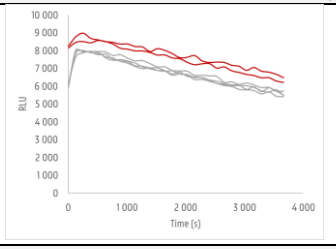 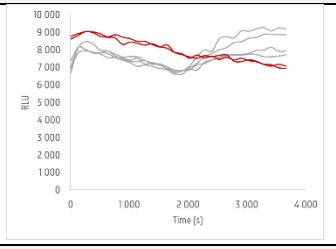	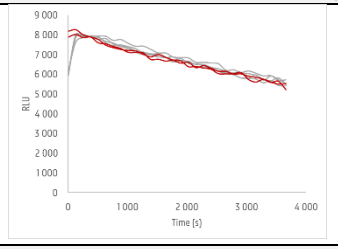 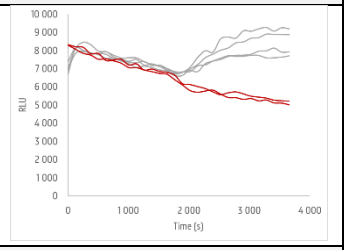
Sample 62	Sample 63	Sample 64
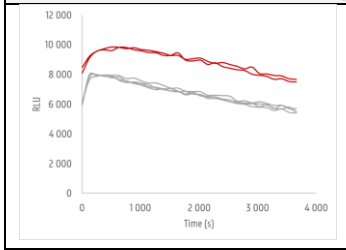 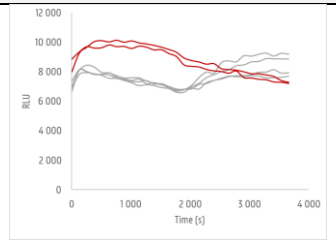	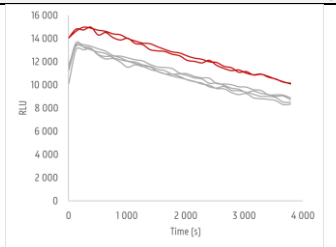 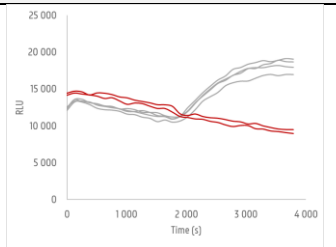	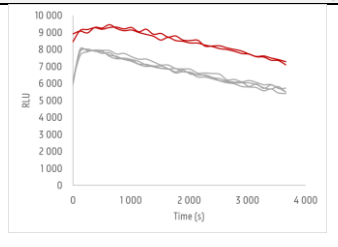 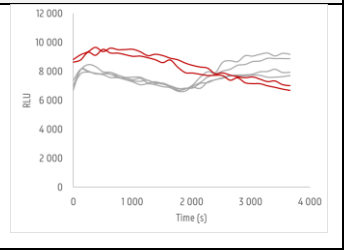
Sample 65	Sample 66	Sample 67
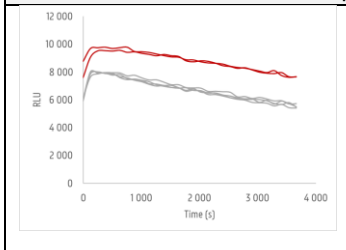 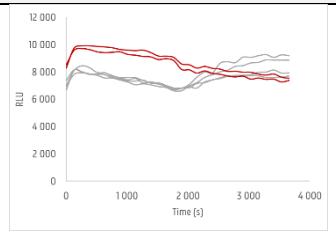	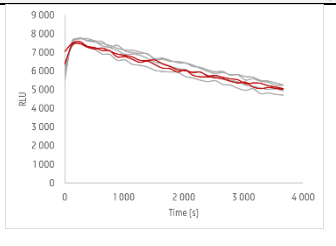 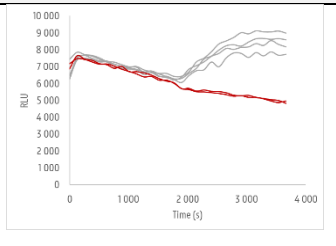	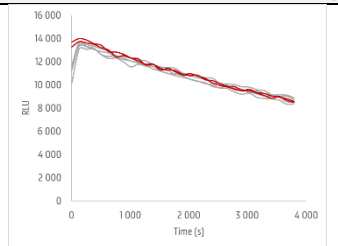 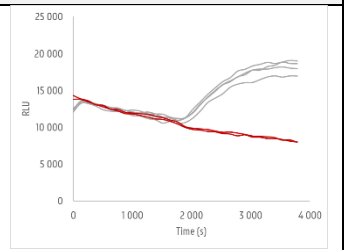
Sample 68	Sample 69	Sample 70
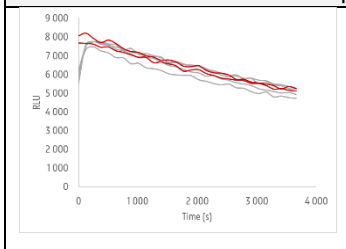 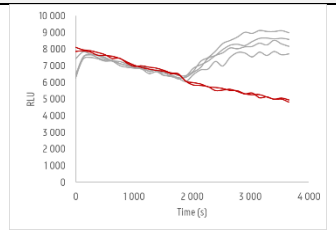	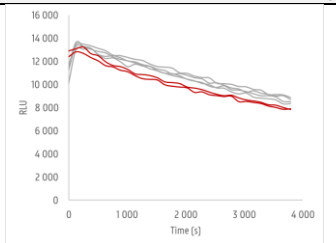 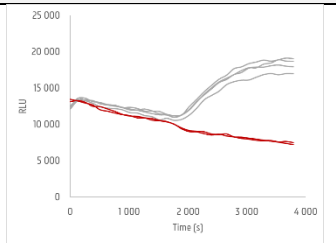	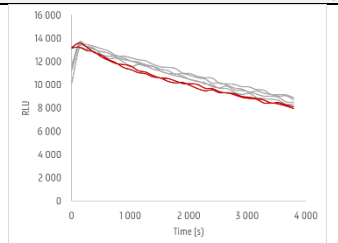 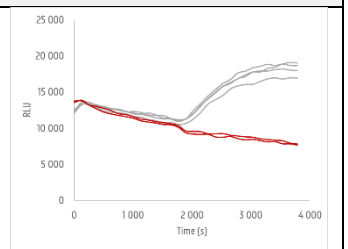

Samples screened positive for opioid antagonists (continued)

Sample 71

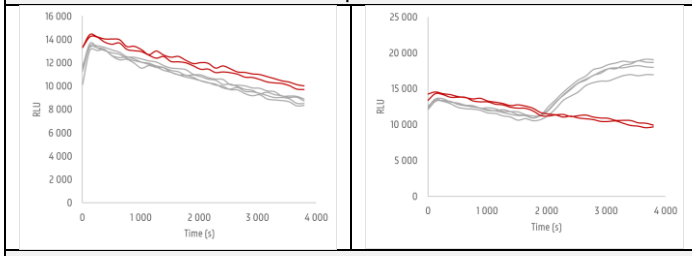

Sample 72

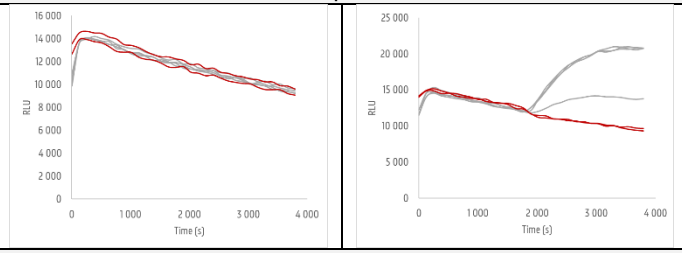

Sample 73

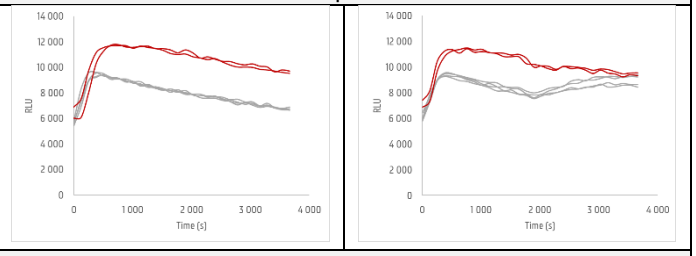

Sample 74

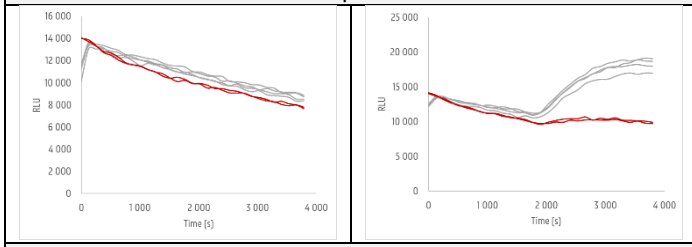

Sample 75

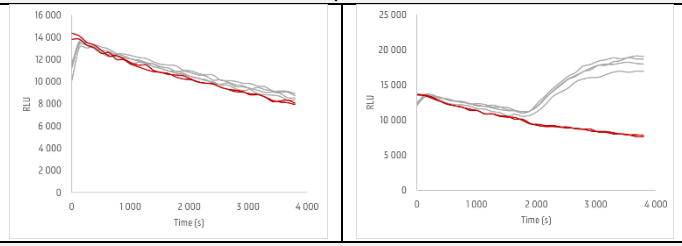

Sample 76

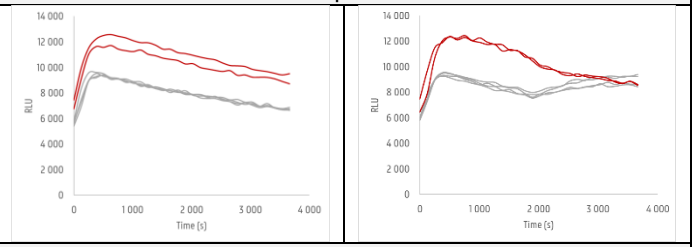

Sample 77

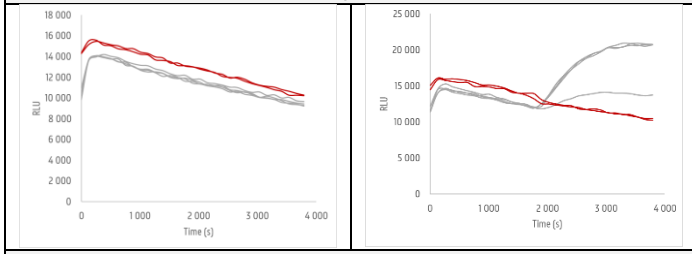

Sample 78

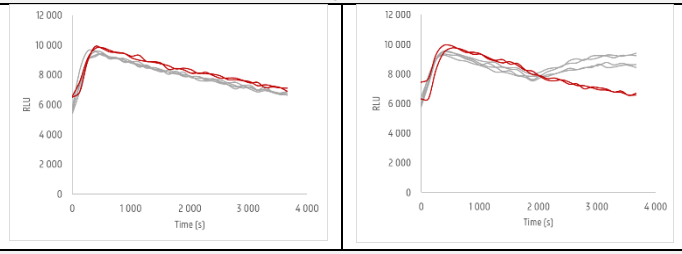

Sample 79

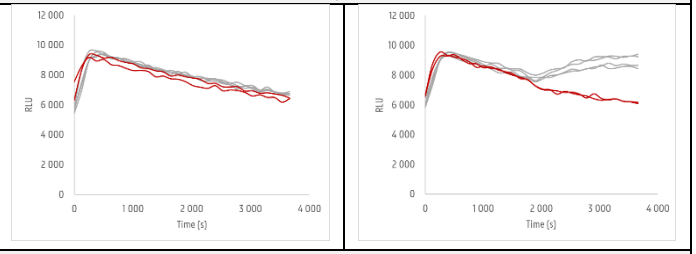

Sample 80

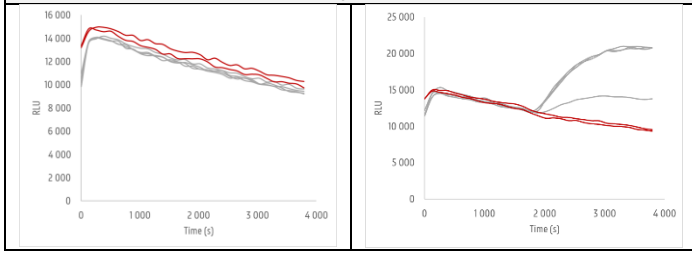

Sample 81

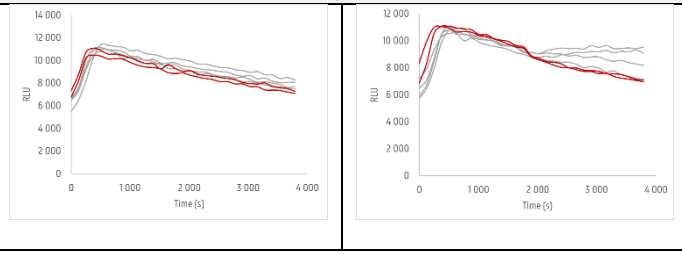

Sample 82

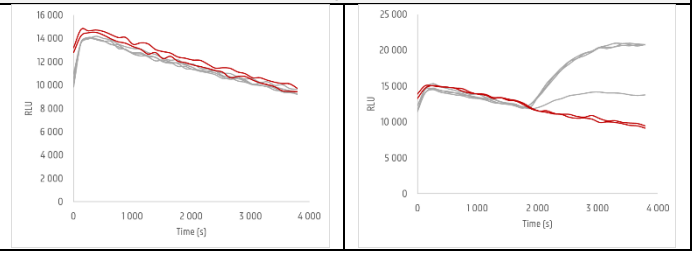

Samples screened positive for opioid antagonists (continued)

Sample 83

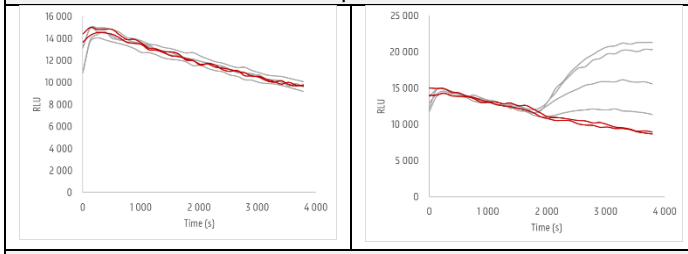

Sample 84

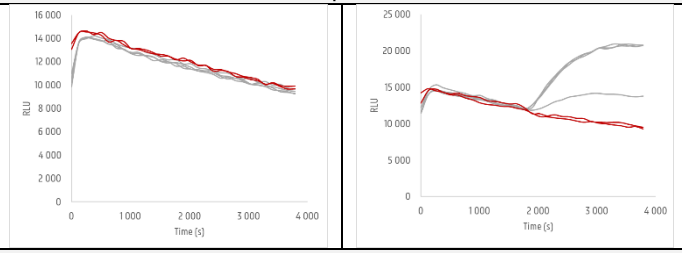

Sample 85

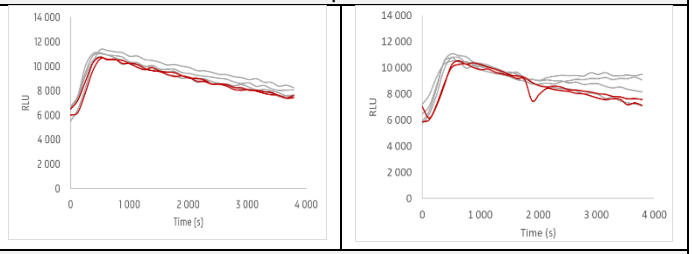

Sample 86

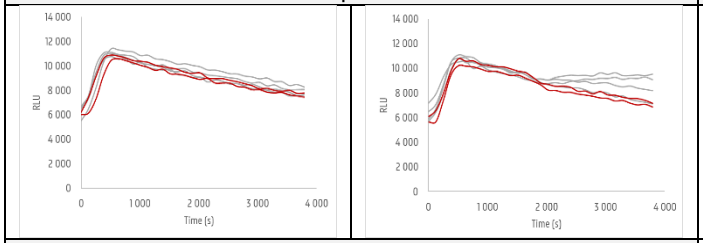

Sample 87

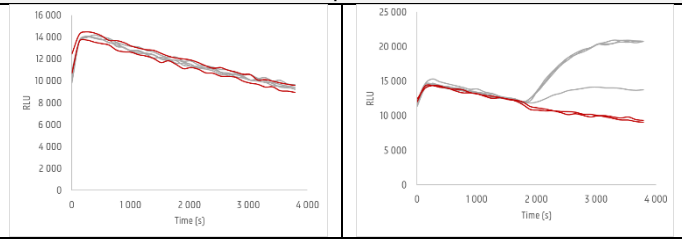

Sample 88

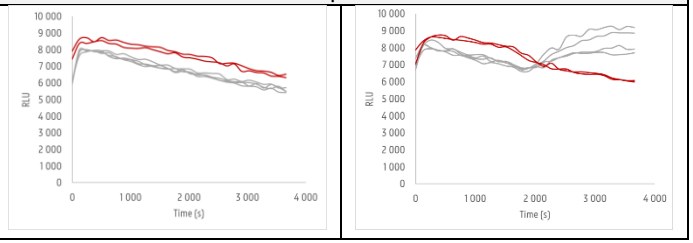

Sample 89

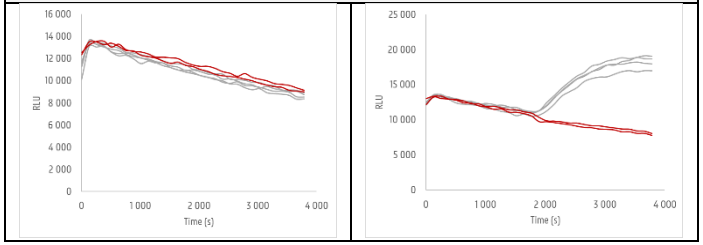

The profiles represent corrected data from the MOR bioassay (1 hour assay time). Each sample is depicted twice, indicating both the original method and the improved method (+ HM injection). x-axis, time in seconds; y-axis, relative light units (RLU) **Legend: Red lines**, sample data (n = 2); **grey lines**, independent blanks (n = 4).

8.6.4. Overview of the falsely scored samples (original and improved method)

Falsely scored samples		
False negative	False positive	False positive for antagonist
Sample 90	Sample 91	Sample 92

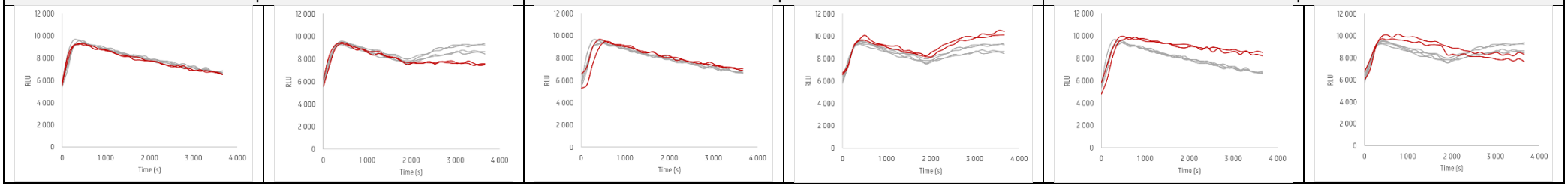

The profiles represent corrected data from the MOR bioassay (1 hour assay time). Each sample is depicted twice, indicating both the original method and the improved method (+ HM injection). x-axis, time in seconds; y-axis, relative light units (RLU) **Legend: Red lines**, sample data (n = 2); **grey lines**, independent blanks (n = 4).

8.6.5. Overview of the samples correctly scored positive for both opioid agonists and antagonists (original and improved method)

Samples explicitly screened positive for both opioid agonists and antagonists	
Sample 93	Sample 94

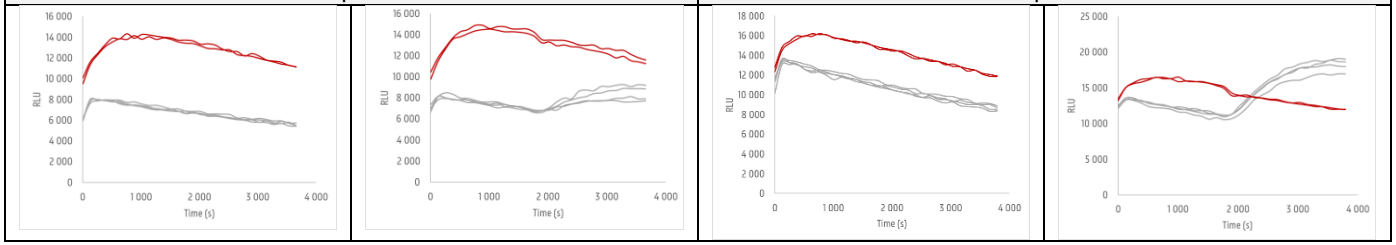

The profiles represent corrected data from the MOR bioassay (1 hour assay time). Each sample is depicted twice, indicating both the original method and the improved method (+ HM injection). x-axis, time in seconds; y-axis, relative light units (RLU) **Legend: Red lines**, sample data (n = 2); **grey lines**, independent blanks (n = 4).

8.7 APPENDIX VII: COMPARISON OF SAMPLES WITH THEIR DUPLICATES

All duplicates were correctly scored. Only profiles of the improved method are displayed.

Samples and their duplicates		
Sample 1	Sample 2	Sample 3
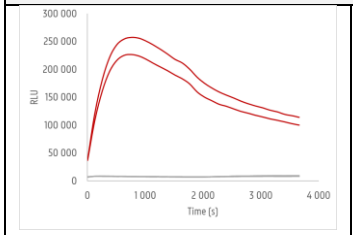 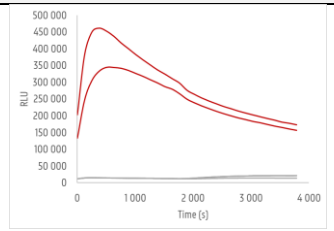	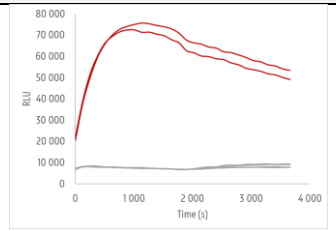	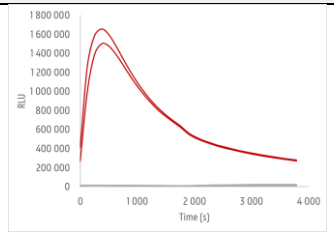 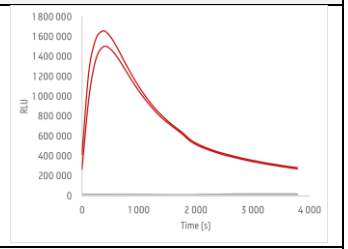
Sample 4	Sample 5	Sample 6
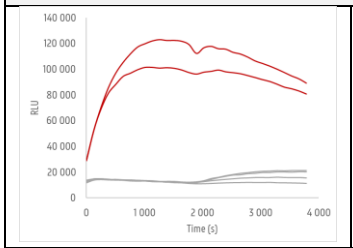 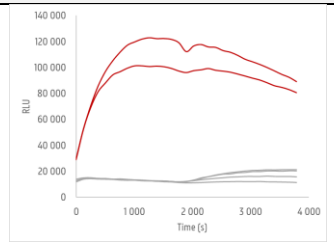	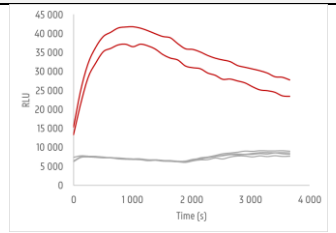	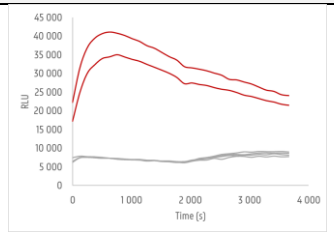
Sample 7	Sample 8	Sample 9
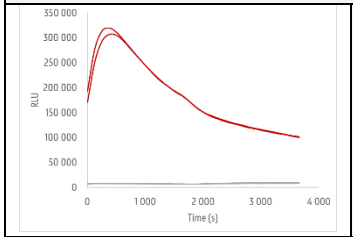	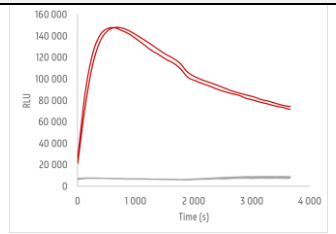	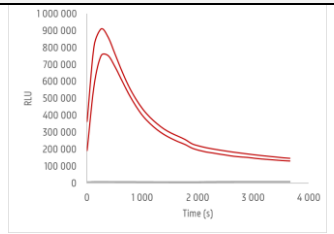
Sample 10	Sample 11	Sample 12
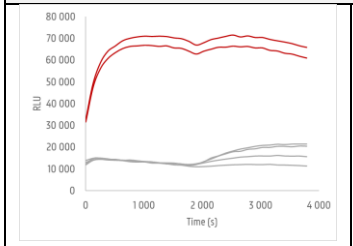 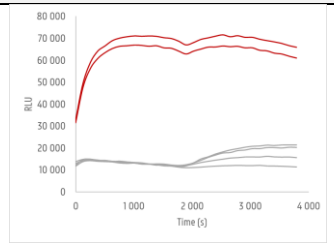	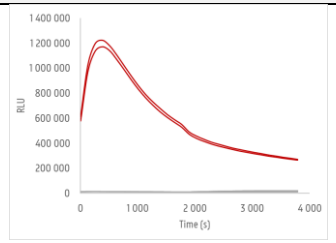 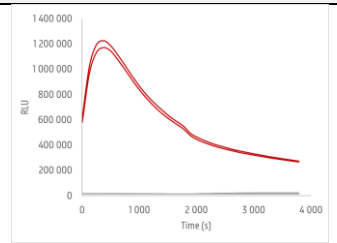	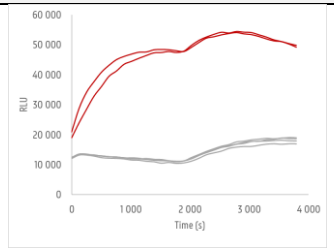 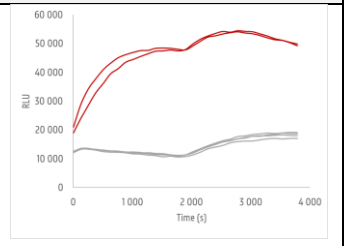

Samples and their duplicates (continued)

Sample 13

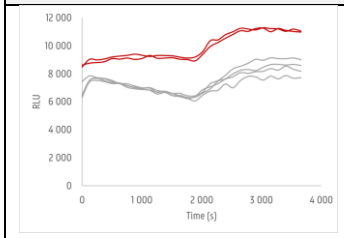

Sample 14

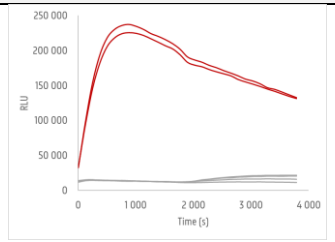

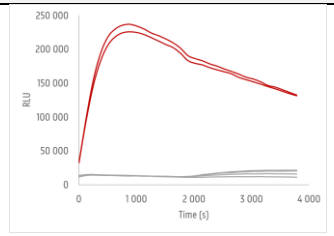

Sample 15

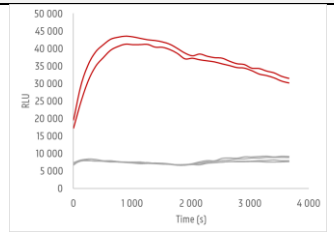

Sample 16

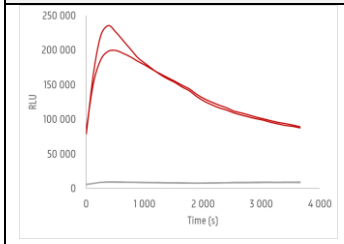

Sample 17

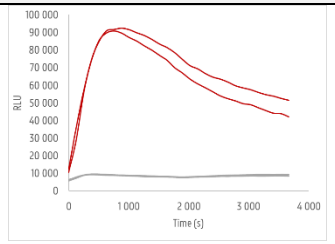

Sample 18

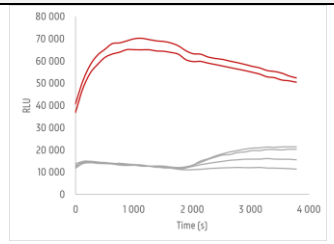

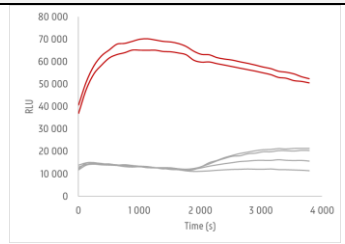

Sample 19

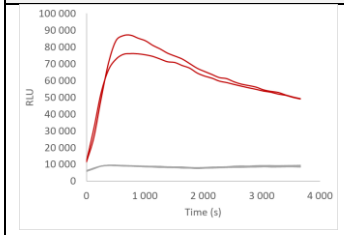

Sample 20

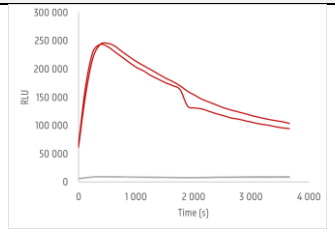

Sample 21

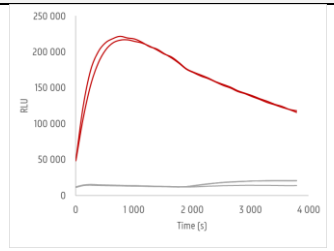

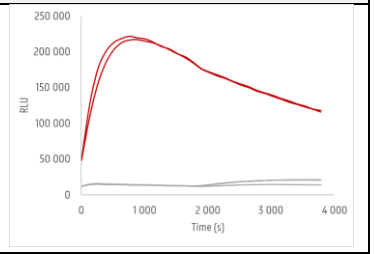

Sample 22

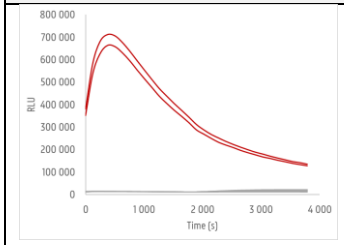

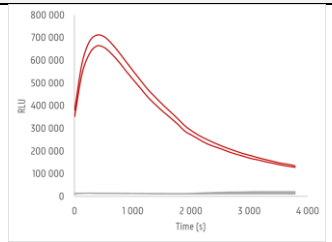

Sample 23

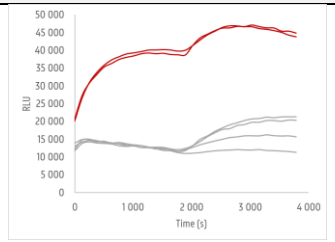

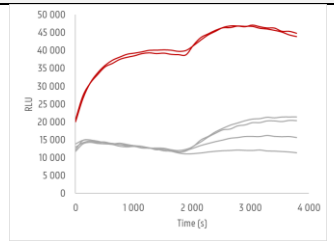

Sample 24

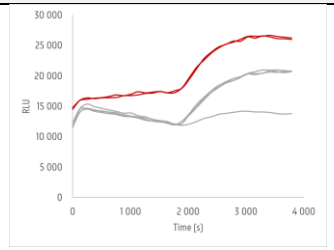

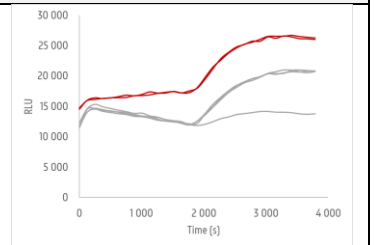

Samples and their duplicates (continued)		
Sample 25	Sample 26	Sample 27
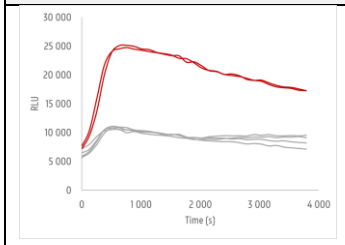	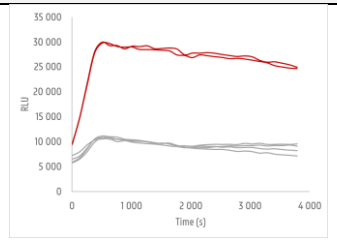 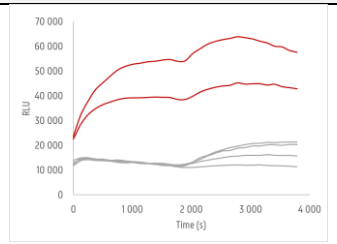	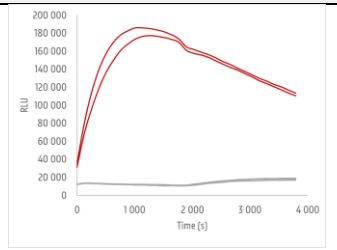 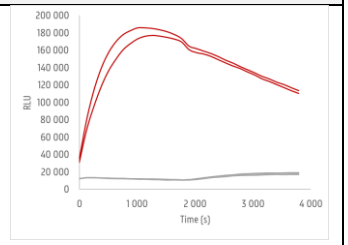
Sample 28	Sample 29	Sample 30
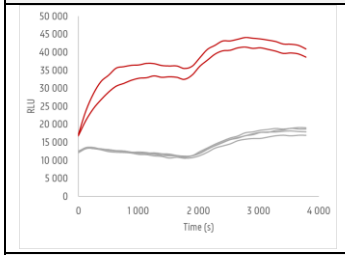	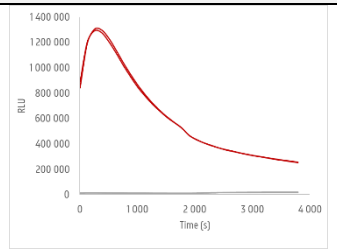	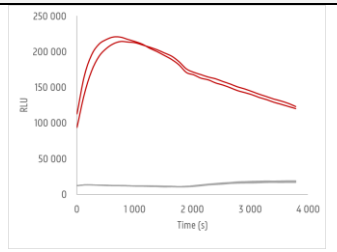
Sample 31	Sample 32	Sample 33
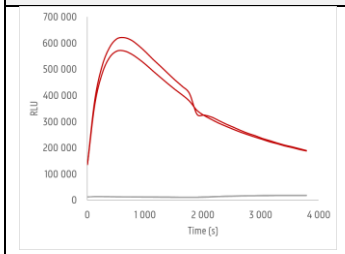	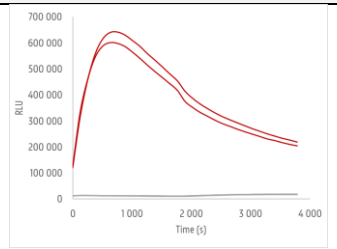	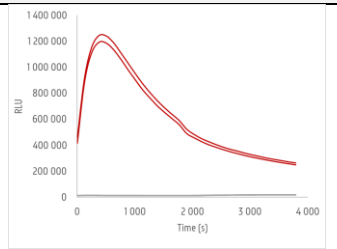
Sample 34	Sample 35	Sample 36
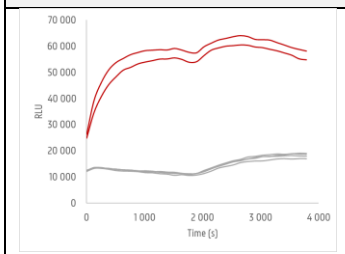	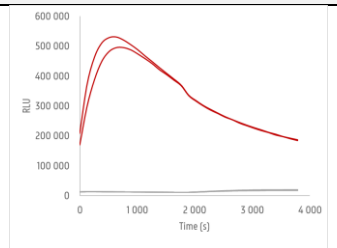	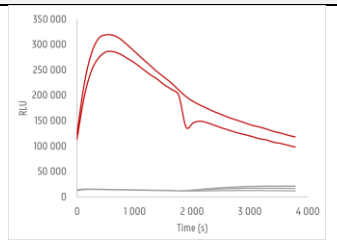

Samples and their duplicates (continued)

Sample 37

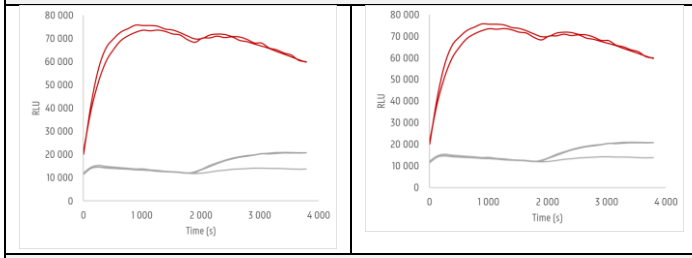

Sample 38

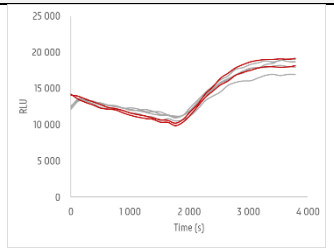

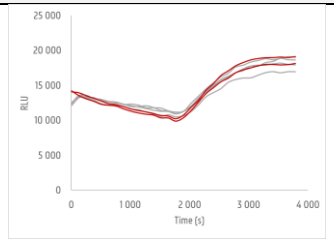

Sample 39

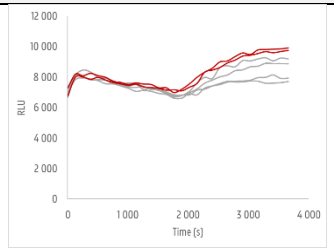

Sample 40

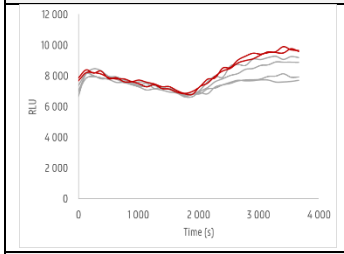

Sample 41

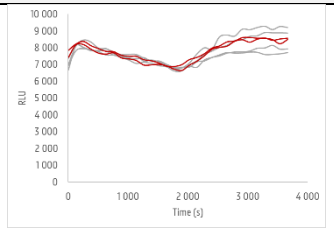

Sample 42

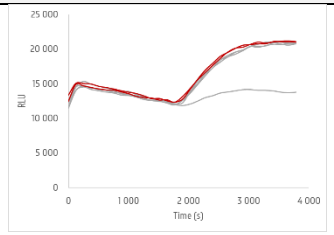

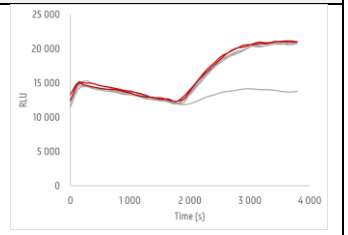

Sample 43

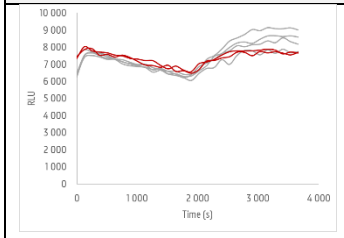

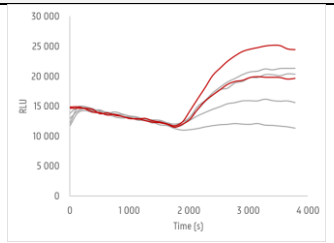

Sample 44

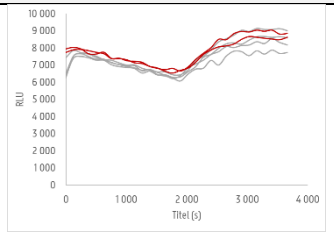

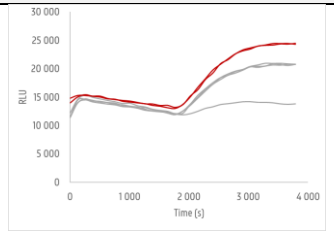

Sample 45

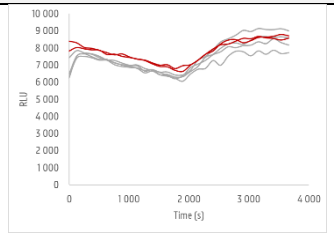

Sample 46

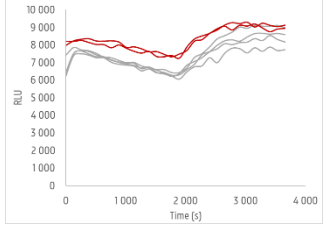

Sample 47

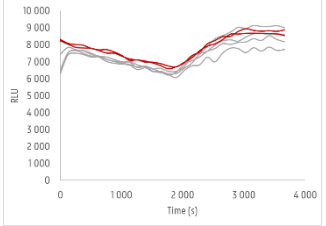

Sample 48

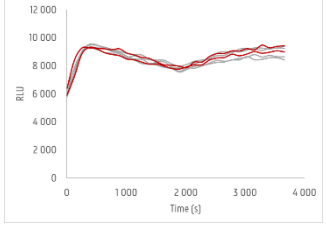

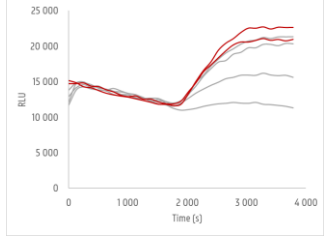

Samples and their duplicates (continued)

Sample 49

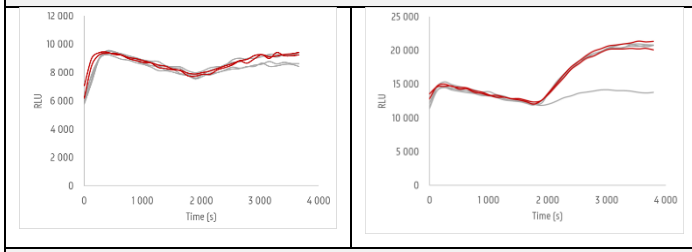

Sample 50

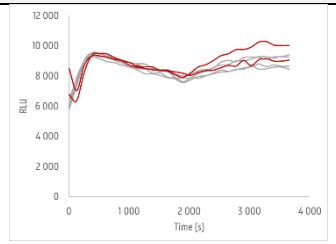

Sample 51

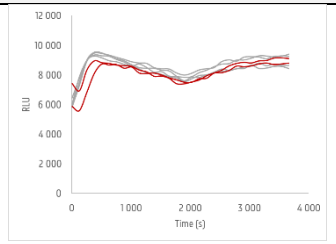

Sample 52

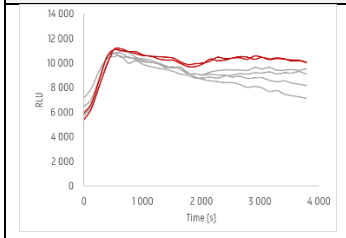

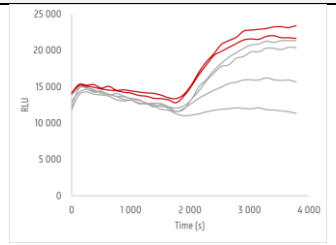

Sample 53

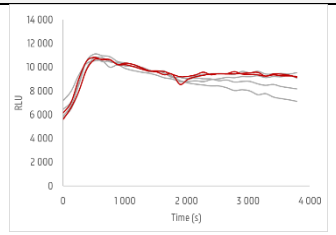

Sample 54

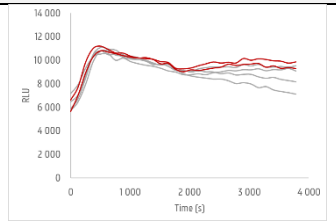

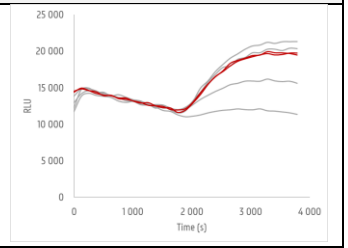

Sample 55

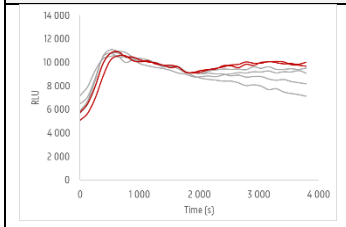

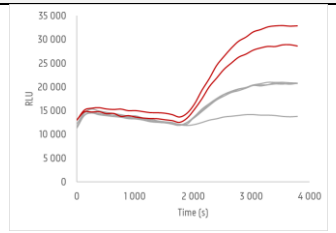

Sample 56

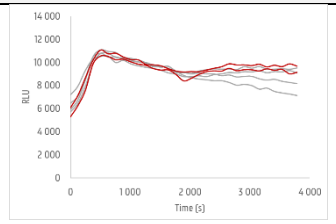

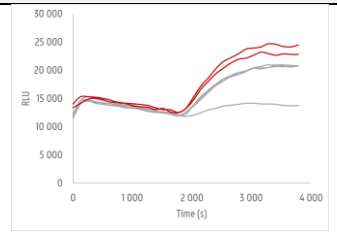

Sample 57

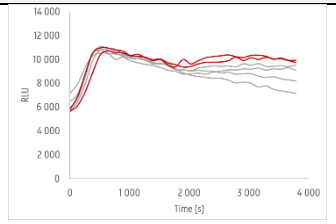

Sample 58

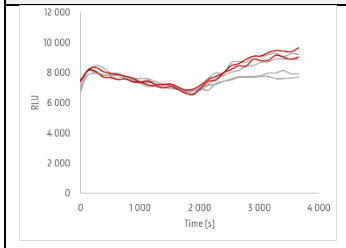

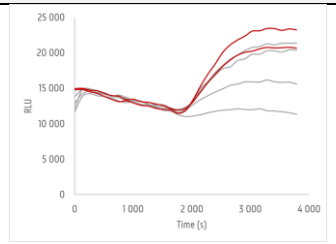

Sample 59

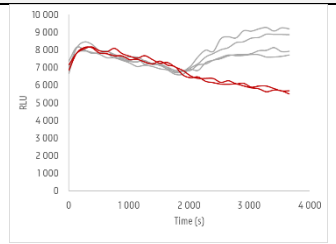

Sample 60

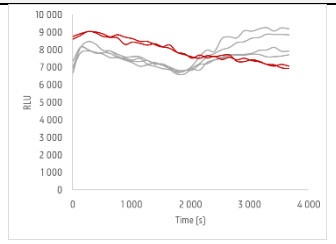

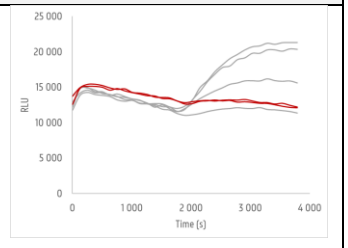

Samples and their duplicates (continued)

Sample 61		Sample 62		Sample 63	
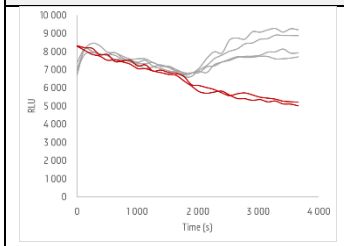		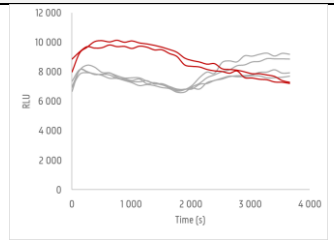		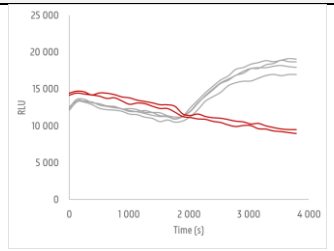	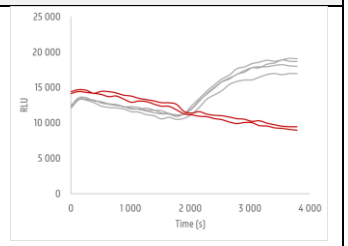
Sample 64		**Sample 65**		**Sample 66**	
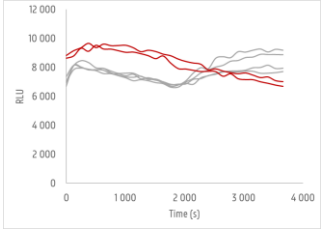		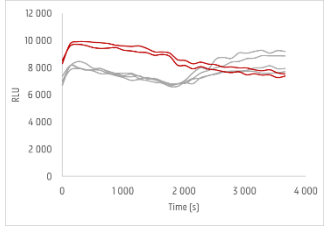	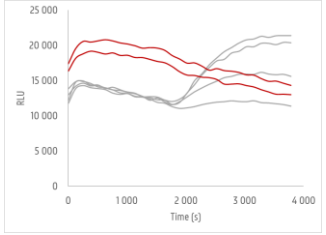	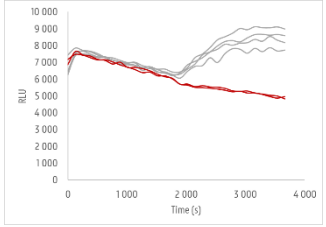	x
Sample 67		**Sample 68**		**Sample 69**	
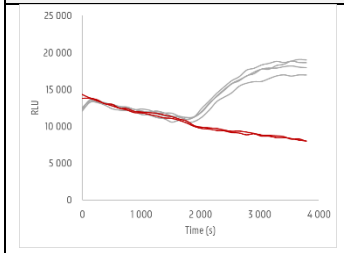	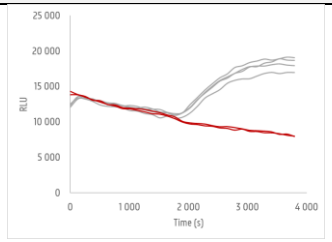	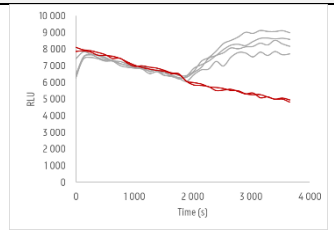		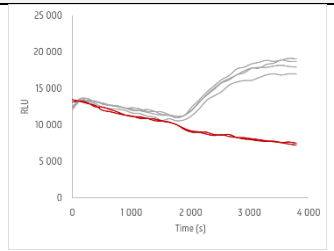	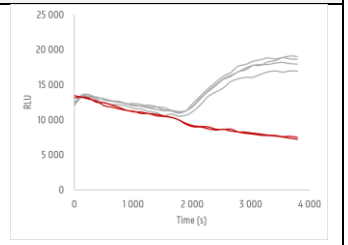
Sample 70		**Sample 71**		**Sample 72**	
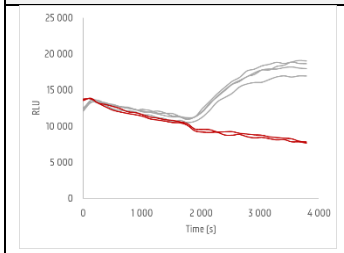	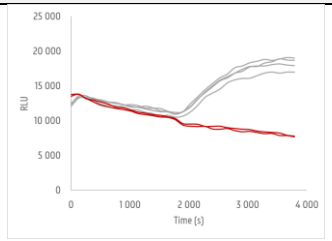	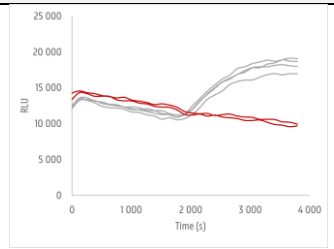	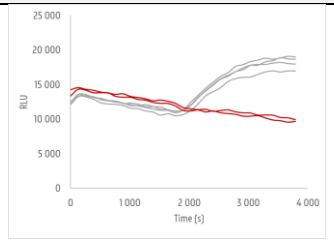	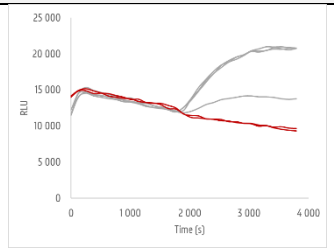	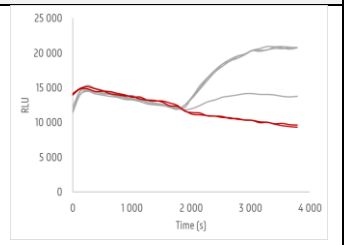

Samples and their duplicates (continued)

Sample 73

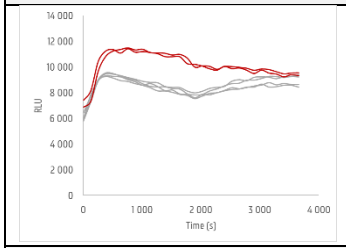

Sample 74

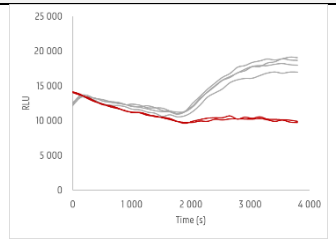

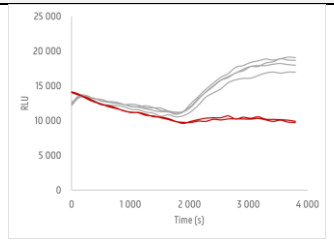

Sample 75

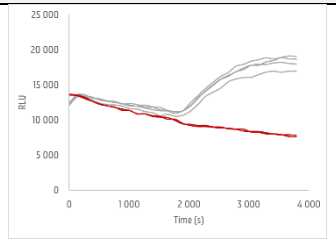

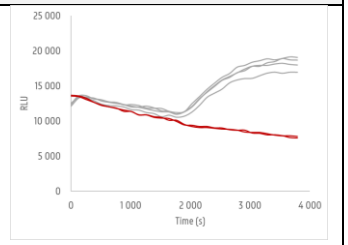

Sample 76

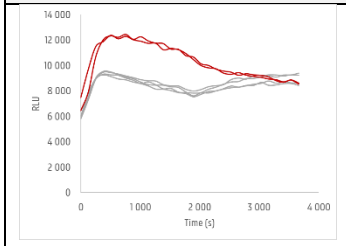

Sample 77

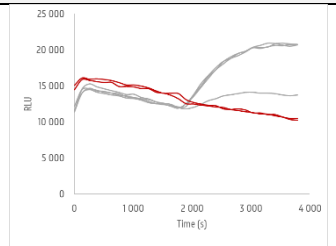

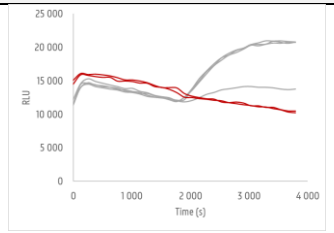

Sample 78

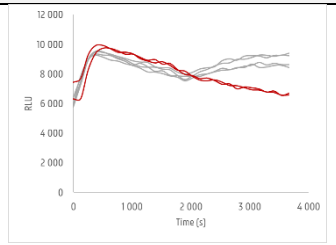

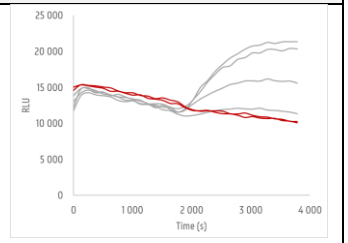

Sample 79

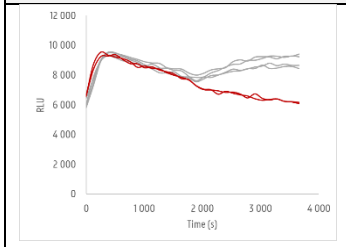

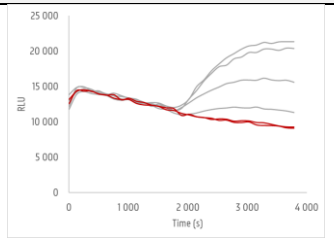

Sample 80

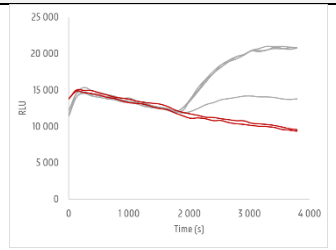

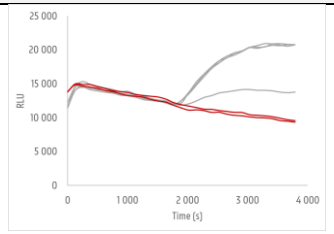

Sample 81

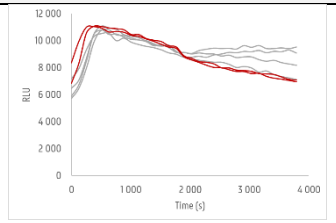

Sample 82

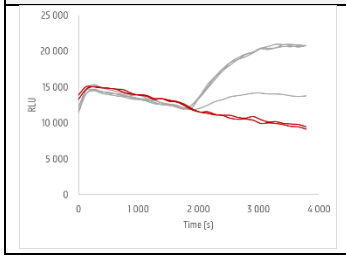

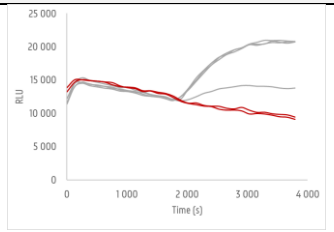

Sample 83

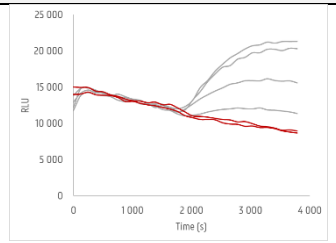

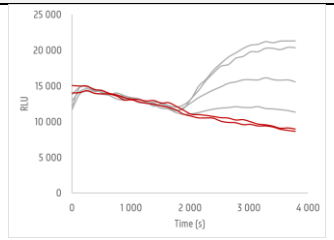

Sample 84

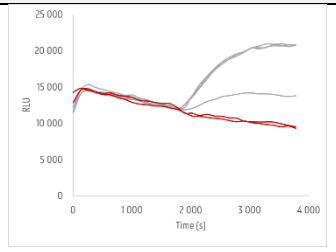

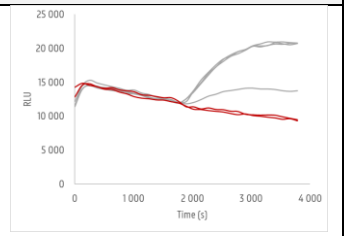

XXX

Samples and their duplicates (continued)		
Sample 85	Sample 86	Sample 87
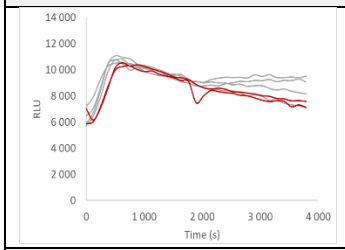	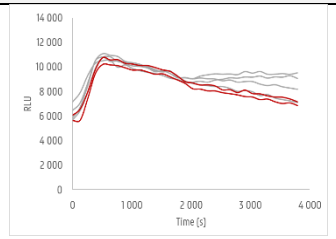	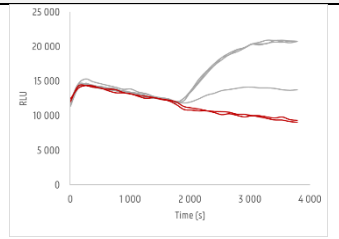 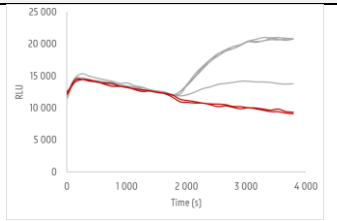
Sample 88	Sample 89	Sample 90
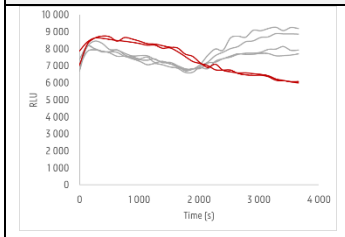	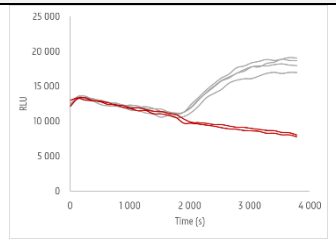	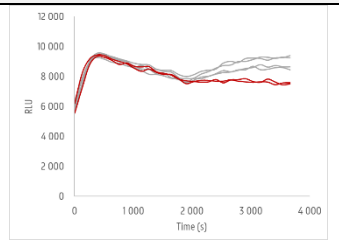
Sample 91	Sample 92	Sample 93
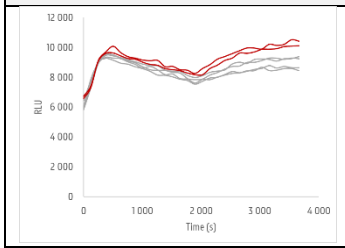	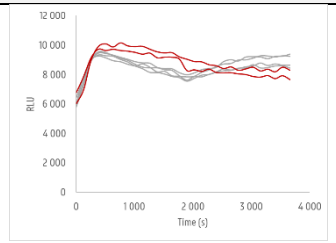	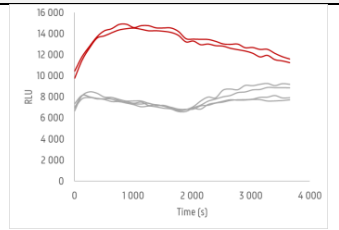
Sample 94		
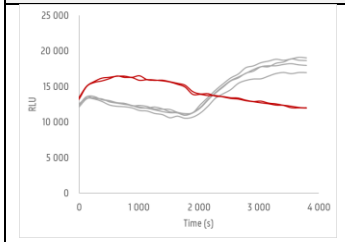		

The profiles represent corrected data from the improved MOR bioassay (1 hour assay time). x-axis, time in seconds; y-axis, relative light units (RLU) **Legend: Red lines**, sample data (n = 2); **grey lines**, independent blanks (n = 4).

8.8 APPENDIX VIII: OVERVIEW OF THE PROFILES OBTAINED FROM 2 HOUR ASSAY TIME

Sample profiles (2 hour bioassay)					
Sample 1	Sample 2	Sample 3	Sample 4	Sample 5	Sample 6
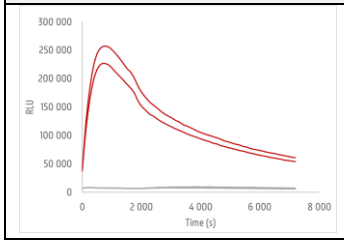	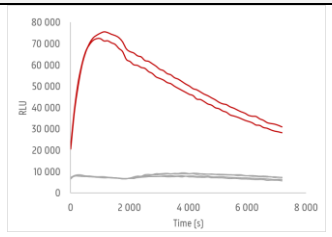	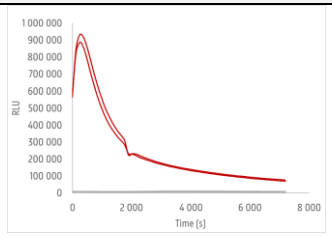	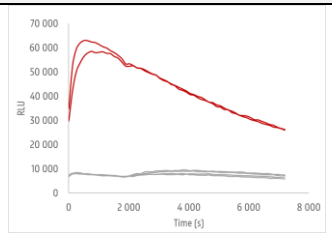	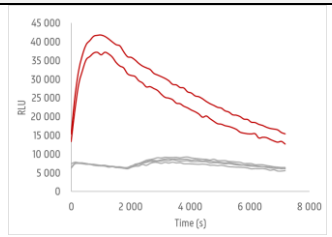	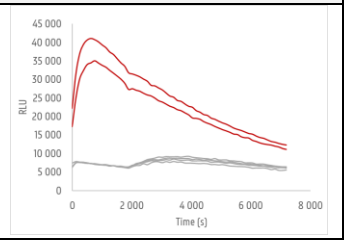
Sample 7	Sample 8	Sample 9	Sample 10	Sample 11	Sample 12
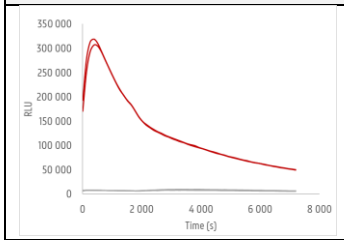	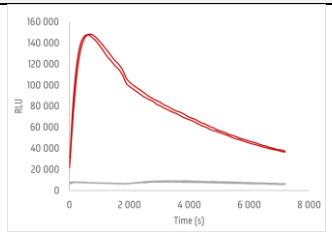	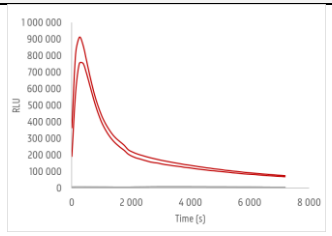	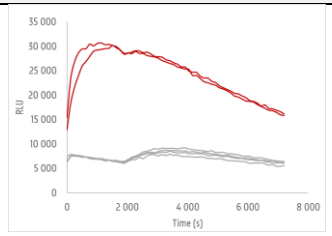	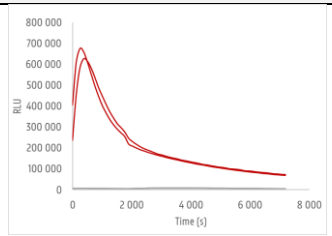	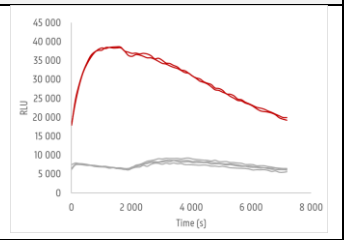
Sample 13	Sample 14	Sample 15	Sample 16	Sample 17	Sample 18
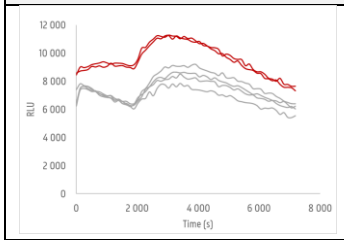	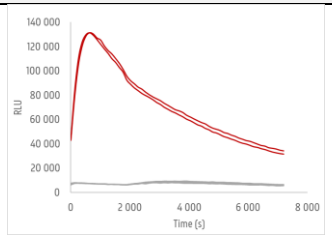	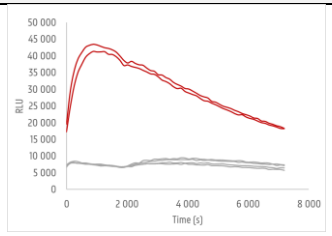	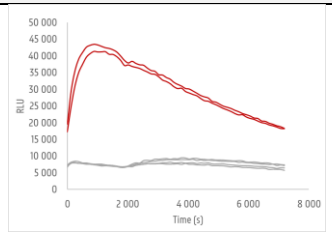	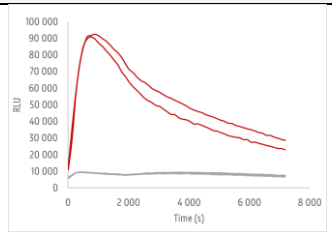	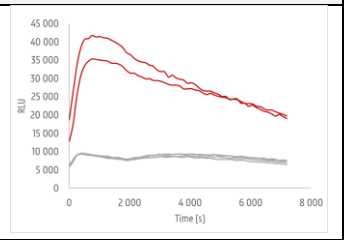
Sample 19	Sample 20	Sample 21	Sample 22	Sample 23	Sample 24
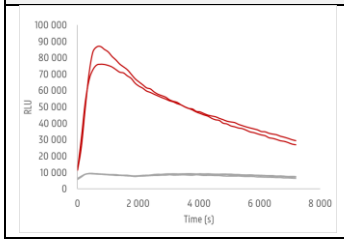	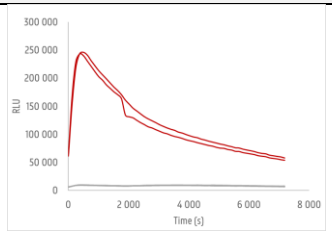	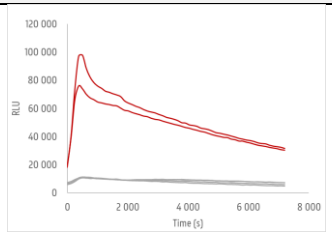	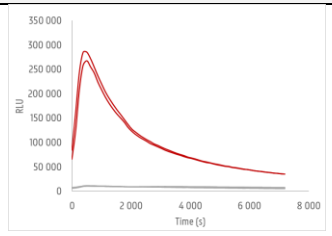	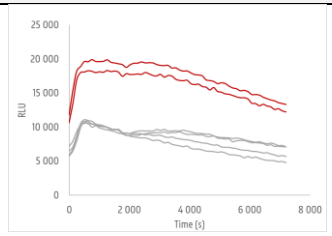	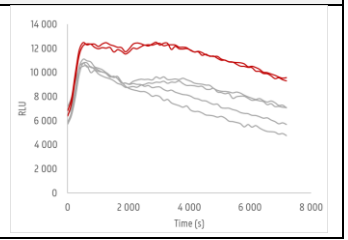

Sample profiles (2 hour bioassay) (continued)					
Sample 25	Sample 26	Sample 27	Sample 28	Sample 29	Sample 30
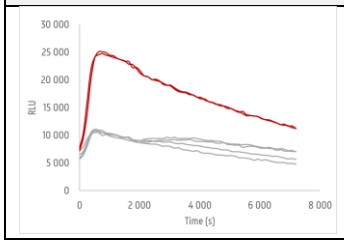	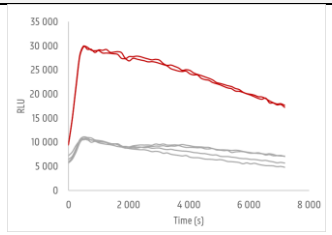	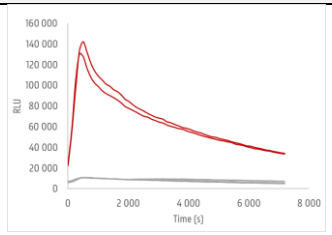	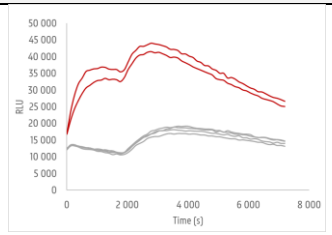	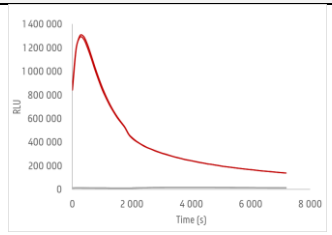	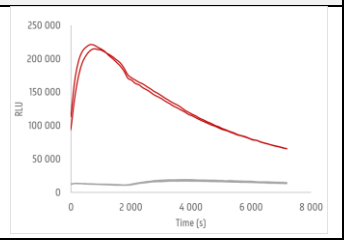
Sample 31	Sample 32	Sample 33	Sample 34	Sample 35	Sample 36
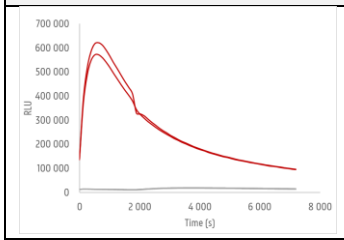	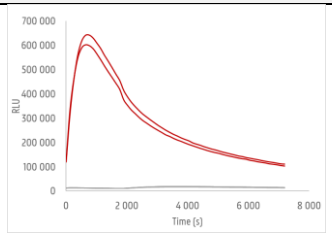	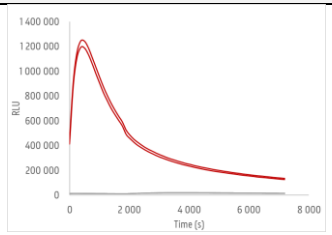	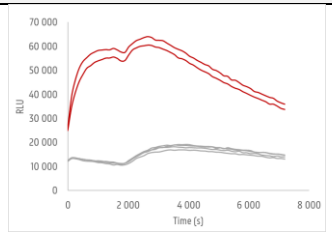	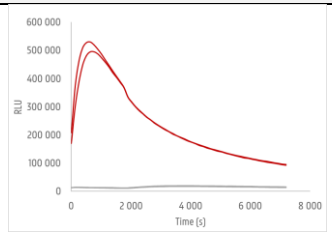	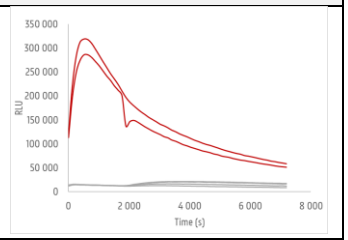
Sample 37	Sample 38	Sample 39	Sample 40	Sample 41	Sample 42
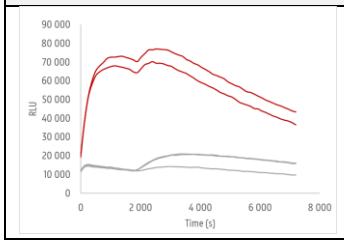	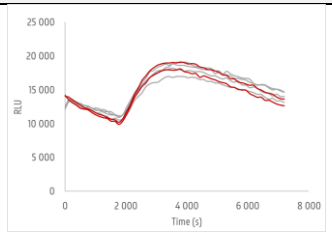	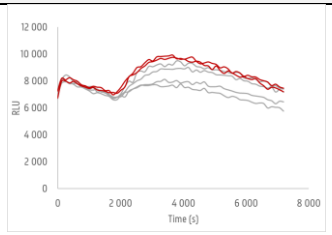	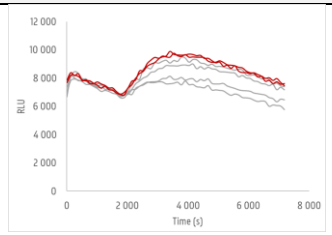	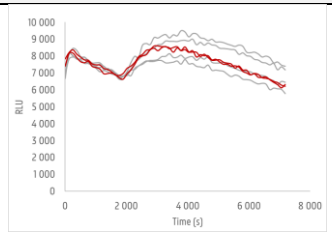	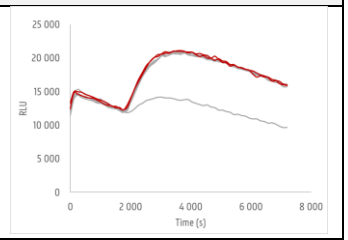
Sample 43	Sample 44	Sample 45	Sample 46	Sample 47	Sample 48
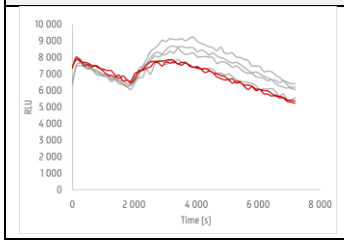	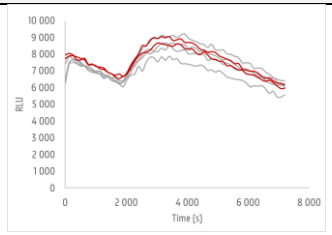	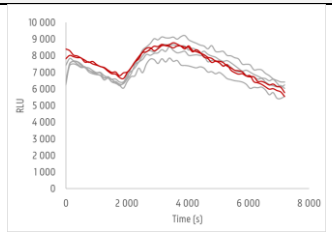	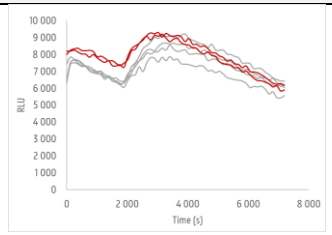	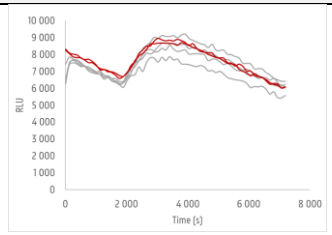	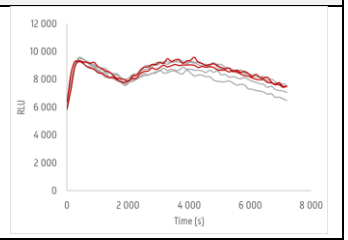

Sample profiles (2 hour bioassay) (continued)					
Sample 49	Sample 50	Sample 51	Sample 52	Sample 53	Sample 54
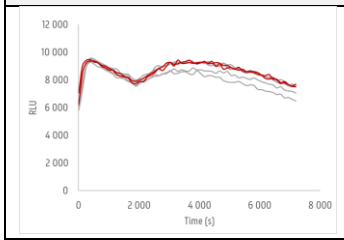	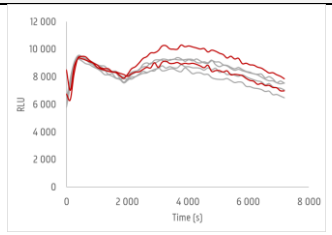	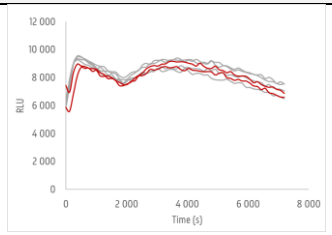	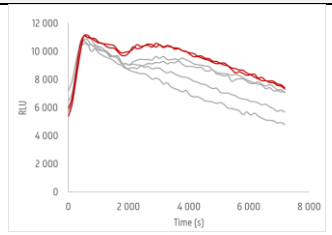	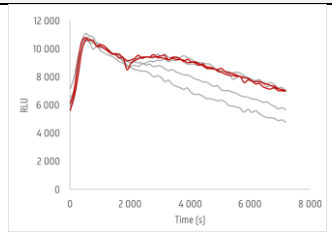	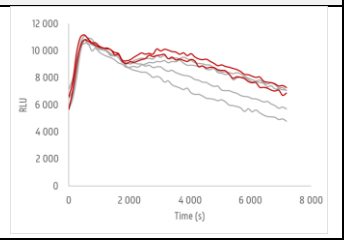
Sample 55	Sample 56	Sample 57	Sample 58	Sample 59	Sample 60
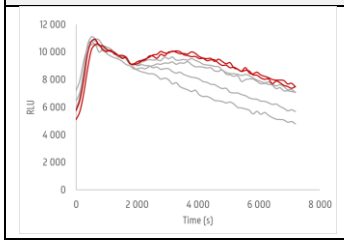	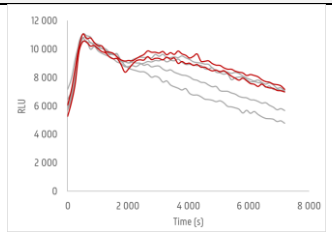	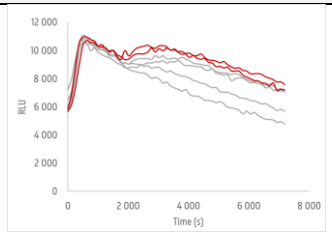	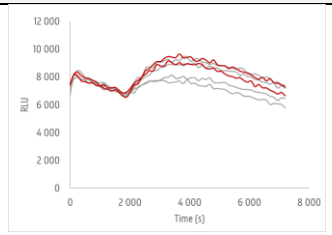	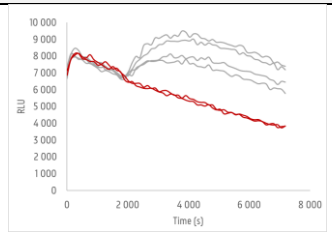	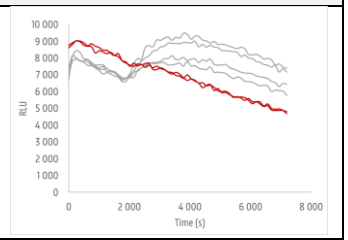
Sample 61	Sample 62	Sample 63	Sample 64	Sample 65	Sample 66
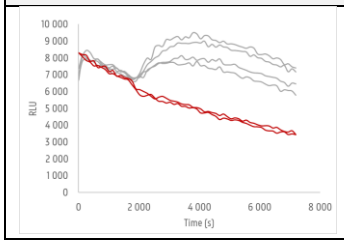	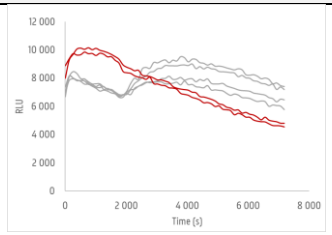	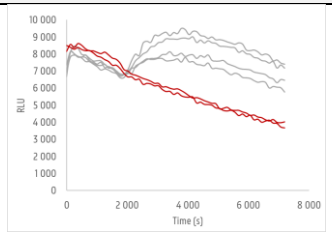	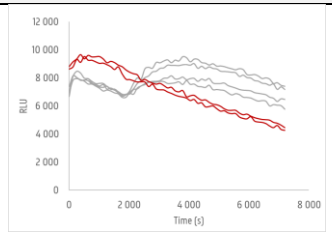	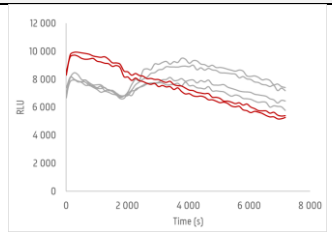	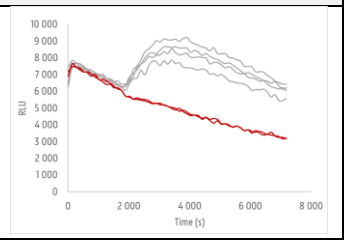
Sample 67	Sample 68	Sample 69	Sample 70	Sample 71	Sample 72
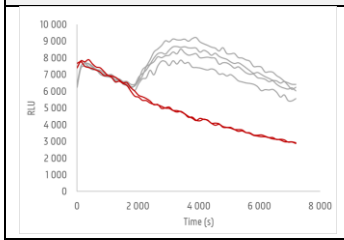	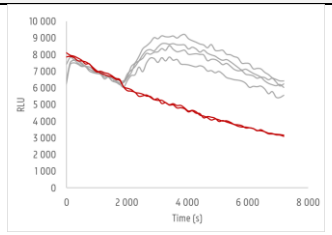	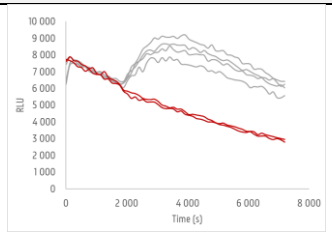	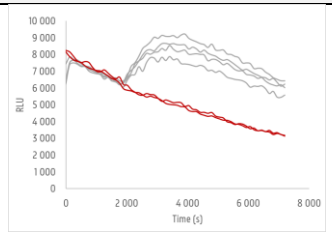	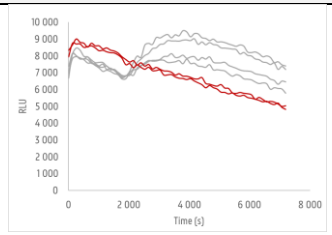	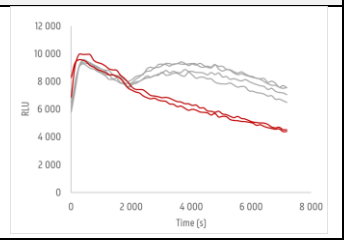

Sample profiles (2 hour bioassay) (continued)					
Sample 73	Sample 74	Sample 75	Sample 76	Sample 77	Sample 78
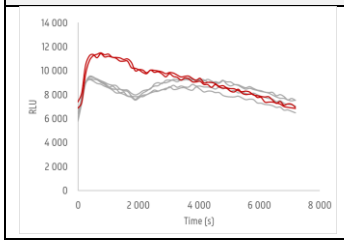	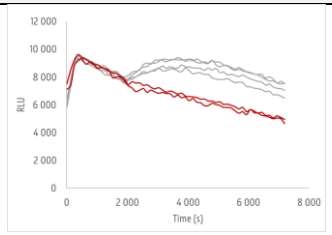	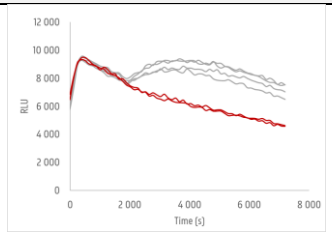	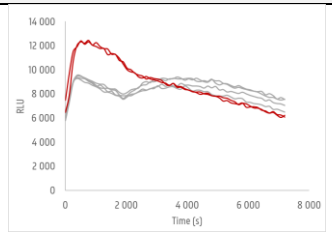	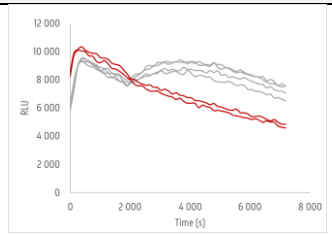	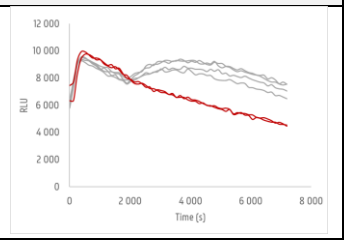
Sample 79	Sample 80	Sample 81	Sample 82	Sample 83	Sample 84
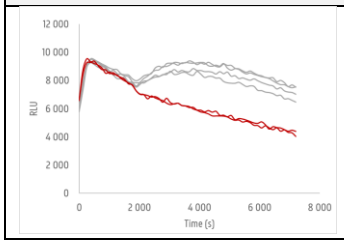	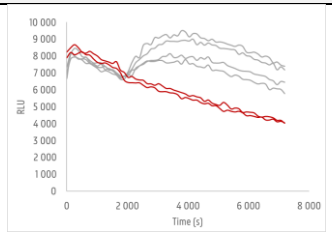	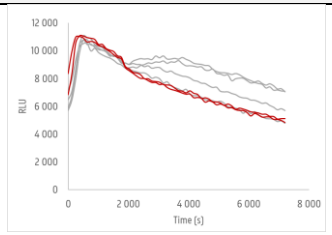	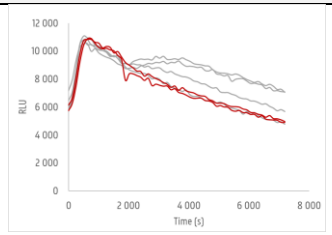	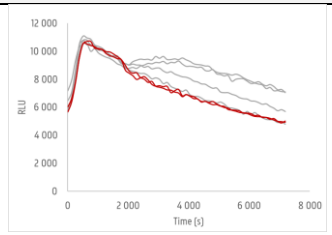	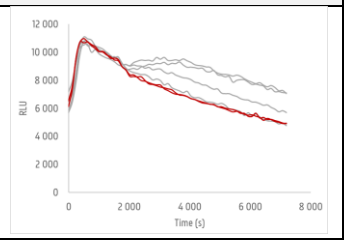
Sample 85	Sample 86	Sample 87	Sample 88	Sample 89	Sample 90
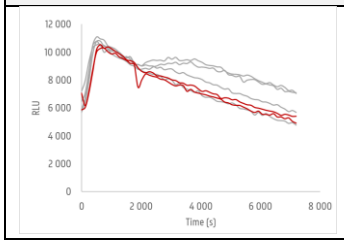	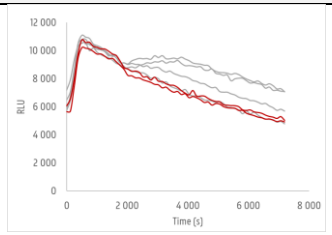	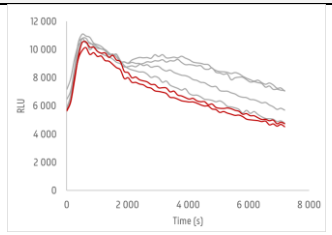	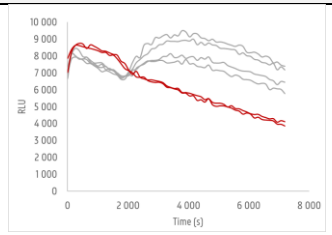	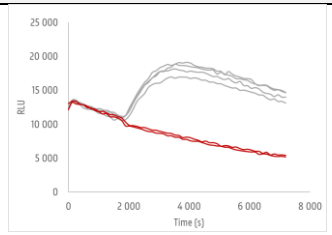	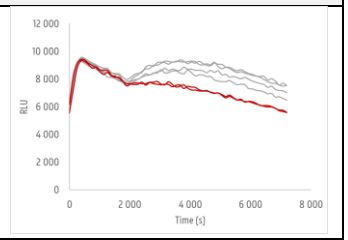
Sample 91	Sample 92	Sample 93	Sample 94		
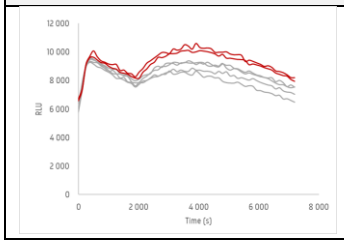	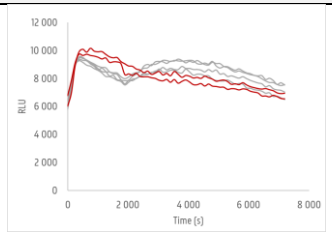	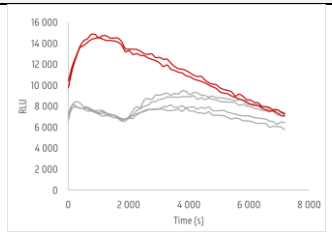	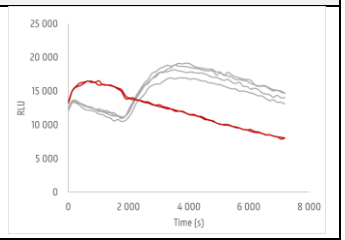		

The profiles represent corrected data from the improved MOR bioassay (2 hour assay time). x-axis, time in seconds; y-axis, relative light units (RLU) **Legend: Red lines**, sample data (n = 2); **grey lines**, independent blanks (n = 4).

8.9 APPENDIX IX: OVERVIEW OF THE OBTAINED CONCENTRATION-RESPONSE CURVES FOR THE SYNTHETIC OPIOIDS

Curves were generated using the GraphPad Prism software (San Diego, CA, USA).

Concentration-response curves: Fentanyl analogues and synthetic opioids

Hydromorphone

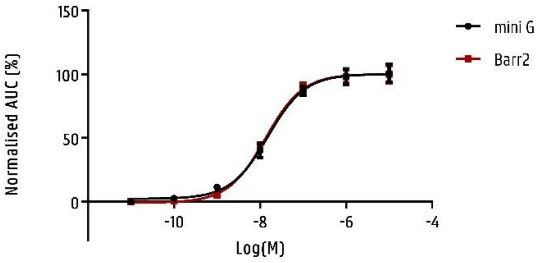

4-fluoroisobutrylfentanyl hydrochloride

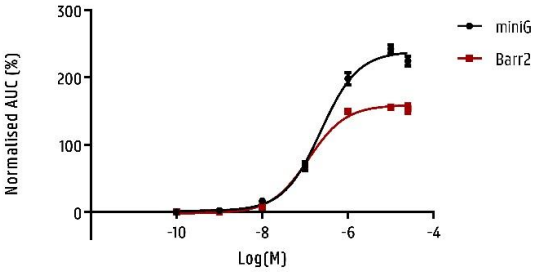

4-methoxybutyrfentanyl

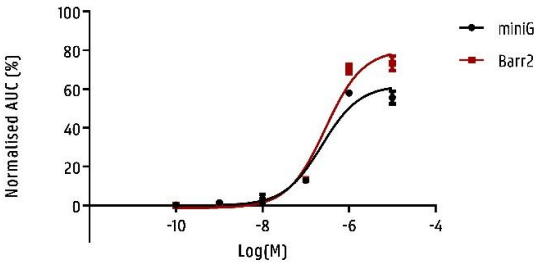

Acetylfentanyl

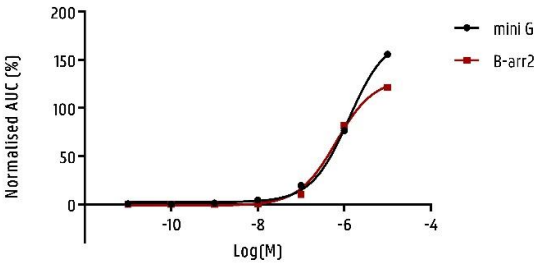

Acrylfentanyl hydrochloride

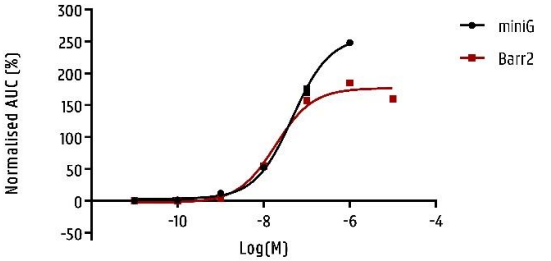

AH-7921

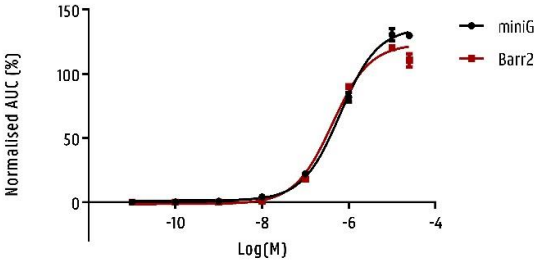

Alfentanil hydrochloride

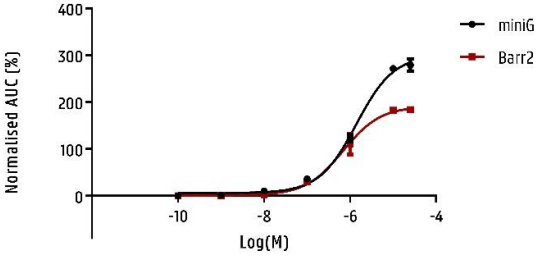

Benzoylfentanyl

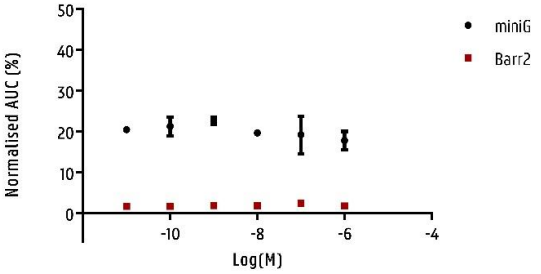

Butyrylfentanyl hydrochloride

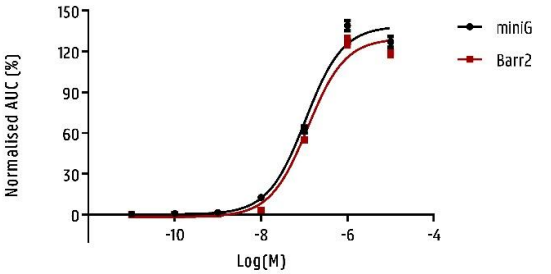

Crotonylfentanyl

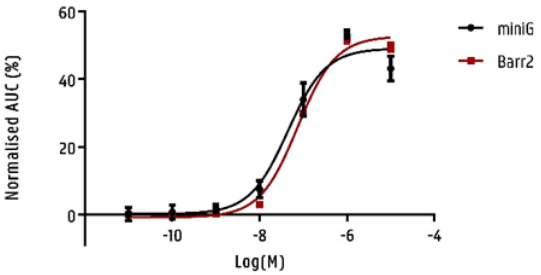

Concentration-response curves: Fentanyl analogues and synthetic opioids (continued)

Cyclopentylfentanyl hydrochloride

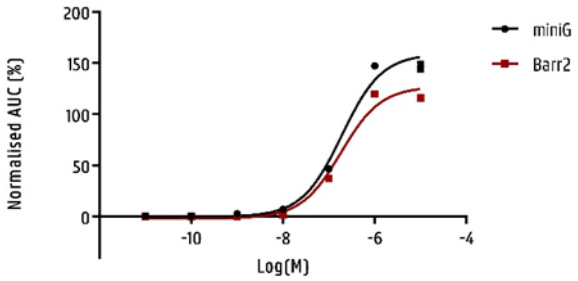

Cyclopropylfentanyl

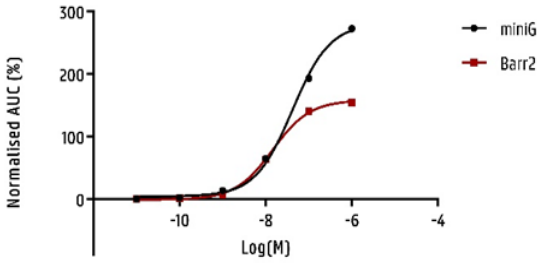

Fentanyl

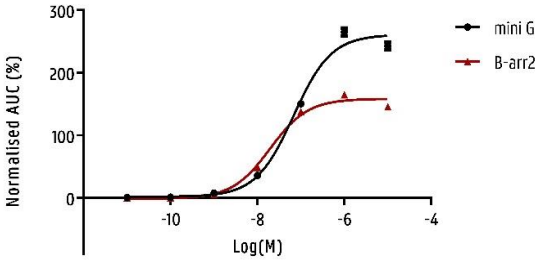

Furanylfentanyl hydrochloride

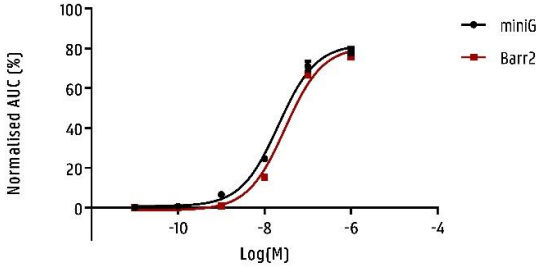

Methoxyacetylfentanyl hydochloride

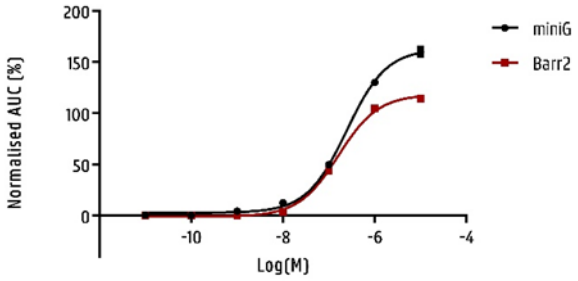

Ocfentanil hydrochloride

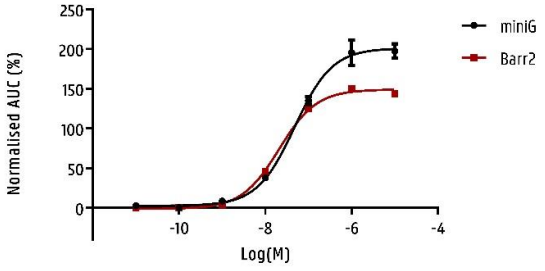

Phenylpropionylfentanyl

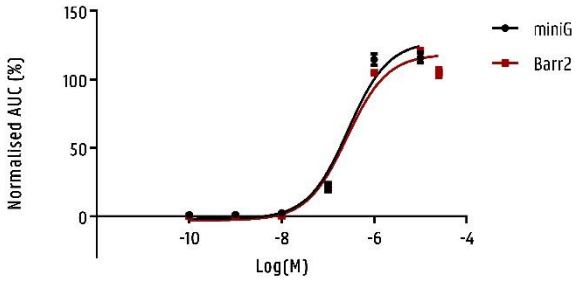

Tetrahydrofuranylfentanyl

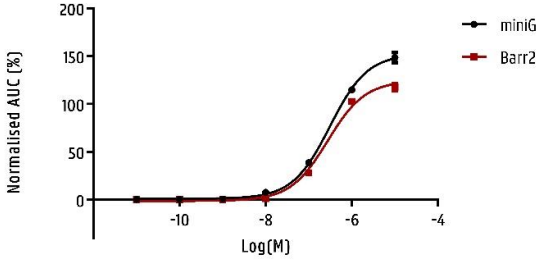

Concentration-response curves: Fentanyl analogues and synthetic opioids (continued)

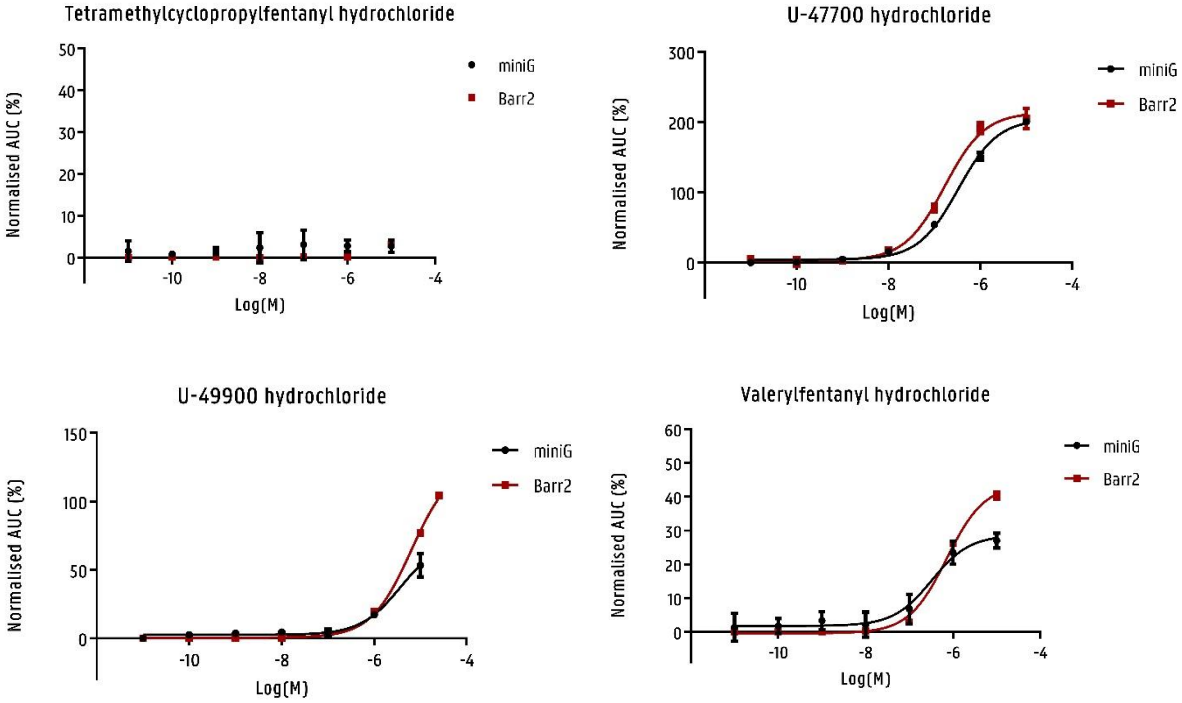

x-axis, logarithm of concentration, y-axis, normalised AUC in %; black curves, mini-G_i assay; red curves, β-arrestin 2 assay

Abbreviations: AUC, area under the curve; **M**, molar; **βarr2,** β-arrestin-2; **miniG**, mini-G_i

8.10 APPENDIX X: OVERVIEW OF THE CALCULATED BIAS FACTOR FOR THE SCREENED OPIOIDS

This table shows a listing of the calculated bias factors (β) of 21 synthetic opioids towards G protein coupling or β-arrestin 2 recruitment. None of these values were found to be statistically significant. Values were calculated using the method described by Winpenny *et al.* (Winpenny, D. 2016) with hydromorphone as the reference standard. We observed no activity for tetramethylcyclopropylfentanyl hydrochloride and benzoylfentanyl in our assay, therefore, it was not possible to calculate pathway bias.

Compound	$\beta = \Delta\Delta\log(E_{max}/EC_{50})$
Hydromorphone	**0**
4-Fluoro-isobutyrfentanyl	-0.05
4-Methoxybutyrfentanyl	0.02
Acetylfentanyl	-0.13
Acrylfentanyl	-0.08
AH-7921	-0.09
Alfentanil	-0.08
Benzoylfentanyl	ND
Butyrylfentanyl	0.13
Crotonylfentanyl	0.26
Cyclopentylfentanyl	0.13
Cyclopropylfentanyl	-0.15
Fentanyl	-0.27
Furanylfentanyl	0.13
Methoxyacetylfentanyl	-0.02
Ocfentanil	-0.17
Phenylpropionylfentanyl	0.15
Tetrahydrofuranylfentanyl	0.11
Tetramethylcyclopropanfentanyl	ND
U-47700	-0.25
U-49900	-0.06
Valerylfentanyl	0.21

Abbreviations: ND, not determined

8.11 APPENDIX XI: POSTER: APPLICATION OF A MU-OPIOID RECEPTOR BIOASSAY (PROMEGA)

The author had the opportunity to contribute to a poster which was presented by Lakshmi Vasudevan at Promega's Discover Glo: Bioluminescent Cell-Based Assay Seminar Tour in Brussels.

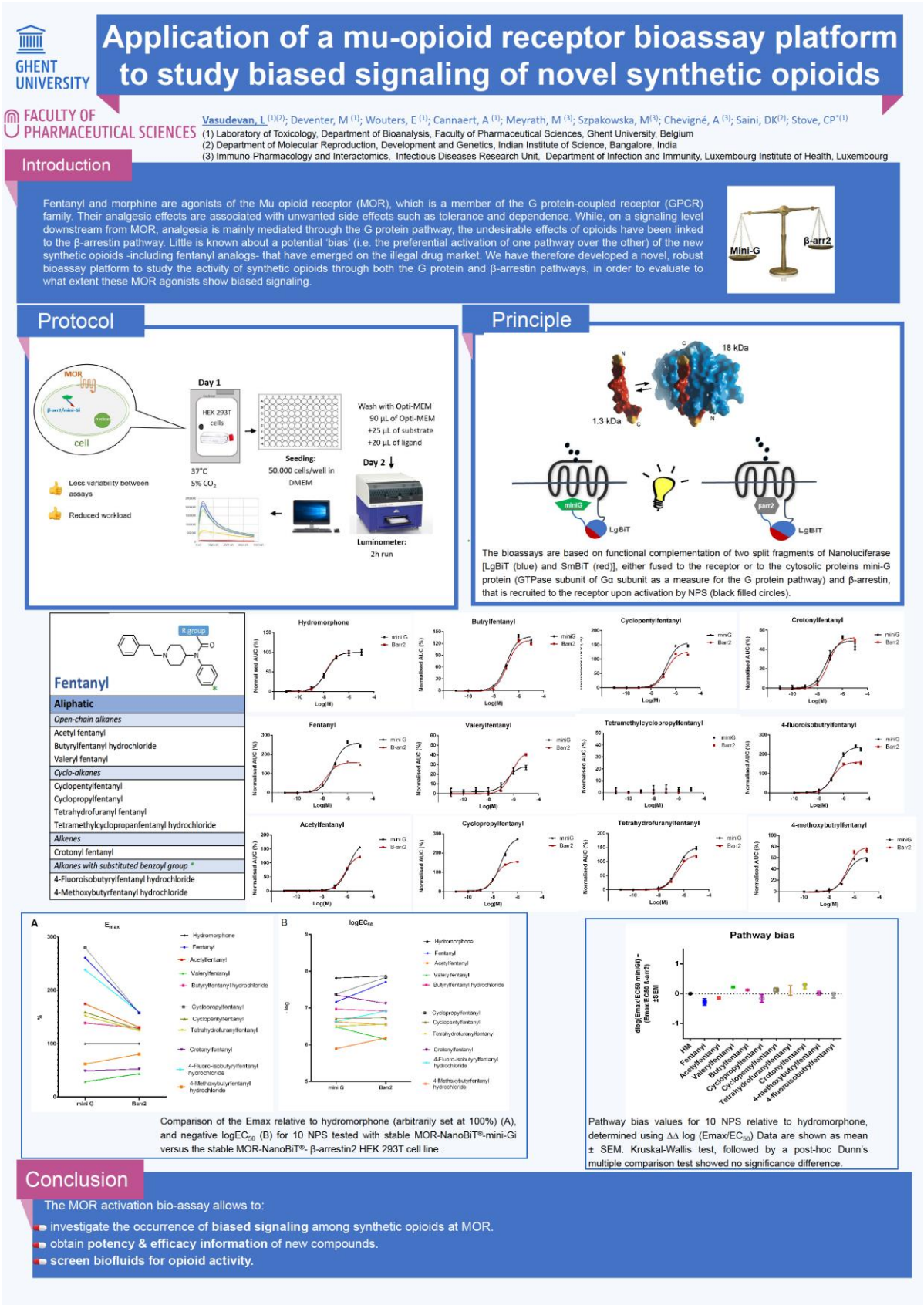

8.12 APPENDIX XII: SUMMARIES OF THE ATTENDED LECTURES IN THE CONTEXT OF INTERNALISATION@HOME

8.12.1. Pillen zonder zorgen: De kunst van het geneesmiddelengebruik by Prof dr. Bouvy (lecture in Dutch)

Prof. dr. Bouvy came to the Faculty of Pharmaceutical Sciences, where he was awarded a medal for being laureate of the Collen-Francqui Chair and gave a lecture about the pharmacist's (changing) role in the optimal use of medicines. He shortly mentioned the importance of evidence-based medicine, which covers the fact that the selection of the proper treatment for patients should be based on evidence arising from randomized controlled trials. However, pharmacists should also bear in mind that expertise of healthcare professionals, his own experience in the field and a patient's opinions are equally important. From originally being exclusively in charge of compounding medications to serving as a medicine distributor due to mass production, a remarkable change in the responsibilities of a pharmacist is noticeable. He has now been assigned the role of a true (pharmaceutical) healthcare professional. Nevertheless, the product continues to be a key element, especially since drug related problems (DRPs) still occur too often in many patients, contributing to ±6% of hospitalizations. From prescription to administration, DRPs can appear throughout the whole treatment process, often lead to suboptimal treatment and are usually preventable. Prof. Dr. Bouvy referred to some examples, like improper storage of biological medicines which leads to their rapid degradation and corresponding therapeutic failure and the fact that older people may struggle to efficiently open blister packs. Therefore, in the light of offering patient-oriented advice, assessment of the risk-benefit ratio, better exchange of information with other healthcare professionals and a multidisciplinary evaluation of polymedication remain important in the prevention of DRPs. Research conducted by Prof. Dr. Bouvy, showed that poor information transfer (in case of hospitalization) and lack of additional patient information (potential comorbidities and lab parameters) are one of the major causes of problems. Ideally, the necessary information is available for pharmacists at all times, but in reality, not enough pharmacists know to how to interpret renal function parameters or potassium blood levels. Additionally, privacy measures hamper this type of approach. In the end, an effective system should be based on three pillars: patient interview, medication records (medication history) and medical records (diagnosis history). These 3 elements should provide optimal pharmaceutical care for every individual patient. The ultimate goal is to develop an approach which allows pharmacists to assess patients' current and potential future problems, regarding to their medication and medical history. Lastly, non-adherence remains an issue according to Prof. Dr. Bouvy. Although various initiatives have already been taken, tackling poor medication adherence should also be a priority in "the pharmacy of the future".

8.12.2. "Pharmacogenetics: do YOU have your DNA passport?" by Prof. Dr. van Schaik

Prof. Dr. Van Schaik was invited at the Ghent University Hospital and presented his area of expertise to a public which contained pharmacy and medicine students, professors and hospital staff. The lecture was initiated by a specific case, concerning treatment failure of anti-depressants in a patient which could not be attributed to non-adherence. Apart from dose and renal function, the effect of a certain drug depends on the metabolising capacity of the liver, consisting of a whole array of enzymes such as cytochromes P450 and the DPD enzyme. During the process of prescribing drugs, it is too often assumed that every individual is equipped with the same capacity. However, this is certainly not the case and it may be the source of a lot of adverse drug reactions (ADRs). Prof. Dr. van Schaik placed particular emphasis on the significance of the possibility of predicting therapeutic response by means of pharmacogenetics, which studies genetic differences primarily related to drug metabolizing enzymes. These differences can explain why in some patients, the same drug does not result in the same blood concentrations or the same outcome and are caused by so-called SNPs or single-nucleotide polymorphisms. SNPs, which are present in more than 1% of the population, can be defined as the substitution of single nucleotides in a gene, resulting in alleles with varying activities. Possession of 2 inactive alleles can make a patient a *slow metabolizer,* whereas *ultra-rapid metabolizers* possess multiple active copies of the allele, which results in extensive enzyme activity. A study was conducted at the Erasmus University Medical Center (Rotterdam) with patients on imipramine (a tricyclic anti-depressant). By non-invasively collecting some DNA, researchers were able to investigate the gene for the CYP2D6 enzyme and saw that the number of active copies was strongly corelated to the dose required for significant therapeutic effect. Pharmacogentics is also a relevant topic in oncology, since some drugs rely on certain enzymes for their conversion into the active metabolite. In theory, with information about a patient's genotype available, it is possible to alter dosage or to switch to a drug that is not affected by a specific enzyme. Pharmacogenetic testing is now relatively easy and is covered by health insurance funds in the Netherlands. An increasing number of patients is screened, often to check if ultra-rapid metabolization rather than non-adherence is the reason for therapy failure. However, one must keep in mind that non-adherence may have a "genetic cause": slow (*poor*) metabolisers often experience side effects much sooner, and therefore consider treatment cessation. Implementing genotypic testing at an earlier stage of treatment can avoid ADRS and facilitate the search for a patient's ideal dose. Unfortunately, gaining information on one's DNA passport is too often done when a patient already experienced drug related problems. According to a study conducted in the US, genotyping before deciding on a treatment is cost-effective. On top of that, it offers a tremendous opportunity for doctors and pharmacists to cooperate. In the Netherlands, genotypic testing is already well established and pharmacists have access to this information, which allows them to provide patients with a more custom-made treatment regimen.

8.12.3. "Precision Medicine in Respiratory Disease, are we beyond fiction?" by Prof. Dr. Maitland- van der Zee.

Prof. Dr. Anke-Hilse Maitland-van der Zee from the Academic Medical Center in Amsterdam was invited to the faculty for Research Day & Student Research Symposium and presented her work on novel biomarkers concerning respiratory diseases. Worldwide, by 2025, respiratory disease such as COPD, lung cancer and asthma will have become the number one cause of death, with new patients every year. Finding the optimal treatment will therefore be of major importance and Prof. Dr Maitland-van der Zee specified 2 relevant rationales. Firstly, "one size does not fit all" when dealing with respiratory disease patients, demonstrated by the heterogeneity in response of asthma patients to standard inhaled corticosteroid treatment combined with bronchodilators. Secondly, to this day, asthma and COPD are still uncurable and patients require lifelong treatment, which stresses the need for improved therapies. The research conducted by Prof. Dr. Maitland-van der Zee focusses on a more precise and patient-oriented way to treat asthma and is based on the finding that different phenotypes, for example asthma with predominant eosinophilic inflammation *vs.* asthma with a high degree of bronchoconstriction, react differently to the same treatment. The assumption arose that certain genetic factors such as SNPs or single-nucleotide polymorphisms that are significantly associated with lung function, may also be associated with asthma phenotypes. SNPs are believed to potentially play a role in different key features of asthma such as inflammation, bronchial hyperreactivity and airway remodelling. Genome wide association studies have been conducted, involving patients who were on either ICS or LABA (Long-acting β-adrenoceptor agonists) and results were then compared to a patient's response to treatment. This allowed to distinguish SNPs that might be of interest for future treatment adjustments. The PUFFIN trail, which analyses if genotype guided therapy, i.e. specific treatment adjustment for patients that carry certain alleles, is now ongoing. To conclude, Prof. Dr. Maitland-van der Zee also had the chance to elaborate on an alternative aspect of respiratory disease research. By using eNose, a device composed of a number of sensors, it has now become possible to detect and recognise different compounds in breath. Implementation of this approach on healthy controls and patients diagnosed with either asthma, COPD or lung cancer and applying principal component analysis, showed that results from different patient groups are remarkably well clustered together. Not only will this allow distinguishing different phenotypes but also it will enable predicting if a tumour is sensitive to specific therapies such as immunotherapy, an appealing feature in oncology research and treatment. We can conclude that promising progress has been made lately in the development of strategies to find a custom-made therapy and treat individual patients more efficiently, but further research on biomarkers and SNPs is required.

Master dissertation submitted to the faculty of Pharmaceutical Sciences, performed in collaboration with the Laboratory of Toxicology.

Promotor: Prof. dr. C. Stove

Commissioners: Dr. M. De Boevre en Dr. A. Cannaert

The information, conclusions and points of view in this master dissertation are those of the author and do not necessarily represent the opinion of the promoter or his research group.